SUSPENDED SEDIMENT FLUX DOWNSTREAM OF THE RETREATING CASTLE CREEK GLACIER, CARIBOO MOUNTAINS, BRITISH COLUMBIA.

by

Michael Strathearn Leggat

B.Sc. (Freshwater Science), University of British Columbia Okanagan, 2006

THESIS SUBMITTED IN PARTIAL FULFILLMENT OF
THE REQUIREMENTS FOR THE DEGREE OF
MASTER OF SCIENCE
IN
NATURAL RESOURCES AND ENVIRONMENTAL STUDIES
(ENVIRONMENTAL SCIENCE)

THE UNIVERSITY OF NORTHERN BRITISH COLUMBIA
November, 2014

Abstract

Glaciers are a major erosive force that increase sediment load to the downstream fluvial system. The Castle Creek Glacier, British Columbia has retreated ~1.0 km in the past 70 years. The dynamics of suspended sediment concentration (SSC) and streamflow (Q) were monitored independently at six sites within its proglacial zone over a 60 day period from July to September, 2011. The time-series were divided into hydrologic days and the SSC response to hydro-meteorological conditions was categorized using principal component analysis (PCA) and cluster analysis (CA). Suspended sediment load (SSL) was computed and summarized for the categories. During the 2011 study period, *c.* 60% of the total SSL was derived from the glacial stream and sediment deposits proximal to the terminus of the glacier; during 'storm' events, that contribution drops to 40% as contribution from diffuse and point sources of sediment within the meltwater channel and proglacial zone increase. While 'storm' events accounted for just 3% of the field season, SSL was 500% higher than the seasonal average, and *c.* 20% of the total SSL was generated in that time.

Table of Contents

List of Tables

List of Figures

Acknowledgements

I would like to express my sincere gratitude to the people and organizations that have supported me through this process. My supervisor, Dr. Philip Owens, has provided me with guidance, support, and encouragement as well as the insight, freedom and flexibility needed to develop, steer and complete this project. Dr. Tim Stott from Liverpool John Moores University was on site for a month of field and laboratory work, and has continually been a valuable and enthusiastic committee member. Dr. Brian Menounos has been a constructive and disciplined committee member who has strengthened this project at every input.

This project would not have been possible without the generosity of AJ Downie, Scott Jackson, Chelton van Geloven, and James Jacklin with the British Columbia Ministry of Environment and John Rex with the British Columbia Ministry of Forests who provided their time to facilitate the in kind use of equipment for this project.

Financial support for this project came from an NSERC Discovery Grant and an FRBC Research Chair Operating Grant to Dr. PN Owens and a UNBC RPA award to MS Leggat.

Several research assistants have contributed to the field and laboratory components of this project. In order of appearance: Barry Forrester, Ian Eccles, Doug Roberts, Maud Barrel, Natalie Saindon, and Sonja Ostertag assisted with field work. Barry Forrester, Ian Eccles, Doug Roberts and Megan Harwood spent many hours in University of Northern British Columbia Landscape Ecology Research Group soils laboratory drying and weighing suspended sediment samples.

Dr. Stephen Déry was readily available for consultation and coordination of field efforts. He and his research team have had an invaluable role in the collection and analysis of meteorological data. Dr. David Scott at the University of British Columbia Okanagan generously made his soils lab available for part of the laboratory analysis. Dr. Mathew Beedle patiently guided the production of GIS imagery; Leticia Gaspar Ferrer facilitated corrections after the fact.

Perhaps most importantly, I have had the continued support and understanding of my family for the countless nights and weekends that I have been unavailable.

1 Literature Review

1.1 Introduction

In British Columbia (BC), glaciers cover 3% of the landmass (*c.* 29,000 km^2) and influence 20% of the watersheds with meltwater and sediment (Austin *et al.* 2008; Moore *et al.* 2009; Bolch *et al.* 2010). Glaciers are sensitive climate change indicators that respond to the ocean and atmospheric circulation patterns that influence winter and summer precipitation and temperature (Déry *et al.* 2009; Moore *et al.* 2009). Glaciers store water during cool and/or wet periods and release water during warm and/or dry periods. Glaciers are powerful agents of erosion that abrade and fracture substrate, making it available for various erosion processes and transport downstream (Dirszowsky 2004; Haritashya *et al.* 2010). The suspended sediment load of glaciated rivers (1-90% ice covered watershed) is higher than the global average (Gurnell *et al.* 1996); this load can be even higher during deglaciation as a result of elevated meltwater production and sediment availability (Gurnell *et al.* 1999; Menounos *et al.* 2005). Currently, BC glaciers are not in equilibrium with climatic conditions and have generally been retreating since reaching their Holocene maxima at the end of the Little Ice Age (LIA) 150 – 300 years ago (Schiefer *et al.* 2007; Menounos *et al.* 2009; Tennant *et al.* 2012). Since the LIA, regional climate has been dominated by a warming trend and annual temperatures have increased by 0.5 to 1.5°C per century (Moore *et al.* 2009). Between 1985 and 2005, glacier area in western Canada declined by 11.5% (Bolch *et al.* 2010). Although current global climate models do not explicitly include glacial evolution, it is expected that they will continue to retreat in response to the projected 1 to 4°C

increase in global mean surface temperature, depending on the emission scenario, over the next 100 years (Collins *et al.* 2013).

In response to glacial retreat, in the near term (10's of years) there is likely to be an increase in meltwater and sediment yield from proglacial rivers and a shift in the timing of the peaks in the hydrograph and sedigraph (Kirtman *et al.* 2013). Moore *et al.* (2009) discuss the effects of climate change scenarios on glacial hydrology. As glacial mass wanes and watersheds become deglaciated, streamflow will approach annual net balance with precipitation, and sediment yield will exponentially approach the 'normal' sub-aerial erosion rate of non-glaciated catchments (Church and Ryder 1972). The magnitude and time scale for the adjustment of hydrologic and geomorphic processes is dependent on climatic conditions, the scale of the geomorphic system, glacial extent and site-specific characteristics that determine the rate of temporal change in streamflow and sediment availability (Tunnicliffe and Church 2011). Many of the watersheds in BC are still responding to the Pleistocene glaciation (Church and Slaymaker 1989).

Glacial processes can affect the timing, quantity and quality of streamflow and suspended sediment load of a watershed. The influence of glaciers on the hydrology, geomorphology and sediment yield of a watershed are of significant ecological, economical, and societal importance. For instance:

- aquatic ecosystems are sensitive to water temperature, and the quantity, quality, and timing of streamflow and sediment; certain species may decline or be extirpated if stream conditions change beyond their niche (Austin *et al.* 2008; Milner *et al.* 2009; Moore *et al.* 2009);

- fine sediment < 63 μm (silts and clays) are the chemically active component of the solid sediment load; they can transport and store nutrients and contaminants (Brown *et al.* 1996; Dirszowsky 2004; Hodson *et al.* 2004; Owens *et al.* 2005; Walling 2005; Hodson *et al.* 2008; Haritashya *et al.* 2010);
- depending on site specific and hydrologic characteristics, bedload can account for 5 – 65% of sediment yield from the proglacial zone and will therefore have implications for downstream channel morphology and ecology (Bogen 1989; Hammer and Smith 1983; Church and Slaymaker 1989; Warburton 1990; Harbor and Warburton 1993; Gurnell *et al.* 1999; Scheifer *et al.* 2010);
- streamflow translates into a dollar value for hydropower operations, and the amount of sediment can determine the lifespan and maintenance requirements of reservoirs, headponds, and turbines (Bogen 1989; Morehead *et al.* 2003);
- there are many anthropogenic interactions that depend on the quantity and quality of water in glacially influenced rivers including, for example, recreational boating, swimming, and fishing; and,
- regulatory agencies that issue water licences and permits for intakes and discharges to surface water may rely on, or have to deal with, upstream glacial influences (Moore *et al.* 2009).

The importance of glaciers, and their rapid retreat since the LIA, has caused researchers to study the processes that influence, and are driven by, these intriguing and valuable landscape features. The focus of this study is on the flux of fluvial suspended sediment < 2 mm through the proglacial zone.

1.2 Research Objectives

The overall aim of this thesis was to assess the influence of hydro-meteorological conditions on suspended sediment flux in a proglacial creek in the Cariboo Mountains of British Columbia during the 2011 field season. The specific research objectives were to:

1. examine the spatial and temporal response pattern of suspended sediment concentration in the proglacial zone; and,
2. determine the sources of streamflow and suspended sediment load under different hydro-meteorological conditions.

In order to achieve these objectives, meteorological data were collected from two automated weather stations in the proglacial zone, and streamflow (Q) and suspended sediment concentration (SSC) were monitored independently at six sites along the proglacial meltwater channels of the Castle Creek Glacier from July 14 to September 11 of 2011. To achieve objective 1, the shape and magnitude of the SSC response to hydro-meteorological conditions was categorized using principal component analysis (PCA) and cluster analysis (CA), and sediment flux processes and source/sink areas were identified using field observations and measurements as substantiating evidence. To achieve objective 2, streamflow and suspended sediment load were computed and summarized for the meteorological categories, as defined in objective 1. In addition, a suspended sediment budget for the Castle Creek proglacial meltwater channel was defined using the results of the analysis in this study and the proglacial sediment parameters defined by Warburton (1990); this helped to quantify areas of sediment sources and storage.

The following introductory sections review relevant work in proglacial zones and on suspended sediment budgets; the challenges of hysteresis and non-linear relationships in SSC and Q data; and the different modelling approaches that have been used.

1.3 Proglacial Zone

The 'proglacial zone' is the area surrounding a glacier that has been influenced by the glacier, and the 'proglacial period' lasts until the completion of deglaciation. 'Paraglacial sedimentation' refers to non-glacial sedimentation processes directly conditioned by the previous glaciation (Church and Ryder 1972; Ballantyne 2002a). The 'paraglacial period' lasts until the effects of the previous presence of ice have diminished, and erosion rates return to that of a non-glaciated catchment under 'normal' subaerial weathering processes (Church and Ryder 1972; Ballantyne 2002a). Recently exposed sediment in the proglacial zone can be in an unstable or metastable state; these initially unconsolidated sediments are subject to rapid and extensive modification and erosion over the proglacial period. Sediment yield can greatly exceed that of otherwise equivalent non-glacial landscapes throughout the paraglacial period (Church and Ryder 1972; Church and Slaymaker 1989; Harbor and Warburton 1993; Hallet *et al.* 1996; Ballantyne 2002b; Hodgkins *et al.* 2003).

A spectrum of geomorphic processes release and rework glacial sediment over a wide range of timescales (Ballantyne 2002a). Immediately after exposure, the unconsolidated and water-saturated till in the glacier forefield begins to adjust to subaerial conditions; loose sediments consolidate as the substrate drains, and slope angles decline (Ballantyne 2002b). More recently exposed surfaces tend to be greater sediment sources than older surfaces and the rate of adjustment following deglaciation can be approximated by exhaustion models

(Ballantyne 2002a, also see *section 1.5.1*). Over time, the eluviation of fines, surface armouring, reduction in surface slope and vegetation colonization act to stabilize the proglacial zone and reduce sediment availability for fluvial entrainment and transport (Warburton 1990; Gurnell *et al.* 1999; Orwin and Smart 2004a; 2004b).

There are many factors that influence the rate of erosion and sediment yield from glaciated watersheds, and no simple linear relationship exists (Gurnell *et al.* 1996); however, global comparisons have found that sediment yields are higher in glaciated watersheds than non-glaciated watersheds (Harbor and Warburton 1993; Gurnell *et al.* 1996; Hallet *et al.* 1996; Richards and Moore 2003). Since the hydrology of a watershed changes as it becomes deglaciated, sediment yield is not static through time and can vary spatially and temporally in response to site-specific characteristics such as the underlying rock type and subglacial deposits, the rate of glacial movement, the character of the glacial drainage system, topography, weather and climate (Gurnell *et al.* 1996). The size of the watershed, extent of glaciation, abundance and distribution of glacial sediments and their connectivity to the fluvial system determine the duration and magnitude of the paraglacial period (Church and Ryder 1972; Ballantyne 2002a; 2002b). Contrary to conventional global sediment yield models that show declining sediment yield as watershed area increases (Syvitski and Milliman 2007), the specific sediment yield for glaciated watersheds (>10 km^2) in BC increases for spatial scales up to 10^4 km^2 as a result of the remobilization of sediments deposited during the Pleistocene (Church and Slaymaker 1989; Tunnicliffe and Church 2011); however, the results for watersheds <10 km^2 are more dependent on physiographic characteristics (Schiefer *et al.* 2001). High sedimentation rates observed in proglacial lake cores (i.e. derived from glacial meltwater) coincide with periods of rapid glacial retreat, but

also periods of rapid advance and glacial maxima due to glacial override of previously deposited sediment (Ballantyne 2002b; Menounos *et al.* 2005; Menounos *et al.* 2009). Downstream sediment yields represent the combined contribution of contemporary paraglacial erosion from active upland proglacial zones and other non-glacial erosion, as well as the reworking of sediment deposited more than 10,000 years ago (Church and Slaymaker 1989; Scheifer *et al.* 2001; Tunnicliffe and Church 2011). As such, it is difficult to partition the relative amount of sediment derived from the two scales of paraglacial systems and contemporary non-glacial processes solely from a downstream perspective (Church and Slaymaker 1989; Ballantyne 2002a; Dirszowsky 2004).

The definition and inclusion of proglacial sediment yields in sediment budget models can help to isolate sediment generated by contemporary glacial and paraglacial processes from contemporary reworking of Pleistocene deposits (Harbor and Warburton 1993). Determining accurate proglacial sediment budgets can be useful for water quality and quantity models that include sediment yield from glacially influenced watersheds (Warburton 1990; Richards and Moore 2003; Orwin and Smart 2004a; Stott and Mount 2007).

1.4 Hysteresis and Non-linear Relationships in Suspended Sediment Concentration and Streamflow Data

Collecting high resolution SSC and Q data requires substantial effort. This section is included to explain the complexity of these types of data, and draws upon the experience of past researchers to justify the need for and usefulness of independent, high resolution data collection.

Empirically, SSC can be related to Q by a simple power function, but simple direct relationships are notoriously poor because of hysteresis loops and non-linear relationships (Gurnell and Fenn 1984; Pickup 1988; Lawson 1995; Hodson and Ferguson 1999; Swift *et al.* 2002; Richards and Moore 2003; Orwin and Smart 2004b; Stott and Mount 2007). In a given high-flow event, scatter in the SSC – Q relationship can result when the sediment wave either lags or, more often, precedes peak Q (Naden 1988; Hodson *et al.* 1998). When plotted against each other with Q as the independent variable, data where the SSC peak precedes the peak Q shows clockwise hysteresis, while anti-clockwise hysteresis occurs when the SSC peak follows the Q peak (Hodson *et al.* 1998; Richards and Moore 2003; Orwin and Smart 2004b; Eaton *et al.* 2010). Hysteresis data contain serial autocorrelation in the residuals, where each data point is related to the others in the series (Naden 1988; Richards and Moore 2003), but not necessarily Q (Hodson and Ferguson 1999). Interpretation of SSC – Q plots and hysteresis loops for a series of sites along a stream can be used to assess sediment availability and suggest which sediment sources are contributing and when they are contributing during a given high-flow event (Hodson *et al.* 1998; Hodson and Ferguson 1999; Orwin and Smart 2004b).

Clockwise hysteresis is more common, and could be considered the background "normal" condition for geomorphically "inactive" systems where fine sediment that has accumulated within the catchment area or the channel since the last high-flow event is evacuated during the rising limb of the hydrograph and is then exhausted as Q peaks (Hodson *et al.* 1998; Orwin and Smart 2004b; Eaton *et al.* 2010). The falling limb of the hydrograph tends to have a much lower SSC, and two equivalent Q values separated by a short period of

time can have instantaneous suspended sediment loads that differ by more than an order of magnitude (Pickup 1988; Orwin and Smart 2004b).

Spatial separation of the sample site from the source of sediment, and episodic mass movement on the falling limb of the hydrograph – commonly a bank failure from undercutting during the event – can result in a "late" or seemingly random pulse of sediment after the initial peak has passed (Pickup 1988; Morehead *et al.* 2003; Orwin and Smart 2004b). This situation can create anti-clockwise hysteresis loops in the SSC – Q plot.

Geomorphically "active" point sources of sediment that are connected to the stream network, such as a bank failure, can be discharged in declining pulses of sediment through subsequent high flow events over a season or several years (Morehead *et al.* 2003; Eaton *et al.* 2010). Additionally, they may become active sediment sources under specific hydrologic or weather conditions such as high Q, spring melt, or heavy rainfall but otherwise be inactive. Diffuse areas of exposed sediment, as found in the proglacial zone, act as transient sediment sources (Warburton 1990; Hodson *et al.* 1998; Orwin and Smart 2004b). The amount of sediment eroded from a particular area is highest immediately following exposure and declines over time as mass movement processes reduce surface slope and sediment availability. These processes can operate at diurnal, weekly, sub-seasonal, and seasonal time scales or over longer periods of time (Warburton 1990; Hallet *et al.* 1996; Hodson and Ferguson 1999; Richards and Moore 2003; Orwin and Smart 2004b).

The processes described above result in a complex relationship between SSC and Q for both "inactive" and "active" geomorphic systems. "Inactive" systems will tend to show more prominent clockwise hysteresis where available fine sediment is entrained during the rising

limb of the hydrograph and then exhausted as the hydrograph peaks. Geomorphically "active" systems tend to have a more complex SSC – Q relationship (Richards and Moore 2003). In proglacial zones, the abundance of unconsolidated fine sediment can cause SSC to track Q more closely (Hodson *et al.* 1998; Hodson and Ferguson 1999). However, the abundance of active sediment sources in these systems will tend to create irregular response patterns, which can include sustained or late pulses of sediment on the hydrograph and anti-clockwise hysteresis. Suspended sediment concentration can change dramatically in a short period of time, and though Q can be a trigger, the suspended sediment response can be unpredictable and thus the two variables are best recorded independently.

1.5 Modeling Suspended Sediment Concentration

The hysteresis and non-linearity that arise from seasonality, source exhaustion, disturbance regimes, and spatial separation of the sample site from the sediment source described above make lumped parameter models that relate SSC to Q inaccurate in supply-limited systems. Such lumped parameter suspended sediment rating curves assume that SSC depends on Q, or that SSC is transport-limited. However, SSC in most fluvial systems depends on the rate of erosion within the catchment and the rate of supply to the channel, not Q (Pickup 1988; Ritter *et al.* 2002). As an exception, in certain locations unconsolidated sediments may be more transport-limited, and in these situations empirical suspended sediment rating curves may be more applicable (Hodson *et al.* 1998; Swift *et al.* 2002; Stott and Mount 2007).

Since the SSC peak tends to occur on the rising limb of the hydrograph, various time lag, hydrograph separation, cross-correlation, log transformation and multiple regression

techniques have been used to predict SSC from Q to correct the suspended sediment rating curve (Hodson and Ferguson 1999). Gurnell and Fenn (1984) tested several of these methods to improve the SSC – Q rating relation for a proglacial system, but none were able to significantly improve upon the estimates made by the ordinary rating curve. They found that a Box-Jenkins transfer function based on a longer time series of SSC and Q data was more accurate and suitable for real-time forecasting of SSC based on Q (Gurnell and Fenn 1984). However, a significant amount of SSC data is required to establish and maintain such models, a continuous record of Q is also required, and the forecasted SSC is relative to the previous SSC.

Building on the past models, Syvitski and Milliman (2007) introduced the BQART model as a global predictor of sediment flux to the oceans. When the model was applied to a database of 488 rivers that drain into the oceans it was able to account for 96% of the long-term sediment yield (Syvitski and Milliman 2007). Glacial sediment is a relatively minor component of this large-scale model, accounting for only 1% of the signal, but they noted that this component would be much more important during and just after glaciation (Syvitski and Milliman 2007). Geographic factors (such as topographic relief, watershed size, geology, latitude, et*c.*) accounted for 65% of the variation between rivers, while climatic and anthropogenic factors accounted for 14% and 16%, respectively. Syvitski and Milliman (2007) state that more advanced models are required to account for the magnitude and timescale of paraglacial and deglacial processes, and that the model includes a general glacial erosion factor as a function of glacial coverage in the watershed. However, specific research has found that glacial cover alone is not a good predictor of suspended sediment yield (Harbor and Warburton 1993; Gurnell *et al.* 1996) and that other factors need to be included,

such as the underlying rock type and sub-glacial deposits, rate of glacial movement, character of glacial drainage system, and the topography and physiography of the basin (Gurnell *et al.* 1996; Scheifer *et al.* 2001).

1.5.1 Modeling Suspended Sediment Yield over the Paraglacial Period

Church and Ryder's (1972) description of the combined effect of deglacial processes over the paraglacial period shows that in-stream sediment yield initially increases following the start of deglaciation and then decreases exponentially to the 'normal' subaerial erosion rate of a non-glacial landscape (Figure 1.1). The inflection point on the falling limb of the model occurs as deglaciation is completed. This model represents the exhaustion of available glacigenic sediment over time through mass movement processes and reduction of surface slope by surface wash, frost sorting, eluviation of fines, and stabilization by vegetation colonization (Ballantyne 2002a). The axes of the conceptual model proposed by Church and Ryder (1972) are scale independent because the response time and magnitude reflect the spatial scale and site-specific characteristics of the catchment. In general, larger systems will have a nested effect of several individual response curves from glacially influenced tributary watersheds and take longer to reach the subaerial norm (Church and Slaymaker 1989; Harbor and Warburton 1993). While primary paraglacial sedimentation can last decades to centuries in small, alpine watersheds (Ballantyne 2002a; Orwin and Smart 2004b), some of the largest rivers in BC continue to have suspended sediment loads greater than the 'geologic norm' as secondary paraglacial processes continue to rework Quaternary sediment deposits (Church and Slaymaker 1989; Scheifer *et al*. 2001; Ballantyne 2002b).

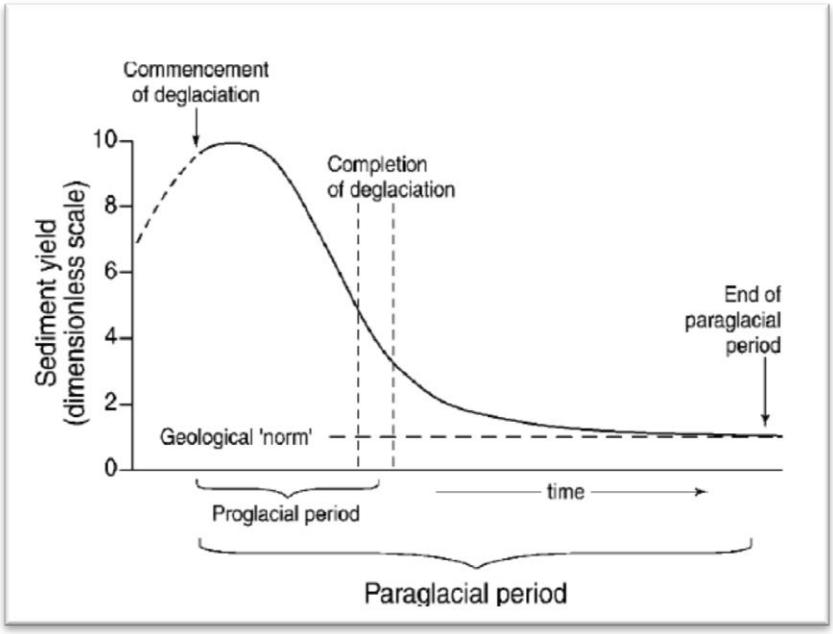

Figure 1.1 Schematic exhaustion model representing sediment yield over the paraglacial period (source: Church and Ryder 1972, pg. 3069).

Embedded within Church and Ryder's (1972) paraglacial sediment yield model is a spectrum of geomorphic processes which includes both primary and secondary paraglacial sedimentation. Primary paraglacial geomorphic systems are directly glacially conditioned (e.g. rock-slope failure due to deglacial stress release, modification of moraines by slope processes, entrainment of glacigenic deposits by rivers), whereas secondary paraglacial systems encompass the reworking of *in situ* glacigenic sediment and paraglacial sediment stores (e.g. talus, debris cones, outwash fans, valley fills) (Ballantyne 2002a). The work of several researchers on primary paraglacial geomorphology is combined into one diagram to compare the rate of paraglacial sediment exhaustion for different processes (Figure 1.2; Ballantyne 2002a). Note that the diagram must be treated with caution because available data are sparse, collected from different locations and are, therefore, not necessarily universally

applicable (Ballantyne 2002a). The y-axis in Figure 1.2 is presented as a proportion of the total, and the contribution of each process to sediment yield will not be equal. All primary paraglacial sedimentation processes follow an exponential decay model following deglaciation (Ballantyne 2002a), which is encompassed by Church and Ryder's (1972) model that extends over the paraglacial period.

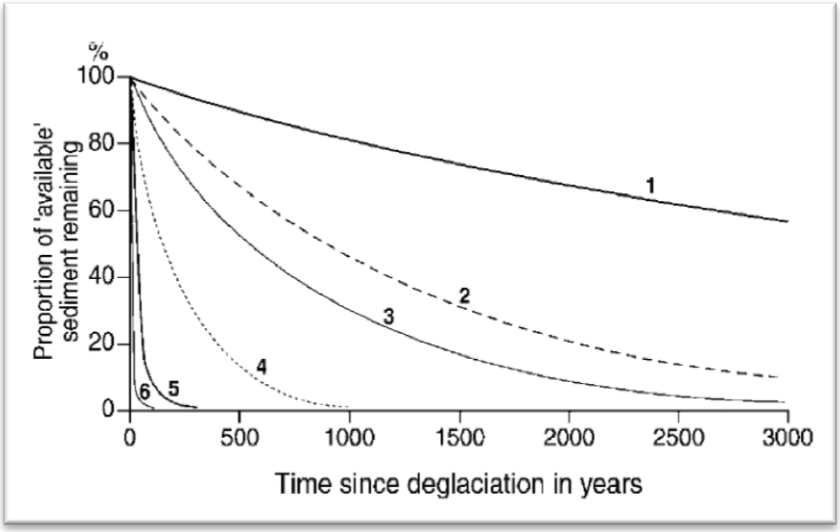

Figure 1.2 Sedimentation exhaustion curves for primary paraglacial processes: (1) rock slope failure; (2) rockfall and talus accumulation; (3) accumulation of large alluvial fans; (4) rock-slope deformation; (5) modification of drift-mantled slopes; and (6) modification of glacier forelands (source: Ballantyne 2002a, pg. 373).

The processes in Figure 1.2 are primary paraglacial processes that are not replenished; the model assumes steady-state conditions with no episodic events or other changes to the system that would rejuvenate or renew the availability of sediment. Additionally, secondary non-glacial reworking of the sediment is not considered in this diagram. Fluvial processes are the dominant non-glacial force that reworks paraglacial sediment deposited on land (Ballantyne 2002a). In the proglacial zone of a retreating glacier, the sediment exposed each year starts at time zero and begins its progression through the

exhaustion model, resulting in dynamic proglacial sediment availability over space and time. The most rapid paraglacial process following deglaciation is the modification of glacier forelands. Mass movement, eluviation of fines, and redistribution and sorting of sediment are often complete within a few decades, and as vegetation colonization occurs normal subaerial weathering rates are approached within *c.* 200 years (Church and Ryder 1972; Ballantyne 2002a). However, secondary paraglacial sedimentation can continue for much longer and is related to watershed size, climatic conditions, and the extent of glaciation and glacial deposits (Church and Slaymaker 1989; Scheifer *et al.* 2001).

1.5.2 Rationale for the Use of Turbidity Measurements to Determine Suspended Sediment Concentration

The spatial and temporal complexity of suspended sediment entrainment, transport and storage precludes predictive models of SSC (Naden 1988). Because of this complexity, it is necessary to have a high sample frequency in monitoring programs that aim to quantify suspended sediment load (SSL) (Gippel 1989; Warburton 1990; Gurnell *et al.* 1996; Navratil *et al.* 2011). Additionally, studies that aim to quantify sediment sources, sinks and processes in a catchment or to establish a sediment budget will likely need multiple monitoring sites (Richards and Moore 2003; Orwin and Smart 2004a; 2004b). Due to the high effort and cost of collecting and analysing physical water samples to measure SSC, turbidity (Tu) is often used as a surrogate measure and sample frequency can be near continuous (Orwin and Smart 2004a; Orwin and Smart 2005; Navratil *et al.* 2011).

Turbidity is a measure of light penetration and is affected by particle size, shape and composition, as well as bubbles (turbulence), water colour, and algae (Gippel 1989; Orwin and Smart 2005; Ginting and Mamo 2006). Turbidity–SSC regressions are especially

applicable in low biologic productivity systems, such as proglacial zones (Swift *et al.* 2002; Orwin and Smart 2004a; Stott and Mount 2007). However, there can be a significant amount of uncertainty in the Tu–SSC relation which culminates from, and is propagated through, various aspects of the data collection and analytical procedure (Navratil *et al.* 2011).

Hysteresis in Tu–SSC data can occur, and has been attributed to changing flow conditions at the monitoring location and different properties of different sediment source materials as they are transported past the monitoring location (Orwin and Smart 2005; Ginting and Mamo 2006; Navratil *et al.* 2011). Unless the SSC sample frequency is high (30 minutes or less), this hysteresis pattern appears as scatter in the Tu–SSC relationship, resulting in a wider spread of the residuals, and a lower R^2 value. However, source materials may be relatively homogenous in the small proglacial catchment area that is the focus of this study, which should limit the amount of Tu–SSC hysteresis from differing source materials.

1.6 Sediment Budgets

While the transport of bedload sediment is hydraulically controlled (i.e. stream competency determines the erodibility and transport distance of sediment), the transport of suspended sediment is typically supply controlled (i.e. sediment delivery mechanisms can be more important than stream competency in determining the amount of material transported in suspension). Suspended sediment can be transported a great distance downstream (Ritter *et al.* 2002); thus, exported from the proglacial zone once entrained.

Fine sediment (i.e. rock flour in glacial meltwater) is the chemically active portion of the solid load transported by a river and is an important vector for the transfer and fate of nutrients and contaminants through both terrestrial and aquatic ecosystems (Brown *et al.*

1996; Owens *et al.* 2005). For fluvial geomorphologists, developing a suspended sediment budget that quantifies the nature, importance and interaction between sediment production, mobilization, transport, storage and yield is a precursor to developing effective sediment management and control strategies aimed at reducing diffuse or point source pollution by fine sediment (Slaymaker 2003; Hodson *et al.* 2004; Owens 2005; Walling 2005; Walling and Collins 2008). The spatial and temporal variability of suspended sediment processes within a catchment can make quantification with direct measurement techniques such as field observations, photogrammetry, erosion pins, profilometers, sediment traps and erosion plots exceedingly complex (Walling and Collins 2008). Thus, there is considerable motivation to find more effective and efficient ways to assemble the necessary data to construct reliable sediment budgets (Harbor and Warburton 1993). As there is no well-defined single procedure that is universally applicable, researchers have focused on integrated approaches that use a combination of complementary techniques to discriminate and quantify sediment sources, fluxes and storage within sediment budget frameworks (Warburton 1990; Harbor and Warburton 1993; Owens 2005; Walling and Collins 2008).

1.6.1 Proglacial Sediment Budget Applications

Proglacial sediment budgets tend to be simpler than equivalent budgets for temperate catchments because of their smaller size, relative lack of vegetation and abundance of unconsolidated material, which make the sources, sinks, and transfers of suspended sediment easier to define. However, a common problem with the definition of proglacial erosion and sedimentation processes is the short time scale of many of the studies due to the high effort involved with collecting data from these often remote locations with extreme climatic conditions (Warburton 1990; Gurnell *et al.* 1996; Hodson *et al.* 1998; Hodgkins *et al.* 2003;

Orwin and Smart 2004a). The definition of sediment budgets over short time scales is subject to partial definition when the recognition and quantification of budget processes are being conducted simultaneously, as such, pilot studies have high value (Warburton 1990). Additionally, Warburton (1990) has noted that data which represent only part of an ablation season may be misleading, as, for example, sediment evacuation during spring freshet may be followed by sediment storage later in that same season. These difficulties are confounded by the fact that each individual ablation season can be markedly different (Hodgkins *et al.* 2003; Jobard and Dzikowski 2006; Stott and Mount 2007; Cockburn and Lamoureux 2008; Haritashya *et al.* 2010), and that sediment sources evolve through the ablation season (Hodson *et al.* 1998; Swift *et al.* 2002; 2005; Haritashya *et al.* 2010). Walling (1978) suggests that 10 years of monitoring are required before the sediment transport system of a catchment can be adequately characterized; however, Warburton (1990) comments that because of the rapid rate of change and condensed frequency of geomorphic events in the proglacial zone, multi-year studies are subject to many of the same limitations.

The proglacial zone can be a significant source and sink of sediment (Warburton 1990; Harbor and Warburton 1993; Hodson *et al.* 1998; Hodgkins *et al.* 2003; Richards and Moore 2003; Orwin and Smart 2004a), and will depend on site-specific characteristics (Harbor and Warburton 1993; Gurnell *et al.* 1996). The function of the proglacial zone as a source and sink of sediment operates at a range of timescales as glacierised catchments respond to weather patterns, and seasonal and climatic trends. Abnormally warm ablation seasons have been shown to increase sediment yield from the proglacial zone (Stott and Mount 2007; Cockburn and Lamoureux 2008), whereas, cooler seasons have been found to increase sediment storage within the proglacial zone (Hodgkins *et al.* 2003; Richards and

Moore 2003). The distribution and intensity of monitoring sites is important in determining and interpreting suspended sediment fluxes because as distance from the glacier increases, so does the potential for sediment storage and remobilization, and therefore modification of transfer patterns (Harbor and Warburton 1993; Orwin and Smart 2004a). Warburton (1990) defined the basic sediment balance equation for the coarse and fine components of a proglacial sediment budget as:

$$\mathbf{Y = SL + TR + M + GL + \Delta VS} \qquad \mathbf{(1)}$$

where: **Y** is sediment yield; **SL** is direct hillslope inputs; **TR** is tributary channel inputs; **M** is the input from moraine deposition; **GL** is the glacial stream input; and **ΔVS** is the change in valley sandur.

Input to the proglacial zone from the glacier can encompasses several sources of meltwater and sediment, including ice melt, snow melt, and subglacial meltwater that entrain supraglacial and subglacial sediment. Glacial stream input is an important component of the proglacial suspended sediment budget (Hammer and Smith 1983; Warburton 1990; Swift *et al.* 2002; Haritashya *et al.* 2010; Orwin and Smart 2004a). Variability among the results of proglacial SSC and Q studies may depend on the characteristics of the glacier, the proglacial zone and underlying geology (Harbor and Warburton 1993; Gurnell *et al.* 1996), as well as antecedent conditions and weather and climate patterns during data collection (Richards and Moore 2003; Coburn and Lamoureux 2008; Moore *et al.* 2009). It is important to note that subglacial, supraglacial and englacial drainage networks evolve, and the timing and amount

of fluvial sediment load can gradually drift or change suddenly within a single melt season (Swift *et al.* 2002), or over multiple seasons (Swift *et al.* 2005; Haritashya *et al.* 2010). When studying proglacial suspended sediment response patterns, the evolution of these drainage networks is significant, and may explain shifts in the pattern as well as seemingly random spikes or decreases in suspended sediment load as the meltwater flow path becomes more or less efficient, and gradually or suddenly exhausts, accesses or abandons sediment sources (Hodson *et al.* 1998). The evolution of proglacial SSC and Q patterns through the ablation season has led researchers to divide data into categories of similar conditions to infer and summarize the processes, controls, and driving factors (Hodson *et al.* 1998; Richards and Moore 2003; Orwin and Smart 2004a).

Richards and Moore (2003) monitored SSC and Q during two ablation seasons at Place Creek Glacier, in the Canadian Coast Mountains and an adjacent catchment that was almost unglaciated. The aspect of the glaciated catchment was northwest with an area of 13 km^2 and 26% glaciated. Using the relatively unglaciated catchment for comparison, they divided the ablation season into four sub-seasons that reflect the Q generation processes: 1) nival; 2) nival-glacial; 3) glacial; and 4) autumn recession. They found that fine sediment was temporarily stored within the fluvial network between the proximal and distal site at low flow, and then re-entrained at higher flow and the response of the catchment to rainfall changed over the ablation season in relation to snow cover and antecedent conditions.

In Orwin and Smart (2004a), the spatial and temporal patterns of suspended sediment flux in proglacial channels of the Small River Glacier, BC, were assessed and ascribed to weather phenomenon. Their analysis, based on that of Hannah *et al.* (2000), combined principal component analysis (PCA) and cluster analysis (CA) (see *section 2.5*) as an

objective way to characterize the ‘shape’ and ‘magnitude’ of the suspended sediment time-series and divide the data into four hydro-meteorological categories: 1) hot and dry; 2) cold and wet; 3) snowmelt; and 4) storm (Orwin and Smart 2004a). Field observations were used to identify sediment sources, paraglacial sedimentation processes and temporary storage within the study site. The study design and analysis procedure for the proglacial zone of the Small River Glacier by Orwin and Smart (2004a) was emulated for this 2011 study on the Castle Creek glacier proglacial zone. As such, some additional detail about their study site and methods are included for reference; similar information for this study on the Castle Creek Glacier can be found in sections 2.1 and 2.2.

The Small River Glacier (SRG) is located in the Canadian Rocky Mountains (53°11’N, 119°30’W), *c.* 47 km east south-east of the community of McBride. The SRG is a small cirque glacier with a south-east aspect. The geology is dominated by limestone with interstratal dolomite and shale units of the Mural and Mahto Formations (Orwin and Smart 2004a). Their study area in the upper basin was 6.86 km^2 and *c.* 50% glaciated with an elevation range of 1750 to 2600 m a.s.l. (Orwin and Smart 2004a). The proglacial zone of the SRG was *c.* 2.0 km^2 with an elevation range of 1750 – 2200 m a.s.l. Average stream gradients were *c.* 15% on two parallel streams and *c.* 21% on a third meltwater stream (Orwin and Smart 2004a). Meteorological data were collected from a central proglacial monitoring station, and SSC and Q data were collected from a network of nine monitoring sites along three proglacial meltwater channels from Julian Day (JD) 288 – JD 238 (July 7 – August 26, 2000). Approximately 10 salt dilutions per site were used to establish stage–discharge rating curves, and SSC was measured in 50 – 100 water samples from each site to field-calibrate the turbidity meters.

1.7 2008 Study on Sediment Fluxes at Castle Creek Glacier

In order to gain a better understanding of suspended sediment fluxes downstream of a retreating glacier, a 34-day study was conducted in the Castle Creek proglacial zone in July and August of 2008 (Stott *et al.* 2009). The study found that SSL and Q were controlled by rainfall and snow/ice melt, sometimes independently and sometimes in concert. The results were used to estimate a 43 ± 2 t km^{-2} increase of suspended sediment yield between a proximal and distal site separated by *c.* 600 m of stream distance, and found that the distal site had more scatter in the SSC – Q relationship than the proximal site. The study highlighted the potential importance of the proglacial zone in modifying SSL and limitations of the SSC – Q relation. Importantly, the study identified that further investigation with a more detailed sampling strategy was required in order to constrain the role of hydro-meteorological conditions on suspended sediment fluxes in the proglacial zone.

In this 2011 study, key limitations identified in the 2008 study were addressed by expanding the network of proglacial monitoring sites, increasing the study length, and independently monitoring Q and SSC to allow for a more comprehensive and quantitative analysis of proglacial suspended sediment flux patterns.

2 Methods

2.1 Study Area

The Castle Creek Glacier (CCG) is an alpine valley glacier located *c.* 35 km south-southwest of the community of McBride, in the Cariboo Mountains of British Columbia, Canada (53°2'N, 120°24' W) (Figure 2.1). The snout of the glacier receded 700 m between 1959 and 2007, and *c.* 1.5 km since its Little Ice Age (LIA) maximum (Beedle *et al.* 2009). In 2005, the CCG had an area of *c.* 9.8 km^2 (Bolch *et al.* 2010). Based on 2011 imagery, the CCG had an area of *c.* 9 km^2; its length and elevation range were *c.* 6 km and 1870 to 2850 m a.s.l., respectively (Figure 2.1; also see *section 2.1.2*). The glacier flows northeast, while the aspect of the accumulation zone is north. The underlying geology is a vertical outcrop of the Windermere Supergroup, which represents a deep-ocean basin turbidite system that formed 700 million years ago (Arnott *pers. comm.* 2011). It was pushed up from the ocean floor about 100 million years ago during the formation of the Rocky Mountains. This bedrock outcrops extensively in the east north-east area of the proglacial zone, and on the west side of the proglacial zone in an area above the terminal lobe of the CCG. Additionally, there is an outcrop along the distal end of the lower till apron, which connects with the east north-east outcrop where the creek flows through a small gorge that marks the end of the immediate proglacial zone. Meltwater from the CCG flows southeast for *c.* 7 km as it leaves the proglacial zone, and then turns abruptly and flows generally northeast, draining into the upper Fraser River basin near McBride after *c.* 34 km.

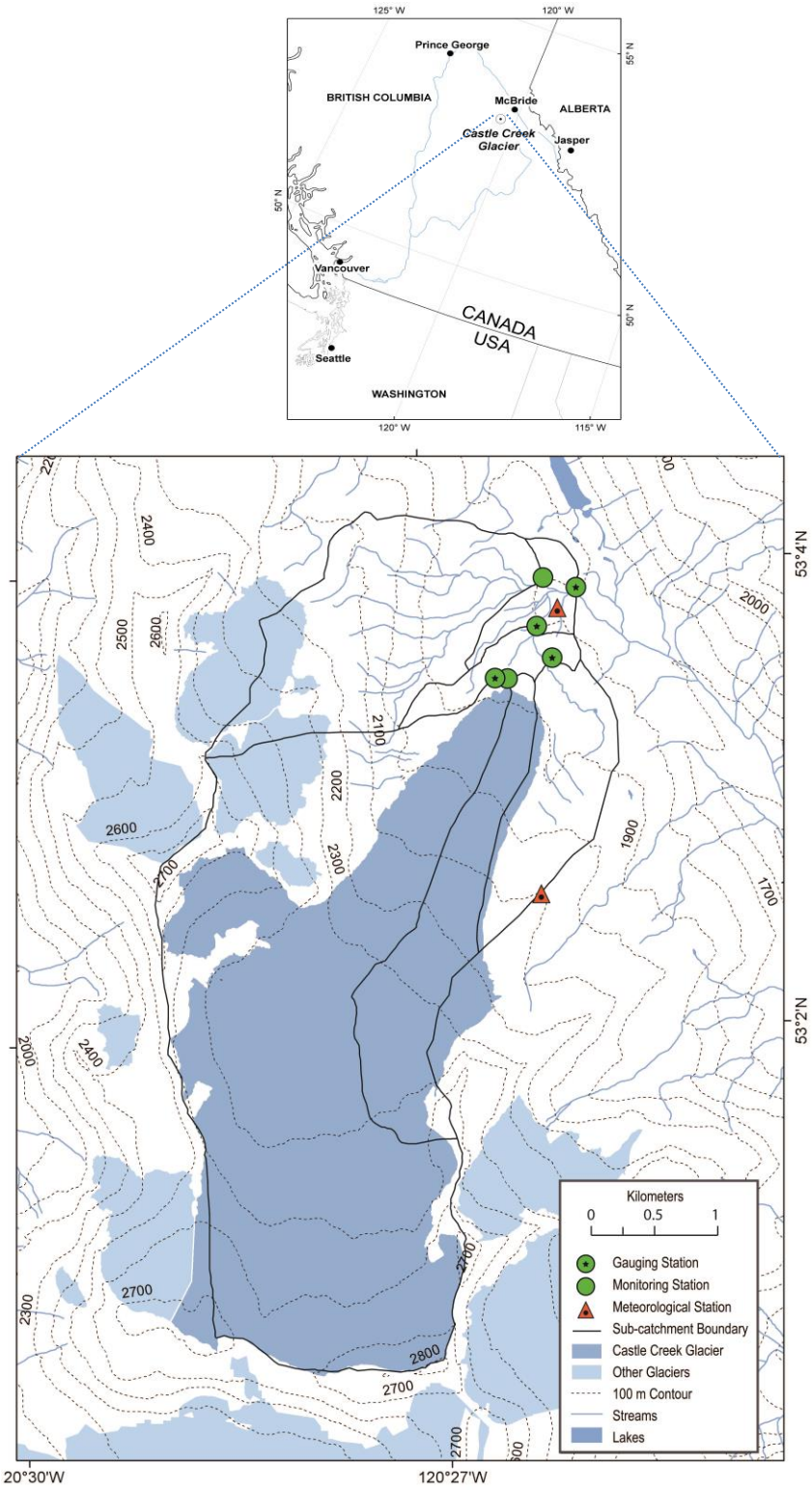

Figure 2.1 Location of Castle Creek Glacier (adapted from Beedle *et al.* 2009). Monitoring locations and sub-catchement boundaries are identified; section 2.1.1 and 2.1.2 provide explanation and methodology. Figure 2.2 includes site names and uses an air photo of the proglacial zone as the base map.

2.1.1 Field Site Observations and Site Selection

The scope of this thesis was on the meltwater channels and sediment sources in the proglacial area from the snout of the glacier *c.* 1870 m a.s.l. to the small gorge *c.* 1800 m a.s.l. The watershed area above the gorge was *c.* 16 km^2 and was *c.* 60% glaciated in 2011 (see *section 2.1.2*), stream distance was *c.* 1.2 km with an average slope of *c.* 3% (see *section 2.1.3*).

The area immediately downslope from the snout of the glacier was characterized by low relief till sheets, outwash fans, abandoned meltwater channels, and bedrock outcrops. The till deposits on the west side of the meltwater channel have been substantially eroded and modified by several abandoned meltwater channels incised to varying depths (up to 10 m) which end at abandoned outwash fans. The east side of the meltwater channel was characterized by two relatively intact till sheets separated by an outwash fan complex (Figure 2.2).

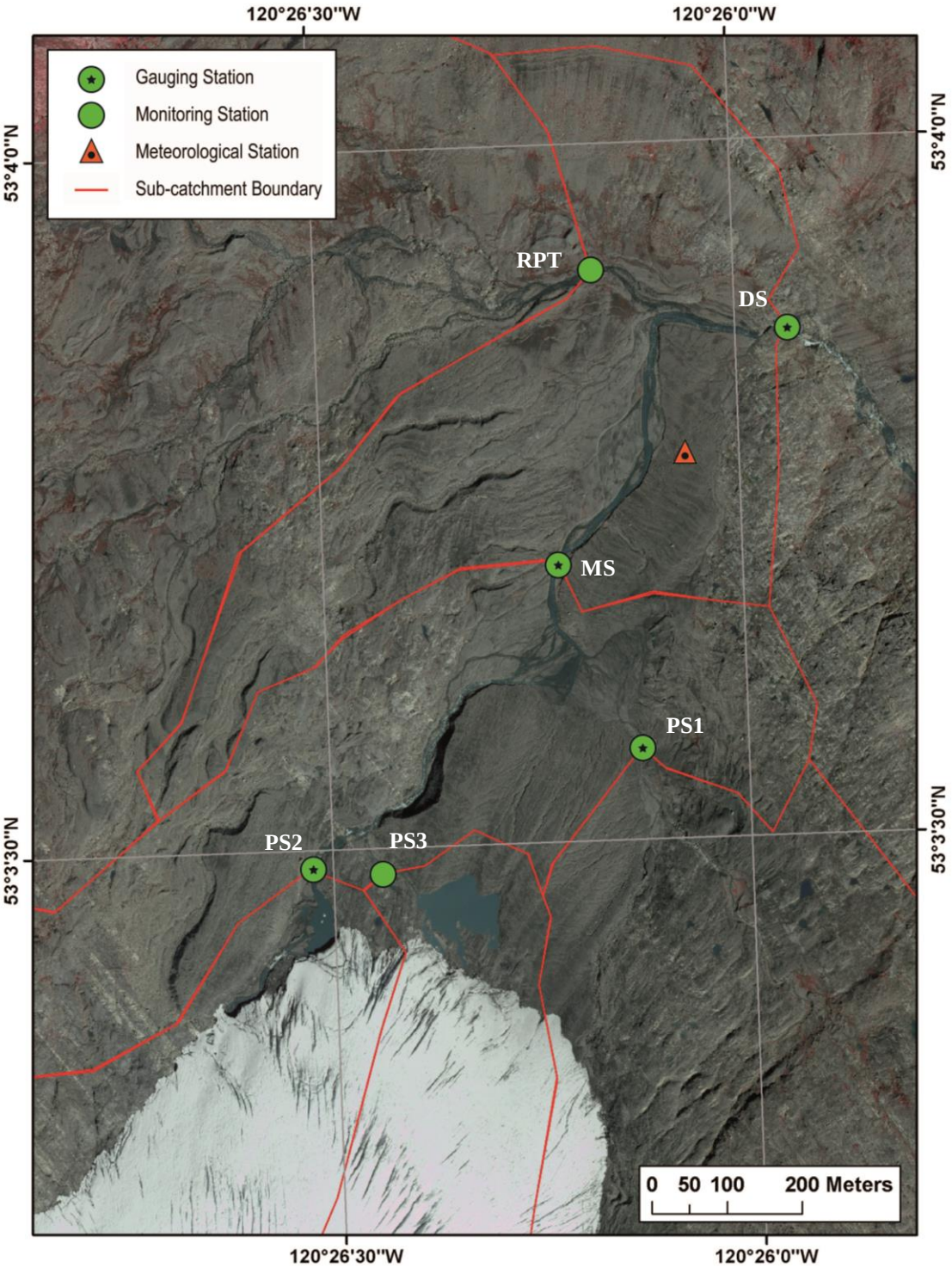

Figure 2.2 Proglacial zone of the Castle Creek Glacier with the 2011 sampling locations, sub-catchment boundaries and lower meteorological station. Turbidity and suspended sediment data were collected at monitoring stations, while water level and streamflow data were additional parameters collected at gauging stations. Site name abbreviations: Proximal Sites 1, 2, and 3 (PS1, PS2, and PS3), Middle Site (MS), Rockback Peak Tributary (RPT), Distal Site (DS).

The main meltwater stream emanated from a subglacial channel portal on the northwest side of the glacial terminus and flowed steeply to a proglacial lake on the west side of the terminus. The outflow from this proglacial lake was mostly bedrock controlled, as was the confluence with another bedrock controlled meltwater stream flowing from a proglacial lake centered at the glacial terminus. From this point, stream slope increased and the channel was bound by bedrock on the left bank and the over-steepened, slumping bank of the upper till sheet on the right bank. In this reach, fine sediment had been washed away leaving behind large cobble and boulders that armour the channel bottom and right bank. The steep single thread channel split at the top of an outwash fan. Much of the left side of the fan was abandoned and elevated from the current channels. The majority of flow was along the right side of the fan where a vertical bank (*c.* 2 m) had been cut along the base of the upper till sheet. There was a gradual decrease in slope and corresponding decrease in stream power and particle size; near the bottom of the fan the stream became braided with wide and shallow channels. A small tributary from the east side of the glacier entered at multiple points from a low gradient outwash plain as dispersed flow converged and curved west around the distal end of the outwash fan (Figure 2.2).

The cumulative meltwater from the CCG flowed generally north with the low gradient till sheet on the right bank, and a series of abandoned meltwater channels and outwash fans on the left for *c.* 400 m. A prominent moraine directs the stream sharply to the east around the distal end of the till sheet. The confluence with a tributary that drained the western side of the watershed and a small cirque glacier/rock glacier on the north aspect of Rockback Peak occurred as the new heading was achieved. From this point, the channel was

relatively straight with a gravel-cobble bed that continued generally east in a single thread to the small gorge, which marked the end of the alluvial proglacial zone, and the study area.

Six monitoring sites were established to assess the spatial and temporal pattern of suspended sediment flux in the CCG proglacial zone (Figure 2.2). Three sites proximal to the glacier monitored suspended sediment input to the proglacial channel from the glacier and the area immediately proximal to the terminus: Proximal Site 1 (PS1) sampled a small ice marginal stream draining the east side of the glacier; Proximal Site 2 (PS2) sampled the main meltwater stream downstream of a proglacial lake on the north-west site of the glacial terminus; and Proximal Site 3 (PS3) sampled a stream flowing north-west from a small proglacial lake roughly centered at the glacial terminus. The Middle Site (MS) sampled the main meltwater channel, downstream of the outwash fan. The Rockback Peak tributary (RPT), which entered the Castle Creek meltwater stream downstream of MS, was sampled *c.* 100 m from the mouth. For the Distal Site (DS), stream gauging was done upstream of the small gorge; however, to ensure complete mixing of water from the RPT with that of Castle Creek, the Tu and SSC sample point was located in the bedrock-controlled reach downstream of the small gorge. The sites PS2, MS, and DS were in approximately the same location as the three monitoring sites that were used in the 2008 study.

2.1.2 Catchment Area

The six monitoring locations were chosen to isolate sediment source and storage areas within the proglacial channel network in order to ascribe the total sediment yield to the proglacial suspended sediment variables (Warburton 1990; Equation 1). Watershed boundaries, catchment area, and glacial cover for the monitoring sites were delineated and computed using a digital elevation model and air photos (Figures 2.1 and 2.2, and Table 2.1).

Table 2.1 Catchment areas and percent glacial cover for 2011 proglacial stream sampling sites.

Site	Total Area (km^2)	Glaciated (km^2)	Un-glaciated (km^2)	% Glaciated
Castle Creek Glacier	8.96	8.96	0	100
PS1	1.24E	0.14E	1.1	11
PS2	9.36E	7.19E	2.17	77
PS3	1.73E	1.64E	0.09	95
MS	12.69	8.96	3.73	71
RPT	2.66	0.5E	2.16E	20
DS	15.68	9.46E	6.22E	60

E – Estimated area

The glacial catchment areas for the three proximal sites were estimated based on the flow lines and topography of the glacier in air photos, and field observations such as stream volume; which cause the total and glaciated area to be flagged as estimates. The cirque glacier/rock glacier in the RPT catchment was estimated based on air photos and field observations, which cause the glaciated and un-glaciated areas to be flagged as estimates for RPT. The glaciated and un-glaciated areas at DS were flagged as estimates because the estimates for RPT were included in the values; however, the effect on the percent glacial cover at DS would be negligible.

2.1.3 Longitudinal Stream Profile

A longitudinal profile of the main meltwater channel from PS2 to DS was collected to help identify sediment storage and source areas based on slope (Figure 2.3). The benchmarks used for vertical control of the water level loggers (see *section 2.3.2*) were tied-in during the longitudinal stream profile to establish relative elevation above the arbitrary datum set 100 m below the highest benchmark.

From PS2 to the confluence with PS3, the slope was a minimum of 0.5% and a maximum of 10%. Below the confluence, the slope increased to 14%, but declined to 7% by the top of the outwash fan. Four transects were surveyed down the outwash fan (OF)

upstream of MS to capture both the inactive area (elevated from the active channel) and the active area.

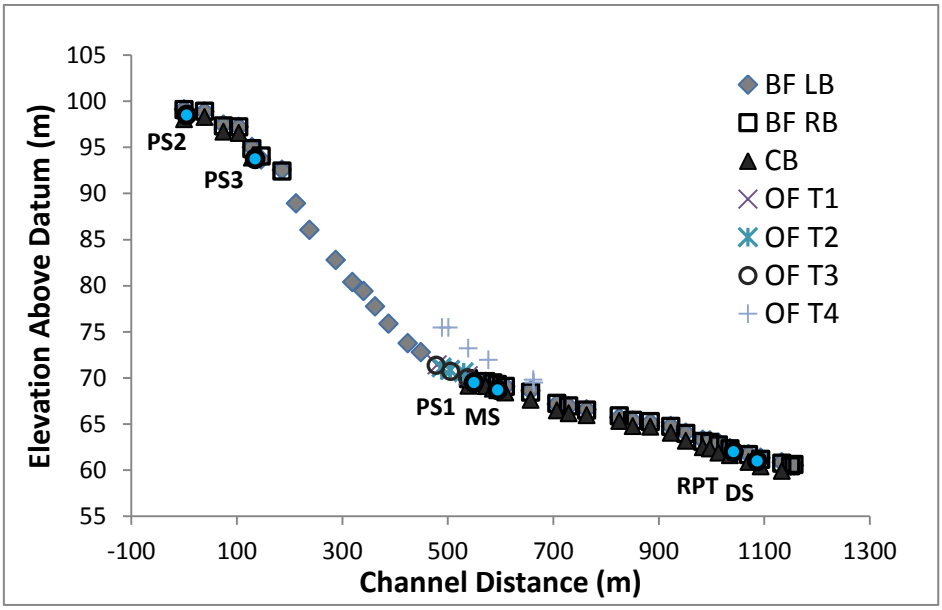

Figure 2.3 Longitudinal stream profile for Castle Creek proglacial meltwater channel. BF LB – Bankfull Left Bank, BF RB – Bankfull Right Bank, CB – Channel Bottom, OF T1 though T4 – Outwash Fan Transects 1 through 4. Datum was arbitrarily set 100 m below the highest benchmark, and zero channel distance was set as the outflow of the proglacial lake upstream of PS2.

The inactive area, OF T4, that began at an abandoned apex was characterized by larger clasts, the stream slope was 6.0% at the top, but declined to 2.5% by the bottom. The existing channel had scoured below and around the apex of OF T4 and had a slope of 7% which gradually declined to where the channel braids. The slope of the braided channels through OF T1, OF T2, and OF T3 was 2 ± 0.3%. Flow converged at the base of the outwash fan just upstream of MS. Stream slope remained gentle (1.5 ± 1.0%) for *c.* 250 m from the base of the fan, past MS, and then increased (2.5 ± 0.5%) just upstream of where RPT entered the main meltwater channel. Stream slope was relatively gentle and consistent (1.5 ±

0.3%) to DS, which was the distal site of this study and the end of the recently exposed (< 60 years) proglacial channel.

2.2 Monitoring and Sampling Strategy

Direct measures of Q and SSC are time consuming and therefore surrogates are needed to achieve a sample frequency that will capture the level of detail necessary to assess the short term variability and rapid fluctuations of these independent variables (Lawson 1995). Water level (WL) and Tu were recorded at a 5-minute interval as surrogates for Q and SSC, respectively. Discrete measures of Q and SSC were collected to develop site-specific rating relations which were then used to compute 5-minute data sets for Q and SSC. The product of these time-series is suspended sediment load (SSL):

$$\mathbf{Q\ (m^3/s)\ x\ SSC\ (mg/L)\ x\ 0.3\ (kg/5\ min) = SSL\ (kg/5\ min)} \qquad \mathbf{(2)}$$

Summary computations used SSL in kilograms per 5-minute time step. Suspended sediment load summaries were divided by catchment area to give suspended sediment yield (SSY) in units of Mass per Time per Area.

During the 2008 pilot study, the confluence of PS2 and PS3 was subglacial (Figure 2.2), and the need for an additional monitoring site was not identified prior to arriving at the field site in 2011. In light of this development, the six monitoring sites were prioritized based on flow volume, and the available equipment was distributed accordingly (Figure 2.4).

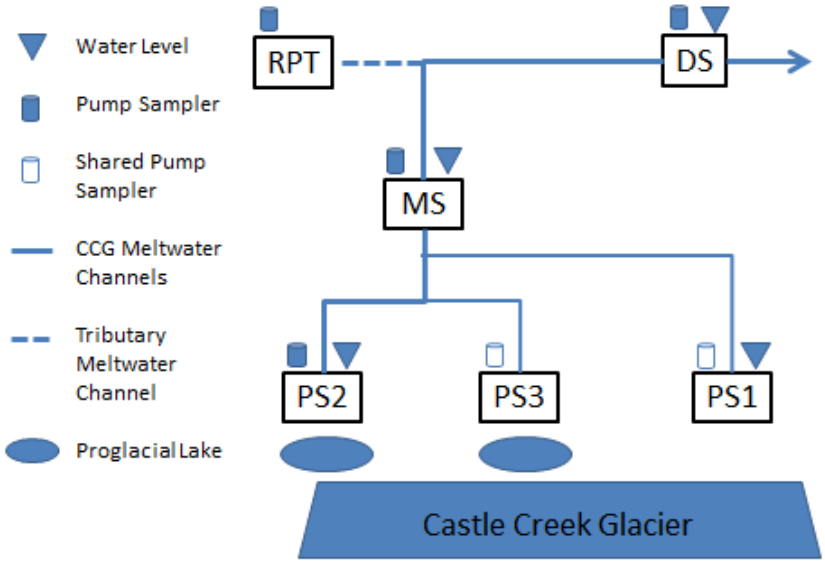

Figure 2.4 - Schematic diagram of the 2011 stream monitoring network at the Castle Creek Glacier.

It was possible to equip all six sites with Tu probes for the duration of the field season. However, only five automated pump samplers and four water level loggers were available. The three sites along the main meltwater stream (PS2, MS, and DS) and the tributary (RPT) were equipped with pump samplers. The remaining automated pump sampler was split between PS1 and PS3. After some initial samples were collected at PS1, the sampler was moved to PS3 for the remainder of the field season. Water level and stream gauging was conducted at PS1, PS2, MS, and DS; the Q record for RPT and PS3 was deduced (see *section 2.4.2).*

2.3 Instrumentation and Data Collection

2.3.1 Meteorological Data

The meteorological conditions of a given region drive the hydrology of that region, which includes the accumulation and ablation of glacial ice. Over the ablation season, proglacial Q can be dominated by snowmelt, ice melt, or precipitation to varying degrees in response to meteorological conditions. Dr. S.J. Déry and his research group have been collecting precipitation, air temperature, total solar radiation, wind speed and barometric pressure data (among other variables) at two sites in the study area (Figure 2.1): 1) in the proglacial zone at *c.* 1815 m a.s.l.; and 2) on a ridge adjacent to the terminal lobe at *c.* 2105 m a.s.l. These meteorological data were imperative to the analysis and interpretation of the fluvial and geomorphological data collected by this study.

The tipping bucket rain gauge at the upper CCG meteorological station was damaged during the onset of a storm event on Julian Day (JD) 234, and data for this event and the remainder of the field season were not collected from this site. Unfortunately, the lower meteorological station was not equipped with a precipitation gauge in 2011. Daily precipitation records from three nearby meteorological stations (Cariboo Lodge near Valemount, Environment Canada ID No. 117393; Crescent Spur, Environment Canada ID No. 1092120; and McBride (upper) snow pillow, BC Ministry of Environment ID No. 1A02P) were collected, weighted by proximity to Castle Creek, and used to estimate the precipitation record following JD 234. Fortunately, this period was dominated by high pressure systems (JD 247 – JD 254), and it was only necessary to estimate precipitation for three days: the storm event on JD 234 (31 mm) that damaged the upper CCG rain gauge, and moderate precipitation on JD 241 (8 mm) and JD 244 (7 mm).

Barometric pressure was collected at both meteorological stations and was needed to isolate water level from the absolute pressure record collected by the submersible pressure transducers (*section 2.3.2*). The lower station was closer in elevation and proximity to stream monitoring sites, and was therefore more representative. Unfortunately, data from this station were prone to erroneous spikes and using the data directly would have propagated these errors to the water level records. Corrections to the barometric pressure record (see *section 2.4.*1 and Appendix 7.1) were made prior to the computation of water level (Equation 3, *section 2.3.2*).

2.3.2 Water Level and Streamflow

Water level (WL) data loggers were fixed vertically in stilling wells using stainless steel bolts and nylon coated aircraft cable. A metric gauge plate was fixed to the stilling well and the assembly was fastened with hosed clamps to rebar driven into the streambed at the sample location. Specific sites for stilling wells were chosen with a suitable downstream control to provide a stable relationship between WL and Q. During site visits, WL was recorded from the gauge plate on the outside of the stilling wells at the beginning and end of Q measurement. Measurement cross sections were selected for having a single channel and relatively straight velocity vectors at the range of WL suitable for wading, but were not necessarily adjacent to the stilling well.

Wireless Hobo U20 pressure transducers (Onset Computer Corporation, Bourne, MA, USA) were used to record WL at the four gauging sites: PS1, PS2, MS, and DS. The data loggers at PS2, MS and DS had a 9 m range with a 0.002 m resolution (± 0.005 m), the logger at PS1 had a 4 m range with a 0.001 m resolution (± 0.003 m) (Onset 2013). The Hobo U20 data loggers record absolute pressure and need to have local (within 2 km)

barometric pressure removed to isolate water pressure, which is proportional to water level (Equation 3):

Abs. Pres. (kPa) – Baro. Pres. (kPa) = Water Pres. (kPa) ∝ Water Level (m) **(3)**

This initial computation was performed within the Hoboware Pro software (Onset Computer Corporation, Bourne, MA, USA); the WL time-series were exported as comma separated files for processing and Q computations (*section 2.4*).

Streamflow (Q) measurements were collected using a Swoffer 2100 impeller type current meter on a top-set wading rod (Swoffer Instruments, Inc., Seattle, WA, USA). Following the mid-section method described in the Resource Inventory Standards Committee Hydrometric Manual (RISC 2009), Q measurements take 30 to 40 minutes and ± 5 – 15% error can be expected, varying with flow conditions (Navratil *et al.* 2011). During the field season, 10 Q measurements were made at DS, eight at MS, eight at PS2, and four at PS1; targeting the wadeable range of streamflow for each site. The near continuous WL records were converted to Q in units of volume per time using rating curves that were established for each site using discrete rating points (see *section 2.4.2*, and Appendix 7.1).

A key component of WL monitoring is establishing and maintaining vertical control so that the WL record can be corrected in the event that the vertical reference point changes during the monitoring period (i.e. the pressure transducer moves) (RISC 2009). The stilling wells were surveyed-in to local benchmarks (painted points on boulders) at the beginning of

the season. Ideally, WL would have been measured from these benchmarks during each field visit to ensure the reference point had not changed; however, given time constraints and the amount of field equipment that was being transported between sites, such a task was unrealistic. The stilling wells were re-surveyed at the end of the field season, and when there was an event that obviously affected the vertical reference point.

2.3.3 Turbidity and Suspended Sediment Concentration

Past researchers have found that suspended sediment in proglacial streams tends to be well mixed, as long as consideration is given to site-specific hydraulics (such as backwater or recirculating eddies) and to avoid the influence of upstream tributaries (Gurnell *et al.* 1992; Richards and Moore 2003). A USGS DH-48 was used to ensure that SSC and Tu sample locations were representative within the stream cross-section. Once the sites were selected, rebar was driven into the stream bed and 30 mm pipe was fastened over the rebar. For sites with a stilling well, the second rebar was driven into the stream bed in a suitable, but slightly different location.

At each monitoring station, the Tu probe and intake hose for SSC samples were mounted together on a floating apparatus attached to a piece of larger pipe (40 mm) that used the smaller (30 mm) pipe over the rebar as a slide guide (Appendix 7.2). Hoses and wires were suspended under tension from the top of the rebar to pump samplers and Tu data loggers located a “safe” distance up the channel bank. Each site was powered by a 12 V deep-cycle battery charged by a 10 W solar panel. As water level changes, the proportional depth of the sample point changes, which can lead to uncertainty in the procedure (Navratil *et al.* 2011). The floating apparatus kept the intake hose and Tu probe at a set depth from the water surface; ideally, above the streambed and the effect of coarser sediment transported in

saltation. As water level increases, the proportional depth from the surface of the sample point within the water column decreases, which was acceptable since suspended sediment (typically < 2 mm) and wash load (< 0.063 mm) tend to be well mixed within the water column.

Each of the six sites was equipped with a Hobo U12-008 data logger (Onset Computer Corporation, Bourne, MA, USA) programmed to record DC voltage output from an Analite 195 Turbidity (Tu) probe at a 5-minute interval. The Analite 195 turbidity probes (McVan Instruments, Scoresby, Australia) use 90° optics and employ infrared light in accordance with ISO7027 to measure Nephelometric Turbidity Units (NTU). The range of the Analite 195 is 0 – 400 NTU, which equates to 0 – 4 V output, and linearity is 1% in the 0 – 1 V range (McVan 2003). The record from the Analite 195 Tu probes was limited by the range of the Hobo U12 data loggers, which is 0 – 2.5 V with an accuracy of ± 2 mV or ± 2.5% of absolute reading (Onset 2013). Since SSC was the target variable, converting the Tu record from V to NTU was not necessary.

Automatic water samplers (ISCO 6700 Teledyne Technologies, Inc., Lincoln, NB, USA) were deployed to collect physical water samples to measure SSC. The sample interval and strategy varied from discrete 800 mL samples every 2, 3, 4, and 6 hours, to 800 mL daily composites of a 100 mL intake every 3 hours. The sample frequency was dependent on the capacity of the field team, and scaled back to daily composite samples once enough (100 – 150) discrete samples were collected to establish a Tu–SSC relationship for each site. Site specific relationships were developed for each of the Tu probes from measured SSC in water samples. These site- and Tu probe-specific relations were then used to calculate a near continuous record of SSC from the near continuous record of Tu (*section 2.4.3*). The daily

composite samples collected from JD 218 – JD 254 were used as a check and backup data set for the calculated SSC record.

Water samples were measured with a graduated cylinder (to determine volume) and vacuum-filtered in the field through pre-dried and pre-weighed Whatman ashless 8 µm filter papers, labelled, and stored. Upon returning to the UNBC Landscape Ecology Laboratory, the samples were unpacked, dried for 24 hours at 105 °C, re-weighed, and SSC was calculated as a mass per volume (Equation 4):

(Dry sediment and filter (mg) – Dry filter (mg)) / Sample volume (L) = SSC (mg/L) **(4)**

The error associated with this gravimetric method has been estimated at *c.* 4%, but was likely higher in this study since samples were not dried in the field (Gurnell *et al.* 1992; Orwin and Smart 2004a). Past researchers have found that there is little (*c.* 4%) to no statistical difference between 8 µm filter papers and 4 µm filter papers because the effective pore size is rapidly reduced as sediment clogs the 8 µm filters (Gurnell *et al.* 1992; Hodgkins *et al.* 2003; Orwin and Smart 2004a). Furthermore, during the 2008 study at Castle Creek it was determined that the use of 8 µm filters underestimated the total flux of sediment in the range 63 to 0.45 µm by about 7% (Stott *et al.* 2009).

2.4 Data Processing and Computations

After reviewing the time-series data, it was identified that JD 195 – JD 254 (July 14 – September 11, 2011) had the most consistent data coverage, and all data sets were trimmed to

this 60 day period prior to computations and analysis (Julian Day calendar included in Appendix 7.5).

Time-series quality assurance and quality control (QA/QC), rating curve development, computations and summaries were done using the Aquarius Whiteboard Time-Series Software (Aquatic Informatics, Inc., Vancouver, BC, Canada). Data summaries were exported from Aquarius as comma separated files for statistical analyses (see *section 2.5*) in Microsoft Office Excel and IBM SPSS Statistics 20.0 (IBM Corporation, Armonk, NY, USA).

2.4.1 Time-series QA/QC

The raw time-series data sets were reviewed and erroneous data were corrected or deleted and filled using Aquarius Whiteboard. In some cases the erroneous data were left in as the best possible information. The following paragraphs describe the quality assurance and quality control (QA/QC) review and revision of raw time-series data.

The 5-minute barometric data from the lower meteorological station contained several erroneous spikes (Appendix 7.1), which were removed using an upper rate of change threshold of 1 mbar per 1 hour (Déry *pers. comm.* 2011). Missing data were linearly interpolated and then averaged with the record from the upper meteorological station. The validity of the corrected file was confirmed with Dr. SJ Déry and used to compute raw WL records from the absolute pressure recorded by the four Hobo pressure transducers.

In the 5-minute interval WL data, 28 cases of partial ice-damming in the vicinity of PS2 were recorded. During these events, ice calving into the proglacial pool became grounded in the outflow channel and was slowly moved downstream by the force of the

water as bed deformation and gradual melting allowed. Stott and Grove (2001) report similar observations in data from the Skeldal River, Greenland. In the WL data, these events appeared as a sudden increase that was not apparent at other sites, followed by a period of stability and then a sudden drop or gradual decline back to the extrapolation of the time-series before the sudden increase. These events typically lasted several hours, but less than a complete diurnal cycle and predominantly (68%) occurred on the falling limb of the diurnal hydrograph. Some ice calving events were apparent at PS2 and MS as a surge of water from ice dropping into the proglacial pool passed though the proglacial channel, but these were not apparent at DS. In two instances, PS2 remained stable after a sudden increase; this was interpreted as ice impact and offset corrections were applied to the data following the events. On JD 233, following a severe ice impact and wave that knocked over the ISCO water sampler, site PS2 was moved 50 m downstream to a location that was less susceptible to ice impact, ice-damming and waves from calving ice. The record from the original site was matched with the record from the new site using benchmarks to maintain vertical control.

In the Tu data, sudden changes in the records following field visits when the lens was cleaned were minimal, indicating that drift due to bio-fouling was negligible. There were occasional spikes or troughs in the data that could have been erroneous. However, since SSC can change drastically in a short period of time, corrections were only applied for obvious errors or if justified by field notes, and all other data were left in the time-series. The range of the Tu meter was exceeded at PS1, PS3, RPT and DS. These data were left in the time-series for the analysis as the best available information. The duration, character, effect and resolve of Tu exceedances will be elaborated upon in the computational, analysis and discussion sections that follow (see *sections 3.1.3 and 4.1*).

Once the preliminary QA/QC was completed, a 7-point moving average was used to smooth the WL and Tu time-series data, keeping the sample interval at 5-minutes. Discrete measurements of Q and SSC were then paired with WL and Tu values from the smoothed time-series data. These paired values were used to develop WL – Q rating curves (*section 2.4.2*) and Tu – SSC regressions (*section 2.4.3*). In various stages of the analysis, 5-minute data, hourly data, and daily data with respective standard statistics (min, max, mean, total, standard deviation, standardized z-score) were used or used as inputs for further statistical analysis (*section 2.5*).

2.4.2 Water Level and Streamflow Rating Curves

At each gauging site, the discrete Q measurements were paired with the mean WL during the measurement to give a rating point for the development of a rating curve, which was then used to compute a Q time-series from the 5-minute interval WL time-series. Rating curves were developed in accordance with the Water Survey of Canada Hydrometric Manual (WSC 2012). Two rating points were not included in the development of the rating curve for DS because they fell outside of the acceptable range (± 5%) of the data from the curve, and lacked sufficient justification to 'shift' the rating curve (WSC 2012). All other rating points were acceptable. The rating curves used to compute the Q time-series for each gauging site are presented in Appendix 7.1. The dynamic nature of the proglacial stream means that the channel profile and control for each site will be prone to frequent 'shifts' or changes in the relation between Q and WL; as such, the rating curves developed for the 2011 season are not valid for subsequent seasons.

Since high-flow measurements are difficult to obtain because of safety concerns and because high-flow events are typically of a short duration, it is common to extrapolate the

rating curve based on the available data (WSC 2012). According to WSC (2012), rating curve extensions are considered "valid" up to twice the maximum gauged streamflow, and an "estimate" for flow that is greater than that value. Sites along the main meltwater channel of Castle Creek (PS2, MS, and DS) were unsafe to wade when streamflow was greater than *c.* 5 m^3/s. In accordance with WSC (2012), rating curves were developed based on the available data and then extended linearly in log-log space. Based on WSC (2012), the Castle Creek rating curve extensions were considered "valid" up to *c.* 10 m^3/s and an "estimate" for flow > 10 m^3/s.

Field observations of channel geometry, stream slope, high water marks, and water velocity estimates from high-flow events were used as a check during rating curve development. Channel geometry included breakpoints within the channel and bankfull as determined by cross-sectional surveys at lower flow. Stream slope was calculated from the longitudinal profile (see *section 2.1.3*). Flagging tape on rocks was used to identify the high water marks, and velocity was estimated by visually tracking and timing floating debris during high flow.

Two of the streams (RPT and PS3) were not gauged because additional equipment was not available. The Q time-series for RPT was calculated as:

$$\mathbf{RPT\ Q = DS\ Q - MS\ Q} \qquad \mathbf{(5)}$$

Similarly, the Q time-series for PS3 was calculated as:

$$\mathbf{PS3\ Q = MS\ Q - (PS2\ Q + PS1\ Q)} \qquad \mathbf{(6)}$$

This method lumps all inflow or outflow between the gauging locations onto one parameter; the stream being deduced. It strictly assumes that there were no other tributary or ephemeral channel inputs, and does not account for hyporehic zone or groundwater interactions. Based on field observations, this assumption was mostly valid with the exception of storm events that resulted in contribution from the ephemeral channel network, direct contributions and/or overland flow. Since the stream bed was predominantly deformable sediment, some interaction with the hyporehic zone can be expected, which would have varied with flow conditions through the season. However, hyporehic and groundwater interactions were not quantified.

2.4.3 Turbidity and Suspended Sediment Concentration Regression

For this study, the target parameter was SSC, and Tu probes were field calibrated to site-specific conditions using discrete SSC samples to develop regression equations. Automated water samplers were programmed to collect discrete time based (*see section 2.3.3*) water samples for SSC analysis. The SSC samples were paired with corresponding Tu readings for each site, and the fourth-spread (or quartile) method (Jacobs and Dinman 2013) was used to quantitatively exclude outliers from the data set before developing site-specific Tu–SSC relations. The method assumes that the data were normally distributed and drawn from a representative population. For each site, the ratio of SSC/Tu was ranked, and the

difference between the 75th percentile rank and the 25th percentile rank was the "fourth-spread". The median (50th percentile rank) plus and minus 1.5 of the "fourth-spread" was used to define the upper and lower limits, respectively, for the data set. The ranked data that fell outside of these limits were considered to be outliers, and excluded from further analysis. A probability plot correlation coefficient (PPCC) was computed for each site and the critical value (CV) at the 5% significance level was obtained from a PPCC CV table (Filliben and Devaney 2013) for the given sample size. When the PPCC is greater than the CV, the null hypothesis that *the data came from a population with a normal distribution* cannot be rejected (Filliben 1975; Filliben and Devaney 2013). Summary tables of the fourth-spread method, normal probability plots and Tu–SSC regression plots can be found in Appendix 7.2.

Once the outliers were removed, the remaining data were used to develop regression equations (Table 2.2) to compute SSC from the 5-minute interval Tu record.

Table 2.2 Turbidity (Tu) – suspended sediment concentration (SSC) regression equations for the 2011 proglacial monitoring sites.

	Equation	95% C.I.	R^2 value	Sample N
PS1	SSC = 304.6 * Tu – 54.2	57.6	0.43	18
PS2	SSC = 252.5 * Tu + 8.6	2.8	0.79	156
PS3	SSC = 184.0 * Tu – 28.0	9.1	0.85	81
MS	SSC = 213.8 * Tu + 8.1	3.6	0.67	176
RPT	SSC = 468.9 * Tu – 106.8	20.5	0.76	175
DS	SSC = 413.0 * Tu – 23.3	5.4	0.77	169

The difference in the equations was attributed to site-specific conditions, sediment source characteristics and the individual characteristics of the turbidity probes (Navratil *et al.* 2011; *section 1.5.2* and *section 2.3.3*). The 95% confidence intervals for the regressions show that there is greater uncertainty with PS1, PS3 and RPT. As is evident from the equations, estimated SSC could be negative in low turbidity conditions (Table 2.2). Partial days of

negative value data occurred at PS1 and PS3 during low flow. These data were removed from the analysis, and the resulting data gaps were not filled. Missing data due to low flow was considered acceptable as sediment is predominantly transported by high flow (Pickup 1988).

2.5 Statistical Data Analysis

During the ablation season, glacially influenced hydrologic data have a diurnal pattern in response to daily temperature cycles. Warm midday temperatures cause increased snow and ice melt, which slows as temperatures cool overnight. When analysing daily data, dividing days at midnight tends to include part of the falling limb of the diurnal hydrograph from the previous day with the next day, which can influence the analysis of daily data (Orwin and Smart 2004). To mitigate this problem, the approximate time of minimum daily flow was used to divide the data into hydrologic days. This time was specific to this study and would change depending on proximity of the study site to the glacier and characteristics of the watershed. Based on the observation of peaks in the hydrograph, the transit time from the proximal site to the distal site in the Castle Creek proglacial study catchment was *c.* 20 minutes. The daily minimum flow occurred between 06:00 and 09:00, and 06:00 was chosen to divide the time-series data sets into hydrologic days for the analysis.

The statistical analysis of this proglacial hydrologic and suspended sediment data follows the analysis of a similar data set by Orwin and Smart (2004a), which is based on an objective proglacial hydrograph classification technique developed by Hannah *et al.* (2000). The analysis uses two multivariate statistical techniques – principal component analysis (PCA) and cluster analysis (CA) – to reduce large time-series data sets into categories of similar data while maintaining as much of the underlying structure of the data as possible.

Hannah *et al*. (2000) use the analysis to categorize hydrologic days based on the ‘shape’ and ‘magnitude’ of the hydrograph; a method reapplied successfully by Swift *et al.* (2005). Hannah *et al.* (2000) state that the analysis is applicable to any time-series data with an underlying cyclic structure, and Orwin and Smart (2004a) expanded the analysis to included proglacial suspended sediment data, which tends to have a diurnal structure similar to proglacial streamflow data. Through the analysis they were able to infer controls on the pattern of proglacial suspended sediment flux at the Small River Glacier (SRG) using four separate classification procedures (Figure 2.5).

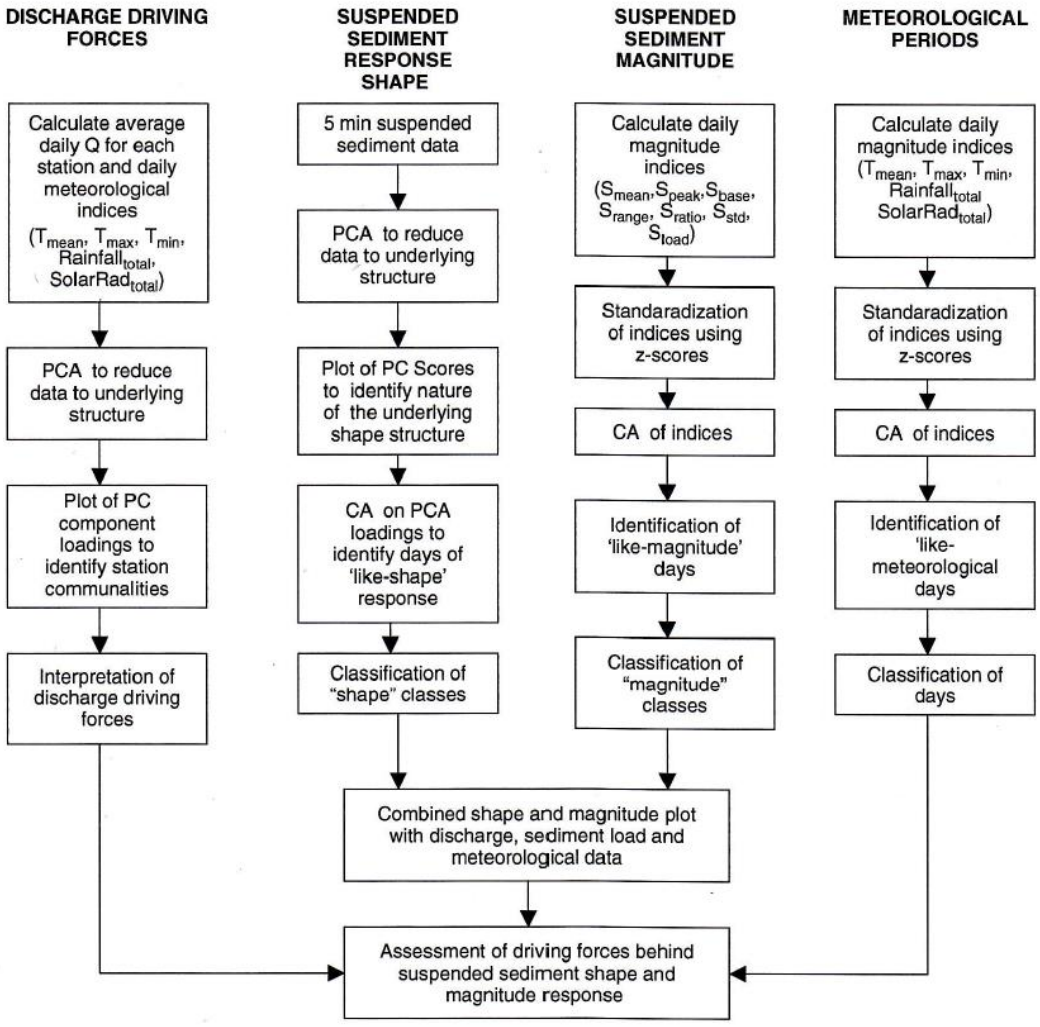

Figure 2.5 Flow chart detailing the classification procedure used to extract suspended sediment transfer patterns (source: Orwin and Smart 2004a, pg. 1527)

The meteorological, Q, and SSC data were categorized using a combination of PCA, CA, and interpretation of data matrixes where "cases" refer to rows of data categories down the y-axis and "variables" refer to columns of data categories across the x-axis (Orwin and Smart 2004a). Mathematically, the data matrix for this PCA must have more rows (cases) than columns (variables) (Hannah *et al.* 2000). The next sections describe the statistical analyses procedures that were performed on the Castle Creek proglacial data set for this

project; the analysis protocol of Orwin and Smart (2004a; Figure 2.5) was followed in order to generate comparable results. The PCA and CA analyses were run in IBM SPSS version 20.0.

2.5.1 Meteorological Periods

A CA was run on meteorological data to group the daily data into categories of similar conditions. The CA of meteorological data included cases of daily values for the variables: mean, maximum, and minimum air temperature; total precipitation; mean relative humidity; total solar radiation; and mean wind speed. The data were standardized (z-scored) and the CA was run using Ward's Method (Tabachnick and Fidell 1989). An agglomeration dendrogram was plotted and used to determine the number of meaningful clusters within the data. The raw data within each cluster were reviewed, and descriptive titles (i.e. 'hot and dry', 'warm and damp', 'cold and wet' or 'storm') were assigned, which were broadly similar to those assigned by Orwin and Smart (2004).

2.5.2 Streamflow Driving Factor

To determine the main driving forces of streamflow (i.e. from glacial meltwater or precipitation), the input matrix for PCA had daily average Q for each site, total precipitation, and solar radiation, average wind speed, and air temperature minimum, maximum and mean as variables, and hydrologic days as cases. The PCA was run using a VARIMAX orthogonal rotation with standard retention criteria. Low communality variables were removed from the analysis and the PCA was re-run on the remaining variables. The Kaiser-Mayer-Olkin measure of sampling adequacy (Tabachnick and Fidell 1989) was used to assess the correlation matrix and suitability of the data set for PCA. Parallel analysis was used to identify the statistically significant eigenvalue for the data (O'Connor 2000). Components

with significant eigenvalues were retained and used to assess the driving factors of streamflow and the proportion of variance in the data explained by each component. A bi-plot of the two dominant components was generated to assess the driving factors of streamflow and descriptive titles (i.e. ‘ablation’ or ‘rainfall’) were assigned after assessing the data explained by the component.

2.5.3 Suspended Sediment Response Shape

To assess the underlying suspended sediment response shape, an independent PCA was run on a data matrix with hydrologic days as variables and a 5-minute time step as cases for SSC data at each site. The PCA was run using a VARIMAX orthogonal rotation with standard retention criteria. Parallel analysis was used to identify the statistically significant eigenvalue for the data (O’Connor 2000). For each site, a scree plot was generated to confirm the break point in the principal components, and that the components with eigenvalues > 1 were retained. Principal component loading scores were plotted against time to reveal the underlying shape of the 5-minute SSC data for each site.

Days with similar suspended sediment response shape were identified by running a hierarchical CA on the principal component loading scores using Ward’s Method. Observations were standardized (z-scored) to remove major variations in SSC magnitude. Low communality variables were removed and an agglomeration dendrogram was plotted to visually identify the number of clusters. The shape structure of the raw data in the clusters was examined and appropriate titles (i.e. ‘diurnal’ or ‘irregular’) were assigned.

2.5.4 Suspended Sediment Response Magnitude

The magnitude classification of daily suspended sediment response shape was determined by running a CA on a data matrix with daily SSC mean, minimum, maximum, range, standard deviation (in mg/L) and daily total SSL (in kg/day) as variables, with hydrologic days as cases for each site. Data were standardized (z-scored) prior to running the CA using Ward's Method, and an agglomeration dendrogram was plotted to visually identify the number of clusters. The magnitude structure of the raw data in the clusters was examined and appropriate titles (i.e. 'low', 'medium' or 'high') were assigned.

3 Results and Discussion (1) - Spatial and Temporal Patterns of Suspended Sediment

In this chapter, objective 1 is addressed by examining the spatial and temporal patterns of suspended sediment flux in response to hydro-meteorological conditions in the proglacial zone. Principal component analysis (PCA) and cluster analysis (CA) are used to categorize and summarize the 5-minute time-series SSC and Q data while maintaining as much of the underlying structure and response pattern as possible.

3.1 Data Sets

The 5-minute time-series data for streamflow (Q) and suspended sediment concentration (SSC) are presented in Figure 3.1, and air temperature (AT) and precipitation (PT) are presented in Figure 3.2; these figures will be a useful reference for the field season summary in *section 3.3.* The Aquarius software that was used to produce the figures does not use Julian Days; refer to Appendix 7.5 for a JD calendar.

PS1 - Q and SSC 5min Data

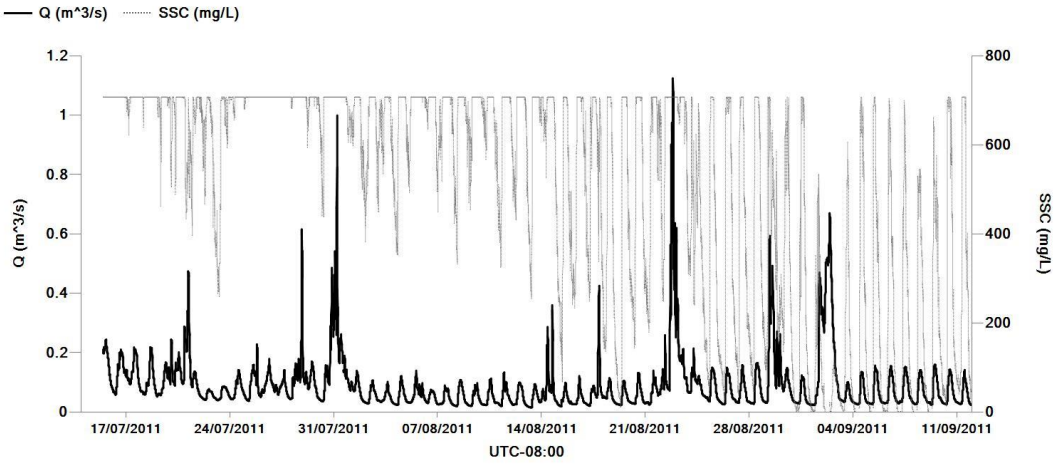

PS2 - Q and SSC 5 min Data

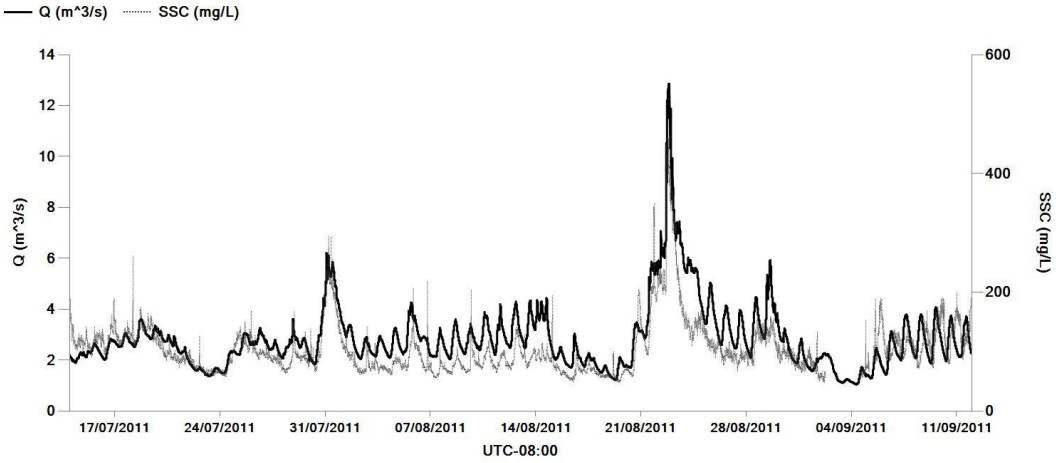

PS3 - Q and SSC 5 min Data

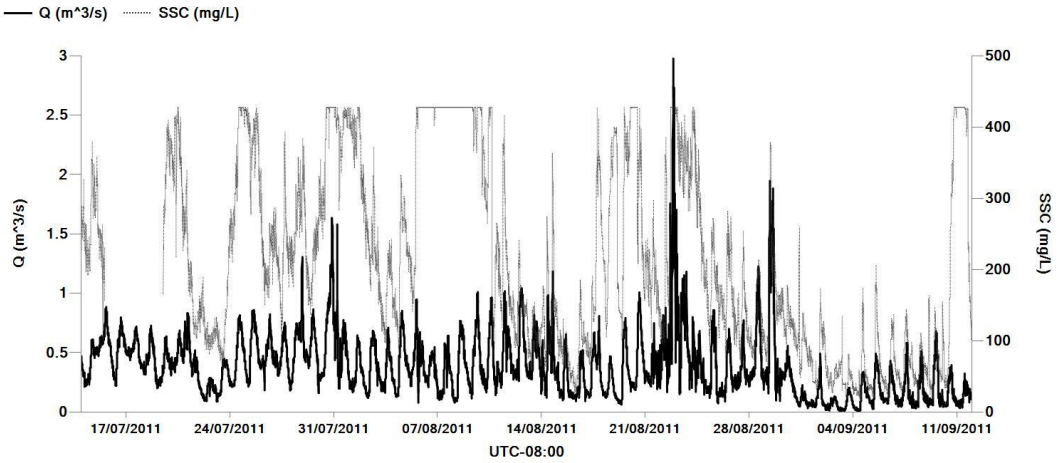

MS - Q and SSC 5 min Data

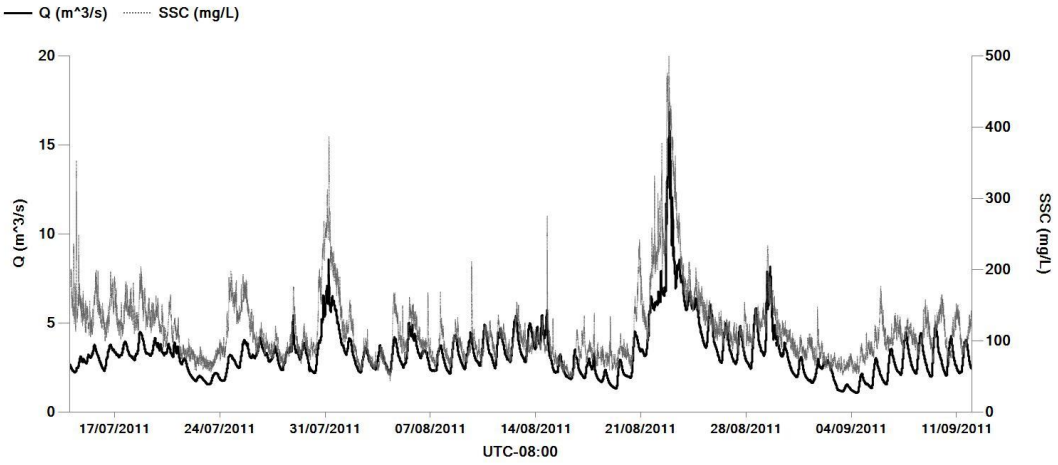

RPT - Q and SSC 5 min Data

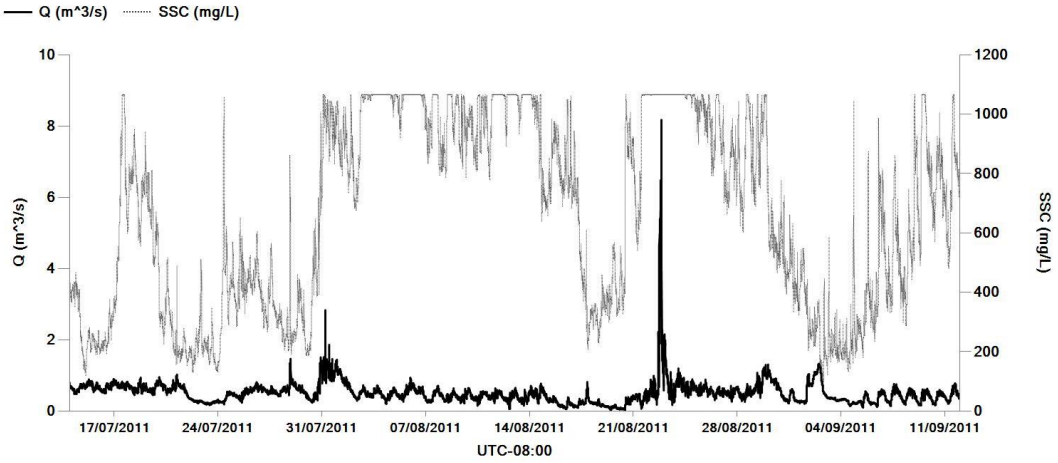

DS - Q and SSC 5min Data

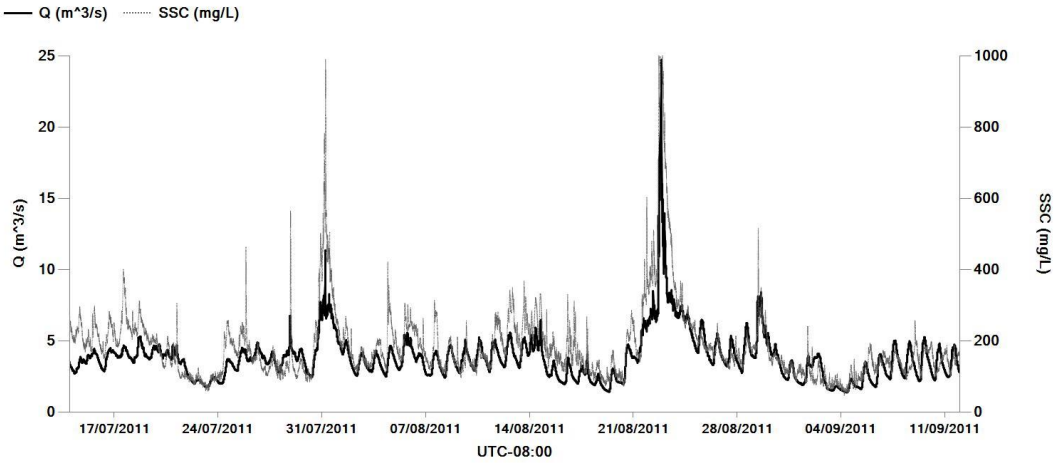

Figure 3.1 Streamflow (Q) and suspended sediment concentration (SSC) time-series (5-minute data interval) from six proglacial monitoring sites, JD 195 – JD 254, 2011 after QA/QC. Scale of y-axis varies according to range of data. Figure presented over two preceding pages. Exceedances in the SSC time-series are described in *section 3.1.3*.

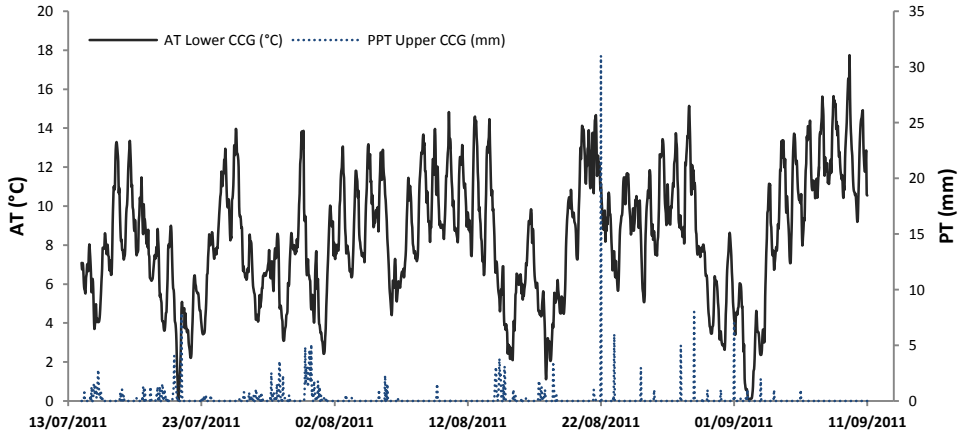

Figure 3.2 Hourly air temperature (AT, °C) from Lower Castle Creek Glacier meteorological station; hourly precipitation (PT, mm) from Upper Castle Creek Glacier meteorological station, estimated daily total precipitation after August 21, 2011.

3.1.1 Field Season Overview

The 2011 field season at CCG captured a mixture of conditions that generated a complex hydrologic and geomorphic response pattern. The following general overview uses category names that are described and summarized in detail subsequently (*sections 3.2* and *3.3*). The first third of the field season, JD 195 – JD 214, switched between 'cold and wet' and 'hot and dry' conditions every few days, transitioning through 'warm and damp' conditions in the process and included a 'storm' event on JD 211 which delivered *c.* 30 mm of precipitation over 24 hours. Discharge and SSC responded to this event at all sites.

Following JD 214, there was a period of 'hot and dry' conditions where Q and SSC data followed a diurnal pattern at most of the sites. During this time, SSC data at PS3

exceeded the range of the Tu meter. These data were likely erroneous as a result of influence from the stream bed since the effect of a high SSC input was not discernable at downstream monitoring locations and the SSC at the other sites was consistent with low-flow conditions. 'Cold and wet' conditions returned on JD 226 for four days, generating a small 'irregular' increase in Q and SSC data at most sites which was followed by low Q and SSC.

The SSC exceedances from JD 215 – JD 225 at RPT may have been the result of low water allowing the sample point to be influenced by material being transported in saltation near the stream bed. Unfortunately, the field team was not on site during this period. On JD 227 the field team returned, and found the RPT sample point close to the stream bed, sustained Tu range exceedances recorded by the logger, and a high amount of sediment in the water samples; the sample location was moved to a deeper location on JD 228. However, on JD 227, the water level was lower than it had been in the time the field team was absent and the Tu was within the range of the sensor, thus, the data from JD 215 – JD225 was accepted and computed as exceedances, rather than removed as erroneous.

Warm weather arrived on JD 231 which was followed by a 'storm event' on JD 234. The warm weather that preceded the event caused meltwater Q to be high; *c.* 6 m^3/s at DS over the 24 hour period before the storm began. The tipping bucket rain gauge was damaged during the onset of the storm; however, an estimated 31 mm of precipitation (see *section 2.3.1*) was delivered by four intense squalls over a six hour period, starting at 16:00 on JD 234. This storm event caused the highest Q and SSC during the field season at all sites. Peak flows at DS were estimated at *c.* 24.7 m^3/s at 21:45 PST and SSC exceeded the range of the Tu meter for nearly three hours at the peak of the event. Five grab samples were collected over a 2.25 hour period (19:30 – 21:45) as the event peaked. Two were collected from

ephemeral channels that drained directly into Castle Creek, one upstream of RPT, and one downstream of RPT; they were measured at *c.* 3600 mg/L and *c.* 2000 mg/L respectively. The grab sample from RPT was measured at *c.* 4200 mg/L; and the main flow of Castle Creek upstream and downstream of RPT was measured at *c.* 1300 mg/L and *c.* 2700 mg/L, respectively. These peak values are comparable to those observed by other researchers (Gurnell *et al.* 1996; Hodson *et al.* 1998), but much less than the 12000 mg/L reported by Orwin and Smart (2004a).

'Hot and dry' conditions followed the 'storm event' on JD 234, but Q and SSC data were 'irregular' at most sites for a few days as storm flows subsided. Cold air temperatures from JD 242 – JD 245 caused Q and SSC to be, generally, low. On JD 241, the estimated 8 mm of precipitation was apparent at all of the monitoring sites in the water level and suspended sediment records. The estimated 7 mm of precipitation on JD 244 increased Q at PS1 and RPT, but a corresponding increase in SSC was not recorded for the event at these two sites. This event was evident at DS, but became more muted at sites further upstream along the main channel and for PS3. The dominance of ice cover in the catchment of the main Castle Creek channel and PS3 will make those sites less responsive to low intensity rain events than RPT and PS1, which have a higher proportion of bedrock and less ice cover in their catchment area.

Following JD 246, 'hot and dry' conditions began, and persisted until the end of the field season, generating low magnitude, but consistent 'diurnal' Q and SSC patterns. The minimum flow for the field season at DS of 1.37 m^3/s occurred from 09:25 – 10:10 PST on JD 247. Following this minimum, warm weather generated meltwater and increased Q and SSC.

As the field season progressed the diurnal peaks in the hydrograph at DS became more pronounced. The time of the daily minimum did not appear to change markedly, but the time from minimum to peak became progressively shorter; the daily peak in the hydrograph occurred at *c.* 18:00 at the start of the field season, *c.* 17:00 in the middle, and *c.* 16:00 by the end of the field season. This trend was likely a result of increasing dominance of ice melt over snowmelt in meltwater as the annual snow pack thins, reducing albedo and meltwater travel time, as well as the seasonal evolution of meltwater channels and flow paths within the glacier (Swift *et al.* 2005; Jobard and Dzikowski 2006; Haritashya *et al.* 2010). The sediment peak tended to occur on the falling limb of the hydrograph, especially during the warm sunny weather at the end of the field season.

3.1.2 Streamflow Considerations

The percent of data at DS that exceeded the maximum gauged flow (5 m^3/s) was 13%. While the uppermost 0.6% of the data exceeded the limit of "valid" extension (i.e. 10 m^3/s), and were considered an "estimate", the 12.4% of the data that were between 5 and 10 m^3/s can be considered "valid" based on the rating curve extension (WSC 2012). Estimated data occurred during the peak of both high flow events at DS. PS2 and MS data were similar; however, there were fewer estimated data points for these sites.

'Offset shifts' were applied to the rating curves for PS2 and MS part way through the field season based on changes to the WL reference point and Q measurements made after the event (see Appendix 7.1). On JD 233, an ice calving event knocked over the water sampler at PS2 and bent the stilling well over. The site was moved on the following day in the hours before the onset of the main high flow event for the 2011 season on JD 234. The data between the ice calving event and moving the site were corrected in the time-series rather

than applying a temporary shift to the rating curve. The shift that was applied to PS2 was determined by rating points collected after moving the site, and was confirmed with survey notes from the established bench marks. The stilling well at MS was bent over (*c.* 50°) during the high-flow event on JD 234. An offset shift was applied to data from the peak of the event and thereafter based on rating points collected after the event; again, survey notes were used to confirm the magnitude of the shift. There were no shifts applied to the rating curves for DS or PS1, and survey notes indicated a negligible change in WL reference point through the field season. Control at DS was the bedrock gorge; control at PS1 was maintained by large boulders. Section control at MS and PS2 may have been affected by scour and aggradation along the channel during the field season, especially during high-flow events. Unfortunately, both of these sites had a change in the WL reference point near the high-flow event and the scope and amount of data collected following the event permits only speculation on the influence of these processes.

The discharge record for two of the six sites was deduced from the gauged sites (Equations 5 and 6, *section 2.4.2*). Ideally, sites RPT and PS3 would have had their own water level loggers, but since additional equipment was not available, this deductive method was the next best option. Based on field observations during the study period, other channel inputs were negligible except during storm events, when precipitation rate exceeds infiltration rate and overland flow converges in ephemeral channels. During these isolated events, the amount of flow entering the system from these channels was variable and difficult to estimate, but likely less than 5% of the flow in the monitored stream network.

3.1.3 Suspended Sediment Concentration Considerations

The fourth-spread method was used as a quantitative basis to exclude outliers from the analysis before developing Tu–SSC regression equations (*section 2.4.3*). The ISCO pump samplers have 24 one liter bottles, thus, a full set of discrete water samples was 24; however, sample sets were not always full as a result of field operational procedures. Four SSC sample sets were subject to corrosion during sample storage, and all plotted as outliers in the Tu–SSC data for PS2, PS3, and MS (Table 3.1).

Table 3.1 Paired turbidity (Tu) and suspended sediment concentration (SSC) sample summary, and results of probability plot correlation coefficient (PPCC) fourth-spread method null hypothesis test; 'YES' means the samples were drawn from a population with a normal distribution.

	PS1	PS2	PS3	MS	RPT	DS
Tu-SSC Samples	24	205	110	202	179	183
Outliers (Corroded)	n/a	47	22	23	n/a	n/a
Outliers	6	2	6	3	4	14
Actual Sample (N)	18	156	82	176	175	169
Fail to reject H_0	YES	YES	YES	YES	NO	YES

There were relatively few outliers in the remaining data (Table 3.1); between 2% and 8% of the samples for all sites with the exception of PS1. PS1 has a low number of paired Tu–SSC samples because of equipment limitation and the necessity to prioritize available equipment (*section 2.2*).

Only four outliers were removed from the RPT Tu–SSC data set, but since the PPCC was less than the CV at the 5% significance level for the sample number, the null hypothesis that *the data were drawn from a population with a normal distribution* was rejected (Filliben and Devaney 2013). Therefore, the quantitative method of excluding outliers from this data set was not statistically sound. A plot of the raw Tu–SSC data can be found in Appendix 7.2;

it is obvious that the RPT data are not normally distributed, which may be a result of multiple sediment sources in that catchment or errors during sample collection. Given the uncertainty in the RPT data, the fourth spread method of excluding outliers from the Tu – SSC data was not modified for this site. The PPCC for the other five sites was greater than the CV at the 5% significance level for their sample number, and so the null hypothesis cannot be rejected. A detailed table on the fourth-spread method and normal probability plots can be found in Appendix 7.2. To maintain consistency in the analysis, linear regressions were used to compute 5-minute SSC time-series from Tu for all sites (Table 2.2, *section 2.4.3*).

Three sites had a substantial amount of data that exceeded the range of the turbidity monitoring instrumentation (Figure 3.1 and Table 3.2). The difference in the maximum SSC value as determined by the regression equation for each site reflect both site specific conditions and the response of the individual Tu probe. Maximum SSC values were included in the Tu–SSC analysis as a better option than omitting Tu monitoring range exceedances (Table 3.2).

Table 3.2 Turbidity (Tu) data summary for the 2011 proglacial monitoring sites.

Data Record	Site					
	PS1	PS2	PS3	MS	RPT	DS
Total days with data record	60	63	62	62	63	64
No. of days JD195 – JD254	58	60	60	60	60	60
Partial days	10	3[b]	2[b]	--	--	--
Partial day exceedance [d]	48	--	13	--	22	1
Missing days	2[a]	1[b]	3[b]	--	--	--
Full day exceedances [d]	4	--	2[c]	--	2	--
Useable days within JD195-JD254	58[a]	56[b]	53[b, c]	60	60	60
% of record useable	97	89	85	97	95	94
Number of 5min data points	16134	16534	15567[c]	17280	17280	17280
Number of 5min exceedances	6332	0	1707	0	2864	33
% of data within Tu range	61	100	89	100	83	100
Max SSC (mg/L)[d]	707.1	640.0	427.4	542.6	1065.1	1009.1

Superscript key: [a] late start of data collection; [b] low water; [c] two days of erroneous data excluded; [d] max SSC value as computed by regression equation.

The amount of Tu data exceedances at DS was less than three hours in total (0.2%). This occurred during a storm peak on JD 234. A grab sample at DS on JD 234 at 19:30 had a SSC of 2736 mg/L, which was *c.* 1 hour before the peak on the hydrograph. PS1 and PS3 were much smaller streams than the main stem of Castle Creek, and thus the effect of Tu exceedances at these sites on the overall sediment budget was somewhat limited. The tributary RPT entered Castle Creek between MS and DS. This stream had a high sediment load and strong influence on the suspended sediment data at DS; therefore, the contribution of sediment from RPT was needed to determine the sediment budget in the reach between MS and DS. For consistency in the PCA and CA analyses across the sites (*section 2.5 and 3.2*) exceedances (i.e. maximum computed SSC (Table 3.2)) were left in the SSC time-series and included in hydrologic daily averages. However, for the computation of suspended sediment load and the suspended sediment budget (*Chapter 4*), exceedances in the RPT time-series were estimated.

Discrete and composite SSC samples from RPT were used along with the SSC record from MS and DS to estimate exceedances in the RPT SSC data between JD 215 and JD 236. The time-series was adjusted to fit with the best information available using multipoint corrections in Aquarius. The difference in suspended sediment load between MS and DS was used for reference, but the assumption that all additional SSL in the reach MS-DS was from RPT was false under certain conditions. The Tu exceedances from JD 215 – JD 225 at RPT were not well supported by independent samples and could be erroneously high as a result of stream aggradation. It was not possible to quantify or correct this potential error, and more confidence can be placed in the RPT estimates after JD 228 because of the new sample location and additional grab samples.

3.1.4 Error and Uncertainty

Navratil *et al.* (2011) assessed nine different uncertainty components in the Tu approach to SSC monitoring using Monte Carlo simulations and found uncertainty associated with automatic pump samplers, stream discharge measurements, and Tu fluctuations at short time-scales to be the greatest limitations. They also identified technical limitations of Tu meters, Tu and water level sample frequency, representativeness of the SSC sample point within the cross section over the range of flow conditions, varying contribution from different sediment source areas, technical field problems, field sampling and laboratory procedures, and the calibration of the Tu–SSC relationship as other sources of uncertainty (Navratil *et al.* 2011). These uncertainty components may be correlated with one another and propagate through analytical computations.

The error in Q data is expected to be 5 – 15% depending on flow (Navratil *et al.* 2011). The cumulative error in Tu–SSC data is expected to be similar (Gurnell *et al.* 1992; Orwin and Smart 2004a; Stott et al. 2009), but would vary with SSC and Q conditions (Richards and Moore 2003; Navratil *et al.* 2011). The 95% confidence intervals are reported for the Tu-SSC regressions in Table 2.2 (*section 2.4.3*), and it is clear that the sites along the main channel produced better data than the smaller and tributary streams. Thus, the sum total of the error for the computed SSL was estimated to be between 15 and 30% of the reported values for the three sites (PS2, MS, and DS) along the main CCG meltwater channel, but would likely be higher for the three sites (PS1, PS3, and RPT) where monitoring was compromised due to limited equipment, equipment limitations, or equipment failure. The precise values reported in this study include this error and uncertainty, which is similar to the 26% error in the proglacial sediment budget by Warburton (1990).

3.2 Principal Component Analysis (PCA) and Cluster Analysis (CA)

3.2.1 Meteorological Periods – Cluster Analysis

The CA of meteorological data allowed the field season to be divided into four categories that, upon reviewing the raw data within the category, were described based on precipitation and air temperature conditions. Those categories and the percent of the field season that they represented were: 'Cold and Wet' (17/60 days, 28%), 'Warm and Damp' (15/60 days, 25%), 'Hot and Dry' (26/60 days, 43%), and 'Storm' (2/60 days, 3%). These categories were used for comparison of streamflow and suspended sediment response under different meteorological conditions (*section 3.3*). Table 3.3 summarizes the field data that were used in the meteorological analysis; a similar table with additional parameters is included in Appendix 7.3. Mean daily air temperature and precipitation have been presented as a time-series in Figure 3.6 following the summary results of the PCA and CA, Figure 3.5 (*section 3.3*)

Table 3.3 Summary of meteorological data from upper and lower meteorological stations for JD 195 – JD 254, 2011. Four clusters of similar meteorological data have been assigned descriptive titles based on air temperature and precipitation.

Meteorological Station:		Lower	Lower	Lower	Upper	Lower	Lower	Upper
Meteorological Cluster	**Parameter**	**AT min (°C)**	**AT max (°C)**	**AT mean (°C)**	**PT mean (mm/day)**	**Rel. Hum. (%)**	**T.Sol. Rad. (W/m^2)**	**W.Spd. mean (m/s)**
Cold and Wet (17 days)	**Average**	**2.0**	**7.3**	**4.8**	**8.0**	**84.4**	**14553**	**4.1**
	Std.Dev.	1.4	1.3	1.2	5.9	4.3	5133.2	1.1
Warm and Damp (15 days)	**Average**	**4.3**	**10.7**	**7.9**	**2.5**	**72.5**	**18195**	**3.6**
	Std.Dev.	1.3	1.5	1.2	2.5	7.9	3657.9	1.0
Hot and Dry (26 days)	**Average**	**7.4**	**14.7**	**10.9**	**1.2**	**58.6**	**22041**	**3.6**
	Std.Dev.	1.2	1.2	1.0	2.0	7.2	3717.6	1.0
Storm (2 days)	**Average**	**5.1**	**12.7**	**8.9**	**31.1**	**79.0**	**14243**	**5.1**
	Std.Dev.	0.6	1.9	0.5	0.1	5.1	6241.7	0.8

Nine of the ‘hot and dry’ days occurred in early September when the approaching autumnal equinox limited the amount of daily insolation and the potential for ablation. Additionally, by this point in the field season, the annual snowpack had mostly retreated from the proglacial zone and ablation zone of the glacier, leaving primarily ice melt to augment streamflow. Had this ‘hot and dry’ weather occurred earlier in the field season when the days were longer and annual snowpack was still present, the Q and SSC response could have been much different. Without these nine days in the data set, the field season was nearly balanced between the three main categories of meteorological conditions.

Orwin and Smart (2004a) used similar titles to describe the meteorological conditions during the 2000 field season at the Small River Glacier (SRG). However, since their monitoring period started 7 days earlier and the proglacial zone of the SRG has a greater elevation range and is steeper than the CCG, they found 16 days fell into a ‘snowmelt’ category. Comparing all meteorological categories between the two data sets, relative humidity and solar radiation were higher, and wind speed was much higher at the CCG in 2011 than at the SRG in 2000. Air temperatures were similar during ‘cold and wet’ periods, slightly higher at the CCG during ‘hot and dry’ periods and slightly lower at the CCG during ‘storm events’. Interestingly, meteorological parameters during ‘warm and damp’ conditions at the CCG in 2011 were similar to ‘snowmelt’ conditions at the SRG 2000. ‘Warm and damp’ days at the CCG were distributed through the 2011 field season, and, based on the title of the category, it is assumed that ‘snowmelt’ days occurred early in the field season at the SRG; however, Orwin and Smart (2004a) do not specify when the ‘snowmelt’ days occurred in their study,

3.2.2 Streamflow Driving Factor – Principal Component Analysis

The PCA of Q and meteorological conditions reduced the data to its underlying components. The two dominant eigenvalues > 1 were used to generate a bi-plot, and descriptive titles were assigned (Figure 3.3). The Kaiser-Meyer-Olkin (KMO) measure of sampling adequacy index for the correlation matrix was 0.532 which indicated that the PCA was a suitable analysis. As a rule of thumb, if the KMO is > 0.5, PCA is a suitable analysis (Tabachnick and Fidell 1989).

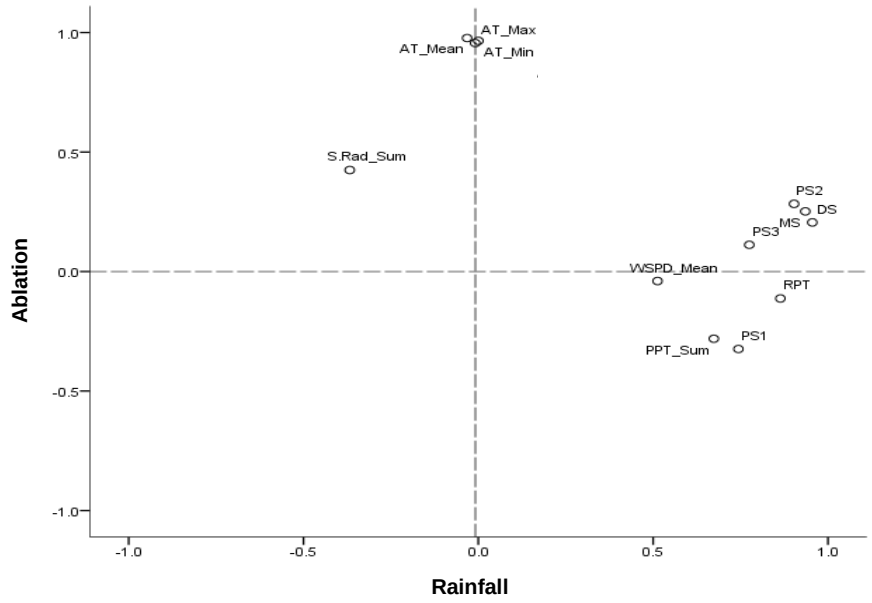

Figure 3.3 Principal component loading of daily meteorological and streamflow (Q) variables on principal component one and two explained 42% (PC1) and 30% (PC2) of the total variance in the principal component analysis. Distance of the variable from the origin indicates relative dominance of the Q generating processes; PC1 and PC2 were interpreted as 'Rainfall' and 'Ablation', and have been titled respectively in the figure.

The two components that were retained from the analysis explained 72% of the total variance in Q data (Figure 3.3). The first component was interpreted as 'rainfall' or stormy conditions and explained 42% of the variance in Q. The second component was interpreted as

‘ablation’ and explained 30% of the variance in Q. Distance from the origin (0.0, 0.0) was interpreted as dominance of the driving factor on Q pattern for the site. Orwin and Smart (2004a) found that the two component solution explained 77% of the total variability in the data from the 2000 field season at the SRG; 55% was attributed to ‘ablation’, and 22% was attributed to ‘rainfall’. In the CCG analysis the days that were represented by ‘rainfall’ were not necessarily days with substantial precipitation, they may have just not scored as ‘ablation’ driven days because they were overcast, cool and/or windy; thus, stormy conditions may be an equally applicable title for the component. The greater influence of the ‘rainfall’ component on Q in the CCG analysis may be a result of the later field season (JD 194 – JD 254 at CCG vs. JD 188 – JD 238 at SRG), and thus a lower influence of annual snowmelt ablation in the 2011 Q data at CCG than in the 2000 Q data at SRG (Orwin and Smart 2004a).

In general, all of the sites plot strongly positive on the ‘rainfall’ axis, but show less variation from the origin on the ‘ablation’ axis. Sites PS2, MS, and DS were along the main stem of the Castle Creek meltwater channel, and all plot close together, and were strongly influenced by ‘rainfall’ and moderately influenced by ‘ablation’ for the 2011 data set. As the distance from the glacier increased, the influence of ‘ablation’ on Q patterns decreased and the influence of ‘rainfall’ increased; which was consistent with the results of Orwin and Smart (2004a). Although the PS3 catchment had the greatest percent glacial cover, it was less influenced by ‘ablation’ and ‘rainfall’ than the sites along the main channel, which suggests a more stable source of flow from deeper within the glacier than the active ablation zone. Two sites, PS1 and RPT, plot negatively on the ‘ablation’ axis. For PS1, this was interpreted as a stronger influence of ‘rainfall’ on Q than ‘ablation’ due to the small proportion of glaciated

catchment area. For RPT, the negative ablation response could be due to independent timing of ablation generated peaks, a muted response from the cirque glacier/rock glacier, or a small proportion of glacial cover.

The precipitation variable plotted positively on the ‘rainfall’ axis and negatively on the ‘ablation’ axis while solar radiation plotted positively on the ‘ablation’ axis and negatively on the ‘rainfall’ axis; which was interpreted as ablation was generated by sunny days, and cloudy days generated precipitation. The air temperature variables indicate a strong positive relation on the ‘ablation’ axis and near neutral on the ‘rainfall’ axis; which was interpreted as warm weather generated ablation, and rainy weather was not necessarily cool. The wind speed variable plots neutral on the ‘ablation’ axis, which could be a result of net balance in the data, rather than no effect, and positive on the ‘rainfall’ axis, indicating that wind speed increased during rainy or stormy weather. The trend of katabatic winds would have been more strongly observed at the lower meteorological station, this trend was muted by averaging the wind speed data from the upper and lower meteorological stations. Wind speed from the lower meteorological station alone would have likely plotted more positively on the ‘ablation’ axis.

3.2.3 Suspended Sediment Response Shape – Principal Component Analysis and Cluster Analysis

Three components were retained in the PCA that was run on the 5-minute SSC data for each site. Principal loading scores were generated and plotted against time to reveal the underlying shape of the components (Figure 3.4). Time on the x-axis is reported in decimal days counting up from zero, and data are reported for the hydrologic day (06:00-06:00). For instance, the first sample is at 06:00, which is 6/24, or 0.25 of a day.

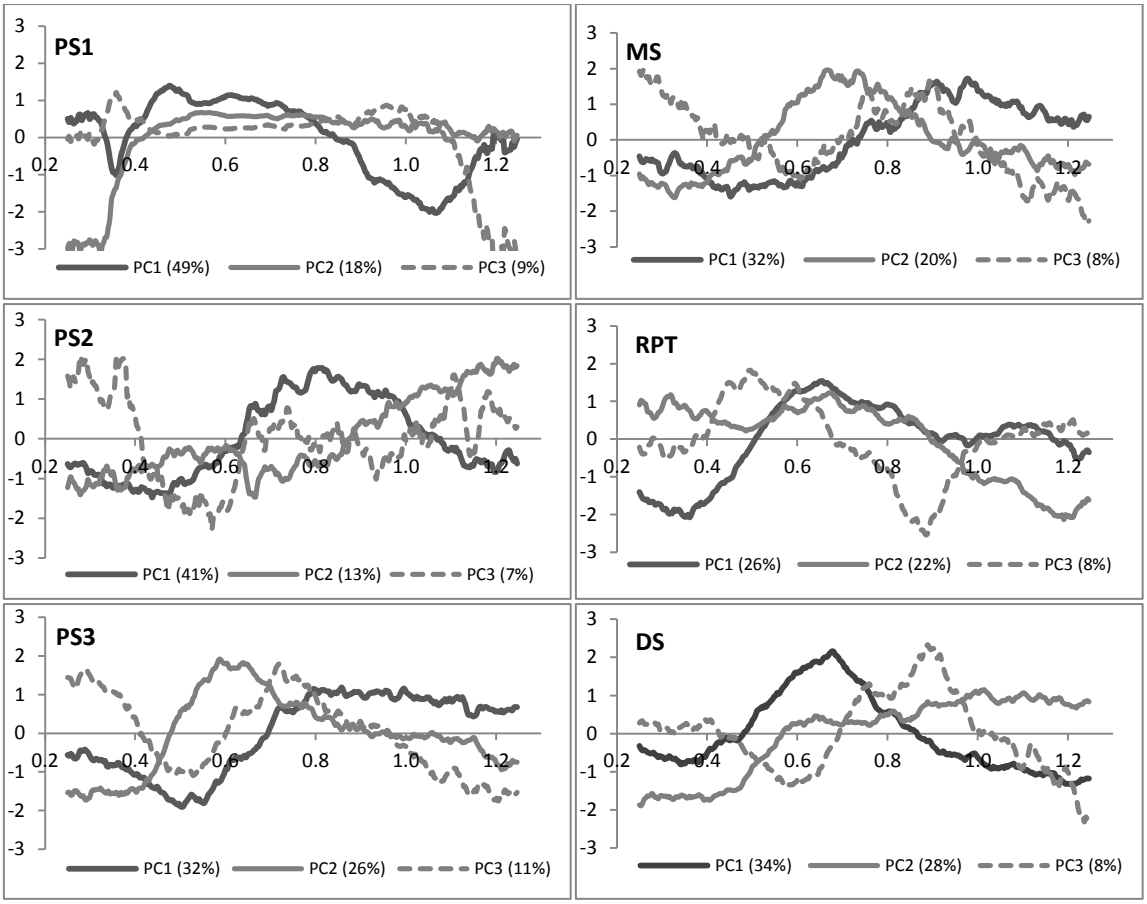

Figure 3.4 Principal component loading score plots for 5-minute SSC data from each gauging station; all full hydrologic days of data were retained as variables for the analysis. Percent of the data represented by each principal component is reported for each site. Time, on the x-axis, is reported in arbitrary decimal days (06:00 is 0.25 of the way through a regular day).

For this analysis, it was necessary to exclude partial days of data, but data exceedances were left in using the maximum value (refer to *section 3.1.3*, Table 3.2). The percent of the data that were represented by each principal component (PC) is reported for each site in Figure 3.4. Since the analyses were run independently for each site, the shape of the PC was not necessarily comparable across sites and the days that were represented by PC1 at one site may not be represented by PC1 at another site. PC1 and PC2 represented an average of 36% and 21% of the data, PC3 represented an average of 8.5% of the data, and an

average of 35% of the data was not represented by the any of the three principal components. All three principal components appeared to have a relatively well defined pattern for PS1, PS3, MS, RPT and DS. The PC3 pattern appeared to be more stochastic for PS2, and appears to be double peaked at PS3, MS, RPT and DS. The results presented by Orwin and Smart (2004a) were similar: PC1, PC2 and PC3 represented an average of 37%, 20%, and 10% of their suspended sediment data, respectively, and PC3 also showed a more irregular response pattern.

A CA was run on the principal component loading scores, and the two cluster solution categorized days as either ‘diurnal’ or ‘irregular’ SSC response shape. Comparisons of the CA results with those from the regression score loading plots (Figure 3.4) confirmed that PC1 and PC2 roughly represented the ‘diurnal’ data as a percentage; *c.* 60% at DS. Most of the data represented by PC3 at PS1, PS3 and MS may be included with the ‘diurnal’ data. However, based on percentage, the data represented by PC3 at PS2, RPT and DS appeared to be categorized as ‘irregular’ data following the cluster analysis. The data that were not represented by any of the three principal components in the first part of the analysis were categorized as ‘irregular’. Similarly, Orwin and Smart (2004a) found that, on average, 75% of their data were categorized as ‘diurnal’ following the CA.

3.2.4 Suspended Sediment Response Magnitude – Cluster Analysis

The CA of the SSC magnitude parameters (see *section 2.5.4*) separated the daily data into ‘high’, ‘medium’ and ‘low’ categories, and was a useful tool for looking at how the magnitude of SSC changed over the field season at a particular site. Sites MS and DS were dominated by ‘low’ magnitude response days; PS2 was dominated by ‘medium’ and ‘low’ response days; PS3 was split across the three magnitude categories; RPT had more ‘high’ and

'low' magnitude days than 'medium' days; and, PS1 had 'high' and 'medium' magnitude response days. Orwin and Smart (2004a) report that on average 80% of their data fell into the 'low' magnitude category and 20% fell into the 'high' magnitude category.

Since each CA was independent from the other sites, the scale of the magnitude analysis varied, which limited the ability to compare the results of this analysis across sites. The mean daily SSC for a 'high' magnitude day at PS2, MS, and DS was 195 mg/L, 336 mg/L, and 449 mg/L, respectively (Table 3.4), while 'medium' magnitude days were 112 mg/L, 161 mg/L, and 238 mg/L, respectively. A given magnitude classification will have a different value for each site because of the differences in the SSC time-series. For example, the number of 'medium' and 'high' magnitude response days at PS2 was greater than at MS, which was a result of lower peak sediment loads at PS2 which allowed the scale of the analysis to be focused on a smaller range than at MS. Essentially, a small number of very high SSC data could stretch the scale so that the majority of the data fall into a lower magnitude category; in which case, the detail of the time-series data could become lost or obscured. Differences in scale between the sites were also reported for this analysis on the data from the SRG by Orwin and Smart (2004a), which they attributed to sediment availability in the contributing catchment area. The analysis could easily be misinterpreted; however, the scale of the SSC data and the results of the magnitude analysis became somewhat of a moot point when SSL was calculated (*Chapter 4*).

Table 3.4 Summary of suspended sediment response magnitude parameters and cluster analysis results. Values computed from daily data. Standard deviation is reported in parentheses.

Site	SSC Magnitude Class	Avg. SSC_{min} (mg/L)	Avg. SSC_{max} (mg/L)	Mean SSC_{mean} (mg/L)	Avg. SSC_{range} (mg/L)	Avg. $SSC_{Std.Dev.}$ (mg/L)	Avg. Std. SSC_{range} (ratio)	Avg. SS_{Load} (kg/Day)	Days (N)	Tot. Days (N_T)
PS1	**High**	433 (168)	707 (0)	644 (63)	284 (168)	80 (55)	1.0 (1.0)	5619 (3698)	36	58
	Medium	16 (40)	683 (52)	292 (99)	667 (54)	233 (36)	27 (196)	2313 (577)	21	
	Low	0**	122	38	146	41	6.0	640	1	
PS2	**High**	119(44)	356 (84)	196 (58)	236 (50)	58 (14)	2.2 (0.8)	108893 (68359)	5	56
	Medium	80 (17)	176 (32)	112 (19)	96 (35)	20 (8)	1.3 (0.6)	29072 (9564)	26	
	Low	65 (10)	111 (18)	81 (13)	45 (14)	9 (3)	0.7 (0.3)	17323 (5572)	25	
PS3	**High**	174 (92)	393 (70)	306 (90)	219 (81)	63 (33)	2.0 (1.6)	13387 (6898)	21	53
	Medium	102 (32)	319 (74)	199 (49)	216 (60)	54 (20)	2.3 (0.8)	7211 (2628)	15	
	Low	43 (28)	192 (78)	92 (40)	149 (71)	33 (16)	4.9 (3.3)	2817 (2305)	17	
MS	**High**	193	499	336	305	84	1.6	301577	1	60
	Medium	88 (30)	311 (72)	161 (39)	233 (53)	47 (12)	2.7 (0.7)	68120 (35730)	8	
	Low	74 (17)	147 (35)	103 (24)	73 (26)	16 (6)	1.0 (0.4)	28630 (13223)	51	
RPT	**High**	752 (180)	1056 (26)	937 (102)	304 (173)	84 (55)	0.5 (0.4)	56235 (24639)	31	60
	Medium	227 (67)	922 (145)	467 (155)	695 (128)	156 (42)	3.4 (1.4)	19008 (9717)	12	
	Low	221 (85)	515 (120)	329 (99)	294 (75)	66 (21)	1.5 (0.7)	13497 (7291)	17	
DS	**High**	211 (108)	968 (45)	449 (152)	757 (71)	189 (50)	5.0 (3.0)	367279 (249474)	3	60
	Medium	162 (41)	396 (116)	238 (53)	233 (120)	51 (25)	1.6 (1.2)	100484 (49369)	17	
	Low	97 (22)	210 (55)	143 (32)	113 (45)	26 (12)	1.2 (0.5)	41631 (15893)	40	

3.3 Shape and Magnitude - Field Season Summary

This section compiles and draws upon several parts of the data collection and analysis presented earlier, and uses field observations to describe the results of the statistical analyses (*section 3.2*) for the 2011 field season. The composite figures in Figure 3.5 summarize daily data and the results of the PCA and CA that were used to categorize the 'shape' and 'magnitude' of the suspended sediment response for each of the sites. Daily mean air temperature and total precipitation are presented with the meteorological CA results for comparison purposes (Figure 3.6). Sites PS1, PS2 and PS3 were missing days in the SSC

shape and magnitude classification due to low water, partial days of data, erroneous data or no data (see Table 3.2, *section 3.1.3*).

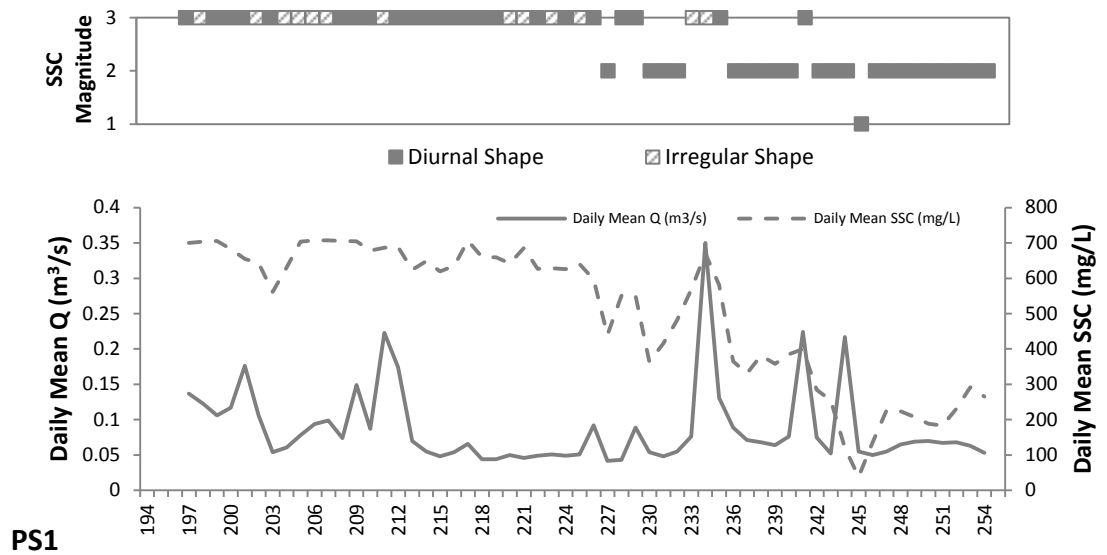

PS1

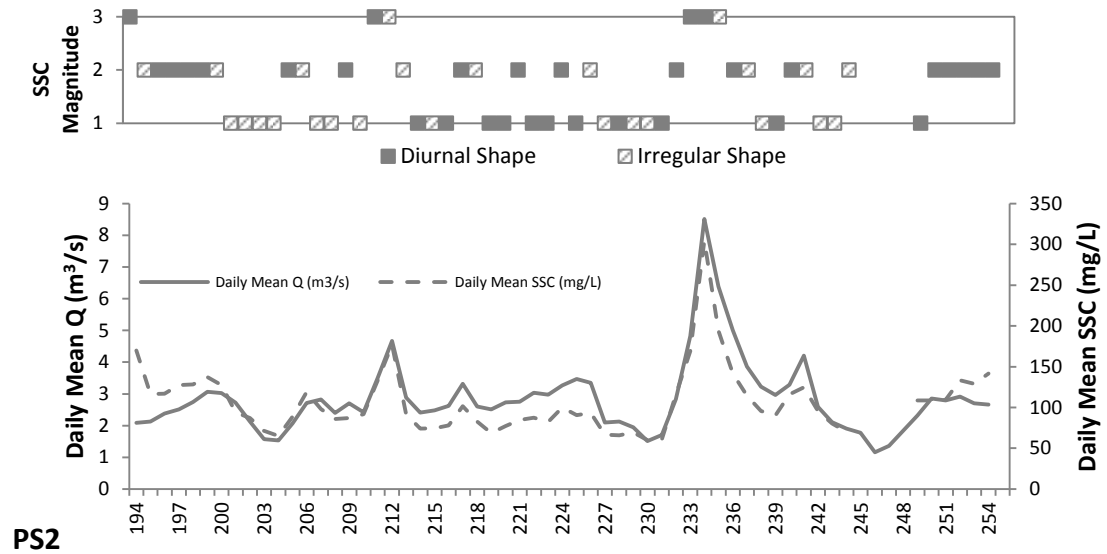

PS2

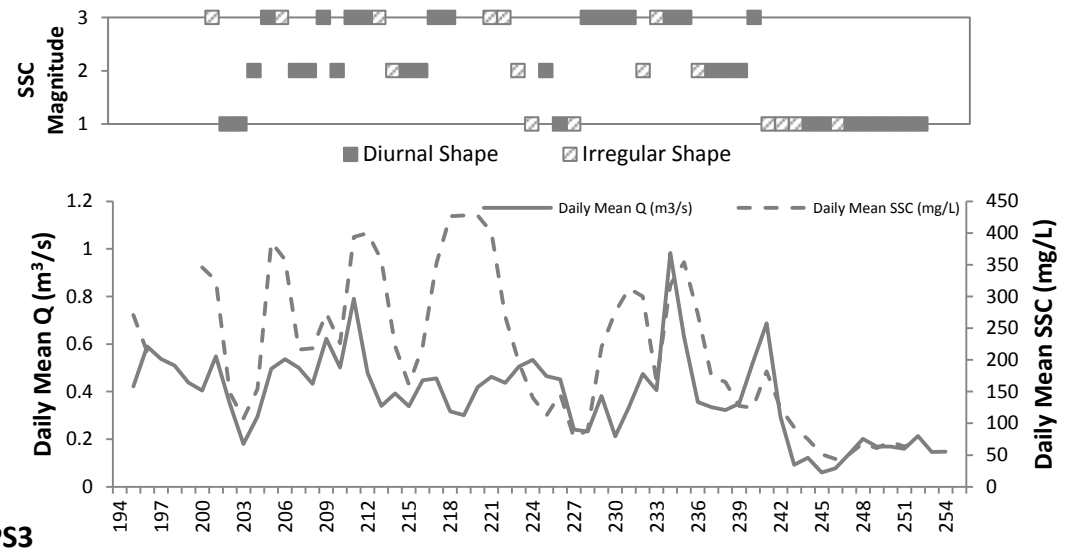
SSC Magnitude
3
2
1
Diurnal Shape
Irregular Shape
Daily Mean Q (m3/s)
Daily Mean SSC (mg/L)
Daily Mean Q (m³/s)
Daily Mean SSC (mg/L)
1.2
1
0.8
0.6
0.4
0.2
0
450
400
350
300
250
200
150
100
50
0
194 197 200 203 206 209 212 215 218 221 224 227 230 233 236 239 242 245 248 251 254

PS3

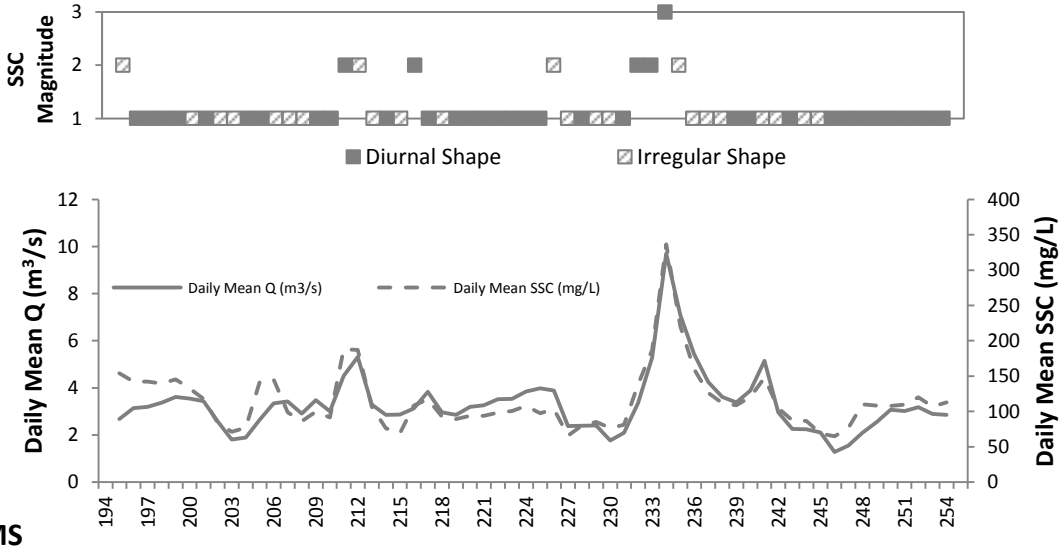
SSC Magnitude
3
2
1
Diurnal Shape
Irregular Shape
Daily Mean Q (m3/s)
Daily Mean SSC (mg/L)
Daily Mean Q (m³/s)
Daily Mean SSC (mg/L)
12
10
8
6
4
2
0
400
350
300
250
200
150
100
50
0
194 197 200 203 206 209 212 215 218 221 224 227 230 233 236 239 242 245 248 251 254

MS

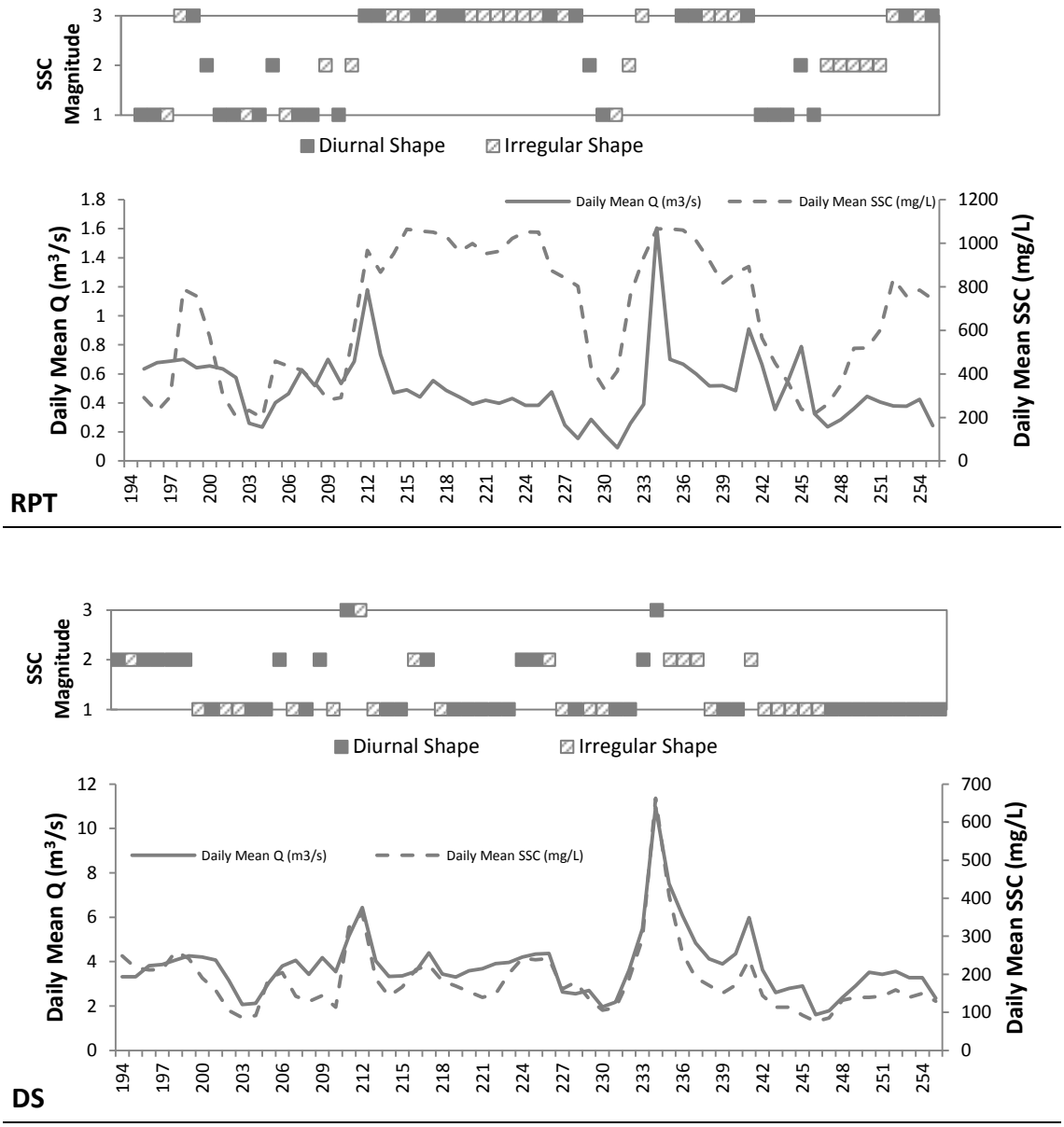

Figure 3.5 Composite figures showing suspended sediment shape (diurnal or irregular) and magnitude (1 = low; 2 = medium; 3 = high) classification results from principal component analysis and cluster analysis and daily mean streamflow (Q) and suspended sediment concentration (SSC) for each of the proglacial monitoring sites. PS1, PS2, and PS3 are missing days in the shape and magnitude classification due to low water, partial days of data, erroneous data or no data (see *section 3.1*). Figure continued over three preceding pages; x-axes in Julian Days.

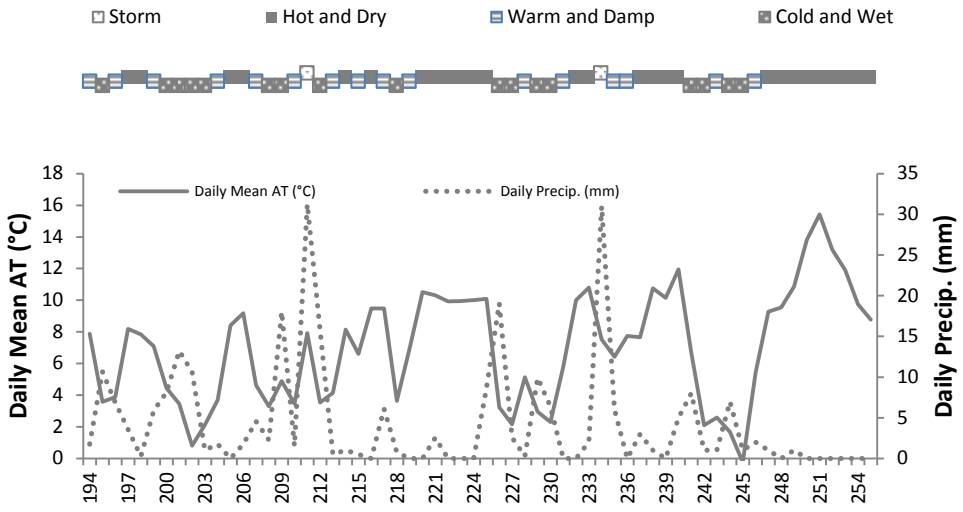

Figure 3.6 Daily mean air temperature (AT) and daily total precipitation presented with results of meteorological principal component analysis ('storm'; 'hot and dry'; 'warm and damp'; 'cold and wet').

The three sites along the main Castle Creek channel (PS2, MS and DS) show a similar 'shape' and 'magnitude' pattern dominated by 'irregular' SSC data on 'cold and wet' days and 'diurnal' SSC data on 'hot and dry' days (Figure 3.5, Table 3.5). The SSC response at these three sites tracks air temperature and precipitation, but, particularly for MS, the response was often not strong enough to cross the threshold to a higher magnitude category. While both 'storm' days were classified as 'diurnal' for PS2, MS and DS, the three or four days following the storm were 'irregular' as storm flows subsided. Successive downstream sites along the main channel show the influence of the tributary streams along the way. Similar to the results of the main meltwater stream at CCG in 2011, Orwin and Smart (2004a) state that the response pattern from three sites along the North Proglacial Stream at the SRG in 2000 was dominated by 'low' magnitude 'diurnal' data, and that 'high' magnitude 'irregular' response data were closely associated with precipitation events. They also found that the SSC magnitude response at a high elevation site was only elevated by

temperature peaks (Orwin and Smart 2004a). Compared to the SRG study, all sites at the CCG were relatively similar in elevation; as such, this high elevation response pattern was not observed. The SSC response at RPT was similar to the response at the Central Proglacial Lower site in the SRG study (Orwin and Smart 2004a), where cool temperatures generated 'diurnal' response data and high temperatures generated 'irregular' response data.

Table 3.5 Summary of suspended sediment 'shape' and 'magnitude' analysis for 2011 proglacial monitoring locations, JD 195 – JD 254: DAYS

Site	Cluster Classification	Cold and Wet (17 days)	Warm and Damp (15 days)	Hot and Dry (26 days)	Storm (2 days)	Days (N) 60	Days (N_T) 60
PS1	Diurnal (Irregular)	15 (1)	12 (2)	18 (8)	(2)	45 (13)	58
	High	10 (1)	8 (2)	5 (8)	(2)	23 (13)	36
	Medium	4	4	13	--	21	21
	Low	1	--	--	--	1	1
PS2	Diurnal (Irregular)	1 (15)	7 (7)	21 (3)	2	31 (25)	56
	High	(1)	(1)	1	2	3 (2)	5
	Medium	1 (6)	4 (1)	12 (2)	--	17 (9)	26
	Low	(8)	3 (5)	8 (1)	--	11 (14)	25
PS3	Diurnal (Irregular)	13 (4)	9 (4)	13 (8)	2	37 (16)	53
	High	7 (1)	4 (1)	2 (4)	2	15 (6)	21
	Medium	1	5 (1)	5 (3)	--	11 (4)	15
	Low	5 (3)	(2)	6 (1)	--	11 (6)	17
MS	Diurnal (Irregular)	2 (15)	10 (5)	23 (3)	2	37 (23)	60
	High	--	--	--	1	1	1
	Medium	(3)	(1)	3	1	4 (4)	8
	Low	2 (12)	10 (4)	20 (3)	--	32 (19)	51
RPT	Diurnal (Irregular)	14 (3)	11 (4)	4 (22)	1 (1)	30 (30)	60
	High	4 (1)	5 (3)	3 (14)	1	13 (18)	31
	Medium	3 (1)	--	1 (6)	(1)	4 (8)	12
	Low	7 (1)	6 (1)	(2)	--	13 (4)	17
DS	Diurnal (Irregular)	3 (14)	8 (7)	23 (3)	2	36 (24)	60
	High	(1)	--	--	2	2 (1)	3
	Medium	1 (3)	3 (2)	6 (2)	--	10 (7)	17
	Low	2 (10)	5 (5)	17 (1)	--	24 (16)	40

The results of the 'shape' and 'magnitude' analysis of suspended sediment response data can be explained by the characteristics of the contributing watershed area. The following sections examine the observed response patterns at each of the six sites with brief reviews of the catchment characteristics and field observations for context.

3.3.1 Proximal Site 1

Proximal Site 1 (PS1) had a small flow volume compared to that of the main stem of the Castle Creek. The influence of its typically high SSC was substantially diluted a short distance from the confluence with the main channel on the low gradient outwash fan upstream of MS (Figure 2.2). It drained an estimated *c.* 1 km^2 area along the east-northeast side of the terminal lobe, which included lateral moraine deposits and the ice-marginal interface; however, the catchment of PS1 was only 11% glaciated (Table 2.1). Much of the deglaciated catchment area was dominated by bedrock and metastable till deposits, but the area proximal to the glacier was dominated by unconsolidated glacial till.

At PS1, 78% of the suspended sediment data during the field season had a 'diurnal' response shape (Figure 3.5, Table 3.5). The sediment load of the small meltwater stream was enriched as it flowed along the unconsolidated till-dominated ice-marginal interface, and its high sediment concentration fluctuated with ablation and precipitation (Figures 3.1, 3.5, and 3.6). The pattern was more apparent as the duration of values that exceed the range of the Tu meter became progressively shorter later in the field season. Both 'storm' events were classified as 'irregular' as a result of sustained 'high' magnitude SS*C*. There was a noticeable decrease in the SSC diurnal range following each storm event, and data fell completely within the range of the Tu meter for most of the time after the second storm event on JD 234. The declining magnitude of suspended sediment response over the ablation season was a result of reduced activity, stabilization or exhaustion of sediment sources along the meltwater channel. Additionally, seasonal snowmelt and ablation potential decline as the autumnal equinox approaches. Any disturbance or redirection of the active channel would likely

reactivate or rejuvenate sediment sources, and glacial advance or retreat could substantially reset sediment availability for the next ablation season.

The four 'high' magnitude 'irregular' response days that occurred from JD 204 to JD207 were a result of full day exceedances driven by ablation, but may have shown a diurnal response shape if data were within the range of the Tu meter. Interestingly, the data show that on JD 244, a ~10 mm rain event and cool air temperatures caused Q to increase while SSC decreased, although the pattern remained 'diurnal'. The JD 244 – JD 245 data were considered valid because all other sites, with the exception of PS3, show a corresponding Q response and low SSC response to this event (Figure 3.1). Upstream of the monitoring station on PS1, there was a tributary that drained a slope dominated by bedrock and metastable till deposits. Low air temperature would have reduced ablation and meltwater production, while rainwater draining from the tributary catchment would have been relatively clean, thus diluting the sediment load of meltwater flowing from the area proximal to the glacier. Other studies have reported a similar proglacial SSC response to rain events when temperatures are low (Sawada and Johnson 2000; Orwin and Smart 2004a)

3.3.2 Proximal Site 2

Proximal Site 2 (PS2) monitored the main flow of the Castle Creek proglacial stream, *c.* 200 m downstream from where it emanated from a meltwater channel portal on the northwest side of the terminal lobe of the glacier (Figure 2.2). The estimated catchment area was *c.* 9 km^2 and 77% glaciated (Table 2.1). Because of the distance between the meltwater channel portal and the monitoring location, there was the opportunity for recently exposed, unconsolidated sediment deposits proximal to the glacier and adjacent to the meltwater stream to enrich the sediment load of meltwater emanating from the glacier. Orwin and Smart

(2004a) observed a similar limitation with proximal monitoring sites located a short distance from the glacier. Ideally, the two sediment sources would be isolated by locating monitoring sites immediately adjacent to the glacier; however, site conditions evolve through the ablation season and the complex geomorphology of the ice-marginal environment limits site selection. Small Q and SSC spikes were observed on the falling limb of the hydrograph, mostly during warm weather, when ice calving into the proglacial pool c. 75m upstream of PS2 caused waves that generated a pulse of water and entrained unconsolidated sediment from the deposits adjacent to the pool; Stott and Grove (2001) observed a similar process on the Skeldal River in Greenland.

Suspended sediment response 'shape' and 'magnitude' at PS2 tended to mirror the trend of ablation driven streamflow, but unconsolidated sediment sources proximal to the glacier were activated by precipitation. About 55% of the SSC data had a 'diurnal' shape and the majority were categorized as 'medium' magnitude (Figure 3.5, Table 3.5). During the 'storm event' on JD 234, available sediment became exhausted during the peak flow and the SSC was much lower on the falling limb than on the rising limb of the event hydrograph (Figure 3.1).

3.3.3 Proximal Site 3

Proximal Site 3 (PS3) drained a proglacial lake that was perched on top of a till sheet in front of the terminal lobe of the glacier (Figure 2.2). Most of the relatively low gradient catchment was exposed within the previous *c.* 8 years (Beedle *et al.* 2009); however, the stability of the deposit appears to have increased rapidly. The estimated catchment area was *c.* 2 km^2 and 95% glaciated (Table 2.1). The source of meltwater to this proglacial lake was primarily beneath the terminus of the glacier, but some meltwater was received from streams

that flowed along unconsolidated sediment at the ice–till interface. Additionally, channels observed on the relatively low gradient area surrounding the lake suggest that runoff from snow melt and storm events can also transport sediment into the lake. The stream that drains this proglacial lake was bedrock controlled and entered Castle Creek *c.* 130 m downstream from the PS2 monitoring location. The suspended sediment response at this site appeared to influence the SSC data at MS, especially during the first part of the field season.

Site PS3 showed a dynamic suspended sediment 'shape' and 'magnitude' response through the field season, responding to ablation, seasonal snowmelt and rainfall (Figures 3.1, 3.5, and 3.6). The extremely high SSC recorded from JD 218 – JD 221, may have been influenced by sediment derived from the stream bed and was not supported by downstream monitoring of SSC at MS; it was, therefore, considered erroneous. While the two full days of Tu exceedances (JD 219 and JD 220) were removed before the analysis, the two partial days (JD 218 and JD 221) were left in, but there was low confidence in the accuracy of these results. Suspended sediment concentration covaried with air temperature and rainfall until the 'storm' event on JD 234. Data with high SSC values were sustained for some time as Q dropped following the event; possibly a function of the amount of time needed for sediment laden water to be flushed out of (or settle in) the lake. The shape of SSC data at this site were 70% 'diurnal', while magnitude responded to air temperature and precipitation peaks. Similar to PS1, as the ablation season progressed, the sediment supply appeared to become increasingly exhausted or transport limited.

3.3.4 Middle Site

The Middle Site (MS) was located at the bottom of an outwash fan complex, downstream from the confluences of the three proximal sites. The catchment area was *c.* 13

km^2 and 71% glaciated (Table 2.1). In addition to the catchment areas of the proximal sites, there was a bedrock dominated area to the west, the till sheet that extended downslope from the terminus of the glacier, and two outwash fans that merged *c.* 100 m upstream of the site. Active mass movement along the right bank of the main channel, between the PS3 confluence and the PS1 confluence, was triggered by snowmelt, precipitation and high flow events.

The suspended sediment response 'shape' at MS was 62% diurnal, and closely mirrors that of PS2 which accounts for *c.* 85% of the flow at MS (see *section 4.1, Table 4.3*). Slightly higher peaks in the SSC data at MS tend to cause the overall magnitude classification to be lower than PS2, 85% of the data at MS fell into the 'low' magnitude category (Table 3.5). Higher SSC peaks during 'storm events' may be the result of sediment sources in the channel, along the channel banks or in the un-glaciated catchment area being activated. Site PS3 was capable of influencing the SSC at MS, which was primarily evident prior to the 'storm' event on JD 211. The input from PS1 has a high daily mean SSC and persistent diurnal pattern, but, because of its low Q, the influence of its response pattern cannot be discerned in the data at MS.

3.3.5 Rockback Peak Tributary

The Rockback Peak Tributary (RPT) drained the northeast aspect of Rockback Peak. The estimated catchment area of RPT was *c.* 3 km^2 and less than 20% glaciated (Table 2.1).The cirque glacier/rock glacier in the top of the catchment had active sediment sources depositing debris via avalanches and rockslides from the mountain above onto its surface. Meltwater was divided over the east ridge of the cirque; a portion flowed east into the Castle Creek catchment, and a portion flowed west into the adjacent drainage. Aggradation of the

outwash fan on the ridge had recently caused RPT to take a more northern route off the ridge. Sediment from this site was characteristically black in contrast to the gray-brown sediment and bluish rock-flour from CCG; this contrast was observed and photographed on site, as well as recorded in suspended sediment and sediment source samples. As the cirque glacier/rock glacier retreats and the alluvial path along the ridge aggrades, this sediment source may divert to the west, away from the Castle Creek catchment. However, for the 2011 field season, RPT was a major source of fine sediment for Castle Creek.

The sediment load of RPT was primarily from the cirque glacier/rock glacier and actively eroding deposits on the adjacent ridge; the response pattern was not necessarily synchronous with the Castle Creek system. An 'irregular' suspended sediment response shape was dominant during 'hot and dry' periods, while other periods tended to have a 'diurnal' response shape. The SSC and Q data responded positively to warm temperatures and precipitation events throughout the season. Following the two 'storm' events, SSC remained elevated for a period of time, which was probably a result of sediment slumping into the channel during the event and slowly being evacuated; Orwin and Smart (2004a) report similar processes and response patterns for one of their sites at the SRG. Warm temperatures caused SSC to exceed the range of the Tu meter for the majority of data from JD 215 – JD219 and JD 223 – JD 225. The range of the meter was also exceeded during the warm weather and 'storm' event that occurred during JD 233 – JD 236. Following the 'storm' event on JD 234, SSC levels remained 'high' for eight days, and then dropped suddenly to a 'low' magnitude response during 'cold and wet' weather on JD 241. Interestingly, on JD 244 streamflow increased in response to a precipitation event but SSC decreased, which was the same response observed at PS1. Similar to PS1, a tributary stream

upstream of the RPT monitoring station drained the bedrock and metastable till mantled slope below the sediment laden ridge where RPT begins; runoff from this tributary may have diluted the SSC in RPT during the event.

3.3.6 Distal Site

The Distal Site (DS) was essentially the combined response of RPT and MS; additional sediment sources were limited to ephemeral channels that were only activated during intense precipitation. These channels and sediment sources would also be active during spring runoff, which was mostly completed before the start of the 2011 field season. At this monitoring site, the catchment area was *c.* 16 km^2 and 60% glaciated (Table 2.1). Additional areas that were not included in the RPT or MS catchments include a low relief till sheet along the right bank of the channel, abandoned outwash channels that carve through thick till deposits along the left bank upstream of RPT, and a moraine and till mantled bedrock outcrop downstream of RPT. 'Shape' classification at DS was very similar to MS, 60% diurnal, while 'magnitude' classification at DS was slightly higher than MS, which was most likely a result of the RPT tributary (Table 3.5). The 'magnitude' response at DS increased with ablation during the early season, but the response diminished later in the field season which was attributed to declining contribution of annual snowmelt.

4 Results and Discussion (2) - Suspended Sediment Load

The analysis of meteorological conditions, streamflow driving factors, and the 'shape' and 'magnitude' of the suspended sediment response has divided the data from the six 2011 monitoring stations into groups of similar data (*sections 3.2* and *3.3*). In this chapter, objective 2 is addressed by computing SSL from the 5-minute time-series SSC and Q data following Equation 2 (*section 2.2*). The SSL time-series are then summarized into hydrologic daily averages and organized into the sub-categories as determined through PCA and CA for each site (*section 3.2*). Building on this analysis, a suspended sediment budget is defined for the 2011 field season for the Castle Creek proglacial zone using the key variables defined by Warburton (1990).

4.1 Suspended Sediment Load

The arithmetic mean of the average daily SSL (kg/day) was computed for each hydro-meteorological, 'shape' and 'magnitude' sub-category (Table 4.1). When summarizing the categories, weighted averages were used to account for the disproportionate number of days in each category; Table 3.5 reports the number of days in each category. A similar table with SSL totals (kg/*x* days) can be found in Appendix 7.4.

Table 4.1 Summary of average suspended sediment load (kg/day) for each sub-category. Averages for 'irregular' response shape data are reported in brackets. The values reported in the body of the table are arithmetic means for the given category. Weighted averages were used to account for the disproportionate number of days in each category for the 'shape' and 'magnitude', and total summary. Table 3.5 reports the the number of days in each category.

Site	Cluster Classification	Cold and Wet (17 Days)	Warm and Damp (15 Days)	Hot and Dry (26 Days)	Storm (2 Days)	Weighted Average summary	
PS1	Diurnal (Irregular)	4927 (5829)	3567 (4736)	2866 (4188)	(17200)	3740 (6400)	4336
	High	6430 (5829)	4320 (4736)	4044 (4188)	(17200)	5177 (6400)	5619
	Medium	2240	2061	2413	--	2313	2313
	Low	640	--	--	--	640	640
PS2	Diurnal (Irregular)	20774 (23451)	26874 (30702)	27595 (30822)	142879	34650 (26366)	30952
	High	(74606)	(109527)	74572	142879	120110 (92067)	108893
	Medium	20774 (26345)	37951 (23263)	28013 (32911)	--	29926 (27462)	29072
	Low	(14886)	12105 (16425)	21096 (26643)	--	18644 (16275)	17323
PS3	Diurnal (Irregular)	7625 (8329)	8568 (5267)	4642 (10877)	29600	7994 (8838)	8249
	High	10932 (15130)	11378 (10915)	11824 (12552)	29600	13659 (12709)	13387
	Medium	8460	6320 (9060)	5818 (9982)	--	6286 (9752)	7211
	Low	2829 (6062)	(547)	1268 (6863)	--	1978 (4357)	2817
MS	Diurnal (Irregular)	33109 (29683)	24089 (58396)	32791 (41514)	191799	39051 (37468)	38444
	High	--	--	--	301577	301577	301577
	Medium	(53905)	(138134)	54363	82021	61278 (74962)	68120
	Low	33109 (23627)	24089 (38462)	29555 (41514)	--	28069 (29574)	28630
RPT*	Diurnal (Irregular)	30471 (13807)	26962 (59615)	34744 (30566)	343410 (42929)	40185 (33176)	36681
	High	64308 (18039)	44417 (78371)	41200 (38843)	343410	72795 (44275)	56235
	Medium	19370 (18153)	--	15374 (15588)	(42929)	18371 (19327)	19008
	Low	15892 (5228)	12416 (3349)	(17563)	--	14288 (10926)	13497
DS	Diurnal (Irregular)	50233 (61070)	53448 (85171)	58527 (70122)	444324	78140 (69231)	74577
	High	(213187)	--	--	444324	444324 (213187)	367279
	Medium	56034 (95476)	82680 (203185)	93841 (74156)	--	86712 (120159)	100484
	Low	47332 (35537)	35908 (37966)	46063 (62054)	--	44053 (37953)	41613

*exceedances in the RPT data set have been estimated

The information in Table 4.1 illustrates where, under what conditions and how much sediment was generated, transported, stored and evacuated from the watershed during the 2011 field season. To simplify the information, it could be presented as percentage of total; however, the distribution of days across categories varied by site and was specific to the 2011 field season, which would make comparisons between locations or over different field seasons difficult, Hannah *et al.* (2000) also report this limitation with the analysis.

As described in *sections 3.2.3* and *3.2.4,* ‘shape’ and ‘magnitude’ parameters were essentially driven by hydro-meteorological conditions at the time of monitoring. Thus, the most applicable division of the field season for the suspended sediment budget was into the hydro-meteorological periods. From there, similar computations of totals and averages can be made, but reported in a simplified format that will also be more useful for modelling applications, assessing subsequent years of data, or comparing results with other sites. Table 4.2 presents the SSL data divided into meteorological categories. The values in the table were computed from daily means or totals as appropriate; max and min values were not instantaneous values, they were max and min of the daily means in the category. Table 4.2 is a good reference for interpreting the other tables presented later in this discussion, and a wide range of summary computations are possible.

Table 4.2 Field season summary statistics for meteorological periods determined through principal component analysis. Streamflow is Q (m^3/s), suspended sediment concentration is SSC (mg/L), suspended sediment load is SSL (t/day), precipitation is PT (daily total mm), and air temperature is AT (daily mean °C). Values in the table have been computed from daily averages or totals of individual hydrologic days (06:00 – 06:00) in the category.

		AT	PT	PS1			PS2			PS3			MS			RPT			DS		
				Q	SSC	SSL	Q	SSC	SSL	Q	SSC	SSL	Q	SSC	SSL	Q	SSC	SSL	Q	SSC	SSL
Cold and Wet	Min	-0.25	0.76	0.042	38.2	0.640	1.51	60.1	7.82	0.060	51.2	0.254	1.77	65.9	11.2	0.184	204	5.13	1.96	86.1	15.4
	Max	6.7	19.1	0.284	706	10.2	4.67	177	74.6	0.687	427	16.8	5.32	187	90.2	1.18	1199	99.0	6.44	360	213
	Mean	2.98	7.96	0.123	506	4.98	2.55	94.3	23.3	0.365	216	7.79	3.04	104	30.0	0.574	525	27.5	3.60	165	59.1
	Days	17	17	16	16	16	17	16	16	17	17	17	17	17	17	17	17	17	17	17	17
	Sum	n/a	135	n/a	n/a	79.7	n/a	n/a	372	n/a	n/a	132	n/a	n/a	511	n/a	n/a	468	n/a	n/a	1005
	Std. Dev.	1.59	6.09	0.073	212	3.12	0.872	29.8	16.7	0.171	116	5.35	1.03	33.8	20.8	0.253	310	25.1	1.21	69.5	49.1
Warm and Damp	Min	2.58	0.0	0.043	136	0.931	1.16	60.9	8.6	0.077	43.7	326	1.28	65.0	7.21	0.092	198	3.35	1.61	75.8	10.6
	Max	9.47	6.86	0.131	707 e	7.14	6.38	194	11.0	0.629	358	19.4	7.10	220	138	0.733	1996	119	7.52	408	271
	Mean	5.54	2.46	0.071	545	3.72	2.79	99.2	28.8	0.365	219	7.55	3.23	109	35.5	0.482	769	35.7	3.69	180	68.3
	Days	15	15	14	14	14	15	14	14	15	13	13	15	15	15	15	15	15	15	15	15
	Sum	n/a	36.9	n/a	n/a	52.1	n/a	n/a	403	n/a	n/a	98.2	n/a	n/a	533	n/a	n/a	535	n/a	n/a	1024
	Std. Dev.	1.87	2.61	0.027	182	1.86	1.34	37.6	26.9	0.160	107	5.57	1.45	42.2	33.2	0.207	527	32.6	1.54	83.7	64.9
Hot and Dry	Min	7.67	0.	0.046	184	1.72	1.36	74.2	15.6	0.138	51.3	0.881	1.55	76.4	10.5	0.235	261	5.24	1.79	85.6	13.5
	Max	15.4	8.64	0.137	707 e	8.30	4.82	169	74.6	0.538	401	117.0	5.28	187	90.0	0.701	1310	52.3	5.46	294	148
	Mean	10.3	1.19	0.068	472	3.27	2.84	107	28.0	0.365	178	7.02	3.27	115	33.8	0.433	818	31.2	3.69	177	59.9
	Days	26	26	26	26	26	26	24	24	26	21	21	26	26	26	26	26	26	26	26	26
	Sum	n/a	30.8	n/a	n/a	85.1	n/a	n/a	672	n/a	n/a	147	n/a	n/a	879	n/a	n/a	811	n/a	n/a	1556
	Std. Dev.	1.82	2.03	0.022	199	1.63	0.647	23.6	115	0.147	110	5.32	0.704	23.5	14.1	0.109	254	11.7	0.73	46.7	26.6
Storm	Min	7.52	31.0 E	0.223	670	13.4	3.50	133	46.2	0.790	318	27.9	4.51	188	82.0	0.685	613	42.9	5.14	323	169
	Max	7.93	31.2	0.350	687	20.9	8.51	304	240	0.983	394	31.3	9.7	336	302	1.61	2337 E	343	11.0	663	719
	Mean	7.72	31.1 E	0.287	678	17.2	6.00	219	143	0.887	356	29.6	7.10	262	192	1.15	1475	193	8.05	493	444
	Days	2	2	2	2	2	2	2	2	2	2	2	2	2	2	2	2	2	2	2	2
	Sum	15.4	62.2 E	n/a	n/a	34.4	n/a	n/a	286	n/a	n/a	59.2	n/a	n/a	384	n/a	n/a	386	n/a	n/a	888
	Std. Dev.	0.29	0.17	0.090	12.1	5.31	3.55	121	137	0.136	53.5	2.37	3.67	105	155	0.651	1218	212	4.11	240	388
Seasonal	Min	-0.25	0	0.042	38.2	0.640	1.16	60.1	7.82	0.060	43.7	0.254	1.28	65.0	7.2	0.092	198	3.35	1.61	75.9	10.6
	Max	15.4	31.2 E	0.350	707 e	20.9	8.51	304	240	0.983	427	31.3	9.7	336	302	1.61	2337 E	343	11.0	662	719
	Mean	6.94	4.42	0.091	506	4.33	2.85	105	31.0	0.383	207	8.25	3.32	115	38.4	0.509	745	36.7	3.81	185	74.6
	Days	60	60	58	58	58	60	56	56	60	53	53	60	60	60	60	60	60	60	60	60
	Sum	n/a	265 E	n/a	n/a	251	n/a	n/a	1733	n/a	n/a	437	n/a	n/a	2307	n/a	n/a	2201	n/a	n/a	4475
	Std. Dev.	3.59	6.84	0.063	197	3.40	1.18	39.9	33.5	0.180	113	6.73	1.32	43.9	41.2	0.240	441	46.1	1.45	90.8	96.6

E – Estimate; e - Exceedance

Table 4.3 and Figure 4.1 report SSL and Q for the monitoring network as percent contribution to the total at DS for each hydro-meteorological category. Mean values were used for the computations rather than totals to reduce the influence of missing days at the proximal sites; raw values are reported in Table 4.2.

Table 4.3 Percent (%) of mean daily suspended sediment load (SSL) and streamflow (Q) relative to the distal site (DS) during meteorological periods determined by principal component analysis.

Meteorological period	Cold and Wet 28% (17 days)		Warm and Damp 25% (15 days)		Hot and Dry 44% (26 days)		Storm 3% (2 days)		Seasonal 100% (60 days)	
Site	% of mean SSL at DS	% of mean Q at DS	% of mean SSL at DS	% of mean Q at DS	% of mean SSL at DS	% of mean Q at DS	% of mean SSL at DS	% of mean Q at DS	% of mean SSL at DS	% of mean Q at DS
PS1	**8.4**	3.4	**5.4**	1.9	**5.5**	1.8	**3.9**	3.6	**5.8**	2.4
PS2	**39.4**	70.8	**42.2**	75.6	**46.7**	77.0	**32.2**	74.5	**41.6**	74.8
PS3	**13.2**	10.1	**11.1**	9.9	**11.7**	9.9	**6.7**	11.0	**11.1**	10.0
∑ PS1 + PS2 + PS3	***61.0***	*84.3*	***58.7***	*87.4*	***63.9***	*88.7*	***42.8***	*89.1*	***58.5***	*87.2*
MS	**50.7**	84.4	**52.0**	87.5	**56.4**	88.6	**43.2**	88.2	**51.5**	87.1
RPT	**46.5**	15.9	**52.3**	13.1	**52.1**	11.7	**43.4**	14.3	**49.2**	13.4
∑MS+RPT	***97.2***	*100.4*	***104.3***	*100.6*	***108.5***	*100.3*	***86.6***	*102.5*	***100.7***	*100.5*
DS	***100***	*100*	***100***	*100*	***100***	*100*	***100***	*100*	***100***	*100*
*****	***(59158)***	*(3.60)*	***(68252)***	*(3.69)*	***(59865)***	*(3.69)*	***(444324)***	*(8.05)*	***(74577)***	*(3.81)*

* Mean SSL (kg/day) and Q (m^3/s) have been included for DS for back calculation purposes; also refer to Table 4.2.

Streamflow was assumed to be conservative throughout the monitoring period in order to compute Q for RPT and PS3 (*section 2.4.2*, equations 5 and 6), as such, there is net balance between upstream and downstream sites (Table 4.3 and Figure 4.1). Suspended sediment load inputs totalling more (or less) than 100% of the SSL at a downstream monitoring site indicate sediment storage (or erosion) within that reach. Based on the longitudinal stream profile (Figure 2.3, *section 2.1.3*) and site observations, in channel storage had the greatest potential to occur on the low gradient outwash fan complex immediately upstream of MS, and there was not likely a significant amount of suspended sediment stored within the reach MS-DS during any meteorological conditions.

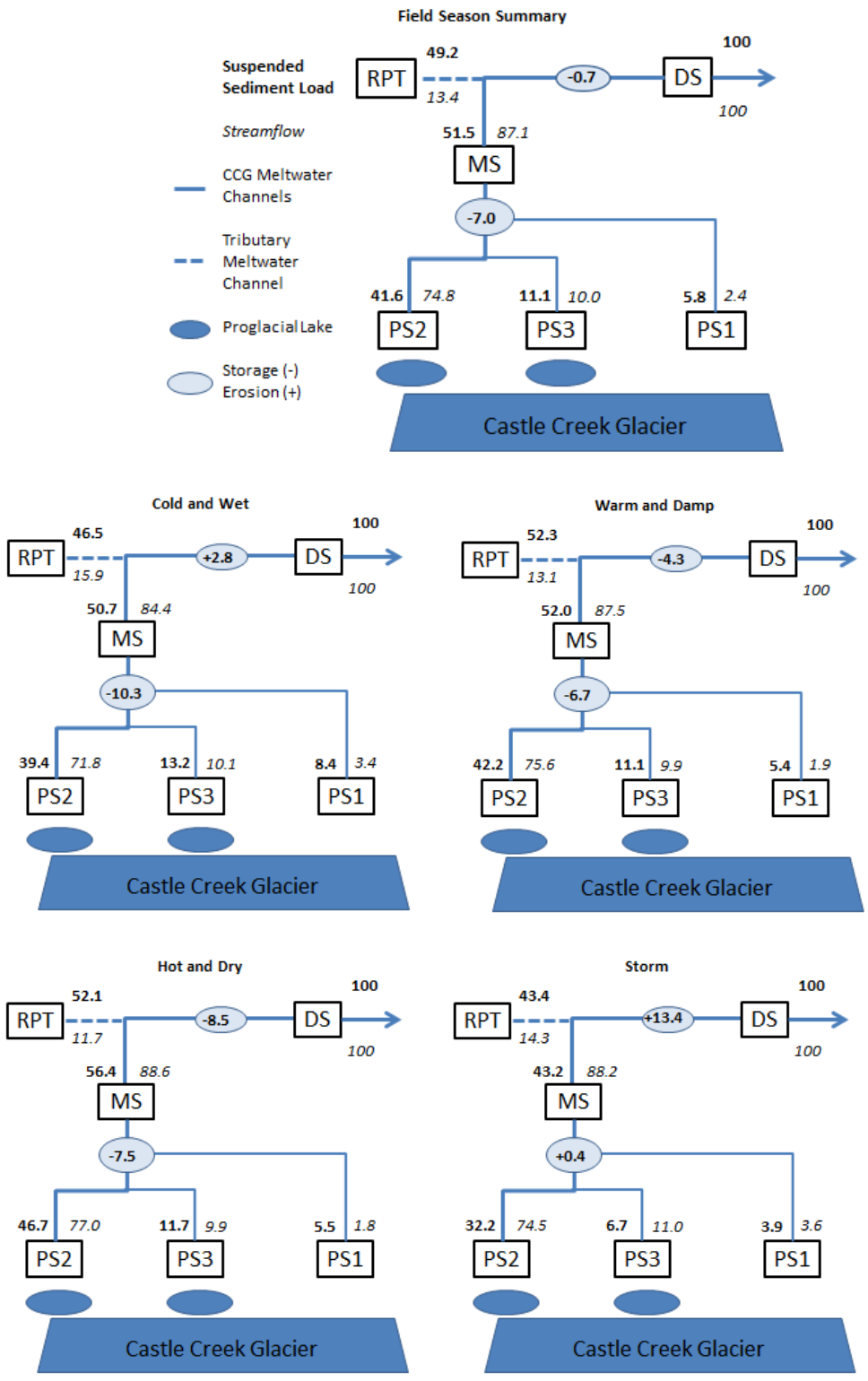

Figure 4.1 – Percent (%) contribution of suspended sediment load (SSL) and streamflow (Q) relative to the total at DS over the 2011 field season and during the four defined hydro-meteorological categories – schematic diagram.

Differences in source contribution to the total SSL at DS during the defined hydro-meteorological categories are apparent in Table 4.3 and Figure 4.1. While the mean daily SSL and Q were similar during ‘cold and wet’ and ‘hot and dry’ conditions at the catchment outlet (Table 4.3), the percent contribution to the total from the monitoring locations varies (Figure 4.1). Glacial melt decreased during ‘cold and wet’ conditions, precipitation activated some in channel and proglacial sediment sources, but low stream competency allowed storage on the outwash fan complex. There is more contribution from PS2 during ‘hot and dry’ conditions in response to ablation Figure 4.1. Comparing between ‘warm and damp’ and ‘hot and dry’, Q values were very similar, but the mean SSL is greater for ‘warm and damp’ conditions and less SSL is derived from the proximal sites.

The seasonal average SSL at MS was 7% less than the input from the three proximal sites, which indicated net channel storage between the monitoring locations. The amount of storage on the outwash fan varied slightly over the three main hydro-meteorological periods; however, during the observed ‘storm’ events, the output from the three proximal stations was slightly less than the SSL at MS. The increase was attributed to sediment contribution from channel bed and bank erosion between the proximal sites and MS associated with high water levels and stream competency. As a seasonal average, the combined SSL of MS and RPT was nearly equal to the SSL at DS, which meant that on average the MS-DS reach was a transport reach. ‘Hot and dry’ and ‘warm and damp’ meteorological conditions show that there was, respectively, 8.5% and 4.3% storage within the MS-DS reach, and ‘cold and wet’ meteorological conditions show 2.8% increase in the MS-DS reach (Figure 4.1). This flux is well within the range of uncertainty of the results (*section* 3.1.4). During ‘storm’ events, the

SSL for the MS-DS reach increased to 13.4%, which was probable given the contribution from channel bed and channel bank erosion, and the contribution from ephemeral channels that drained diffuse proglacial sediment sources. The reach MS-DS had the most ephemeral channels; during the JD 234 ‘storm’ event grab samples from these streams were measured at *c.* 4000 mg/L.

As a seasonal average, RPT supplied 49% of the SSL, but only 13% of the Q at DS, while the respective values for the three proximal sites were 59% and 87% of the SSL and Q Figure (4.1). These values not only highlight the dominance of the glacier on SSL and Q, but also the strong influence of a relatively small sediment laden tributary in the overall suspended sediment budget. Aside from RPT, PS2, the main meltwater channel emanating from the glacier, contributed the majority of the SSL throughout the field season, varying between 32% during ‘storm’ events and 47% during ‘hot and dry’ periods.

As a result of Tu range exceedances, there was greater uncertainty within the RPT analysis. There were 12 days in the RPT SSC time-series that had exceedances filled based on discrete and composite daily SSC samples (*section 3.1.3*). These 12 days account for 6%, 33%, 19%, and 50% of the RPT data for ‘cold and wet’, ‘warm and damp’, ‘hot and dry’, and ‘storm’ event periods, respectively. The estimates are reasonable, given the available information, but compromise the accuracy in the MS-DS reach. The deductive method used to compute Q for RPT strictly assumed that there were no other inflows in the MS-DS reach, which was false during intense precipitation events when ephemeral channels became active and contributed to streamflow; similarly, spring snowmelt could also concentrate in ephemeral channels and deliver sediment from diffuse proglacial sources to glacial meltwater

channels (Richards and Moore 2003; Orwin and Smart 2004a). This assumption in the Q computation affects SSL at RPT and creates additional uncertainty in the reach MS-DS.

In Table 4.4, values are computed based on the seasonal total SSL and seasonal mean Q to show the contribution during the specified meteorological category for each of the sites.

Table 4.4 Meteorological summary of suspended sediment load (SSL) and streamflow (Q) for each site. Values computed as a percentage of the seasonal total SSL (t/day) and seasonal mean Q (m^3/s). Raw values and the number of days of observation for each site in each category are presented in Table 4.2.

Meteorological period	Cold and Wet 28% (17 days)		Warm and Damp 25% (15 days)		Hot and Dry 44% (26 days)		Storm 3% (2 days)		Seasonal 100% (60 days)	
Site	% of seasonal SSL	% of seasonal Q	% of seasonal SSL	% of seasonal Q	% of seasonal SSL	% of seasonal Q	% of seasonal SSL	% of seasonal Q	Total SSL ($x10^3$ kg)	Mean Q (m^3/s)
PS1	**32**	38	**21**	19	**34**	34	**14**	11	**251**	0.09
PS2	**21**	25	**23**	25	**39**	43	**16**	7	**1733**	2.85
PS3	**29**	27	**24**	24	**35**	41	**13**	8	**437**	0.38
∑ PS1 + PS2 + PS3	***24***	*26*	***23***	*24*	***37***	*43*	***16***	*7*	***2421***	*3.36*
MS	**22**	26	**23**	24	**38**	43	**17**	7	**2307**	3.32
RPT	**21**	32	**24**	24	**37**	37	**18**	8	**2201**	0.51
DS	**22**	27	**23**	24	**35**	42	**20**	7	**4475**	3.81
DS-RPT	***24***	*26*	***22***	*24*	***33***	*43*	***22***	*7*	***2274***	*3.30*

% seasonal Q values weighted based on number of days of observation

The two 'storm' days accounted for 3% of the duration of the field season, *c.* 7% of the Q (with the exception of PS1), and 13 – 20% of the SSL (Table 4.4). Interestingly, 20% of the SSL at DS occurred during the 'storm' events, which was *c.* 4% higher than PS2 and MS, and 2.5% higher than RPT. The higher sediment load at DS was likely due to the contribution of sediment from diffuse proglacial sources via ephemeral channels in the reach MS-DS. Sites PS1 and PS3 had a lower percent of their total SSL transported during 'storm' events than PS2, which was likely because of the dominance of bedrock in the PS1 catchment and glacial ice in the PS3 catchment. During the field season, PS1 and PS3 had a

substantial and sustained influence from meltwater flowing over fresh moraine deposits, whereas PS2 emanated from a subglacial meltwater channel portal with a well-established channel bed. Site MS shows influence from PS1 and PS3 in each of the meteorological periods. However, the response pattern of MS was very similar to PS2 because 75% and 86% of the seasonal SSL and Q, respectively, was derived from PS2. The SSL at PS2 showed a greater increase with 'storm' events than the other proximal sites because unconsolidated extra-channel sediment sources proximal or adjacent to the glacier were activated by precipitation and increased streamflow (Table 4.4).

Daily suspended sediment yield (SSY) in Table 4.5 was computed by dividing the mean SSL for a given period (Table 4.2) by the watershed area (Table 2.1, *section 2.1.2*). For total yield, the mean daily SSY values were multiplied by the respective number of days of observation in the category (note that some sites were missing days, as reported in Table 4.2).

Table 4.5 Suspended sediment yield (SSY) for the Castle Creek watershed during the 2011 field season. Mean daily SSY (t/km^2/d) and Total SSY (t/km^2) for each catchment are reported.

Site (km^2)	Cold and Wet (17 days) Mean daily (Total)	Warm and Damp (15 days) Mean daily (Total)	Hot and Dry (26 days) Mean daily (Total)	Storm (2 days) Mean daily (Total)	Seasonal (60 days) Mean daily (Total)
PS1 (1.24)	4.01 (64.3)	3.00 (42.0)	2.64 (68.6)	13.9 (27.7)	3.49 (202)
PS2 (9.36)	2.48 (39.7)	3.08 (43.1)	2.99 (71.8)	15.3 (30.6)	3.30 (185)
PS3 (1.73)	4.49 (76.3)	4.37 (56.8)	4.05 (85.0)	17.1 (34.2)	4.76 (253)
MS (12.69)	2.37 (40.3)	2.80 (42.0)	2.66 (69.3)	15.1 (30.3)	3.03 (182)
RPT (2.66)	10.3 (175.9)	13.4 (201)	11.7 (305)	72.6 (145)	13.7 (827)
DS (15.68)	3.77 (64.1)	4.35 (65.3)	3.82 (99.2)	28.3 (56.6)	4.75 (285)

The total SSY from RPT during the 2011 field season was more than double that of any of the other sub-catchments. However, since RPT was a relatively small sub-catchment, the seasonal total SSY at DS was only 36% greater than MS. Interestingly, the SSY of the

proximal sites tended to be greater than the SSY of MS. However, SSY between MS and DS increased with catchment area, which, as expected (Church and Slaymaker 1989; Schiefer *et al.* 2001; Gurnell *et al.* 1996 Tunnicliffe and Church 2011), disagrees with conventional sediment yield models (Syvitski and Milliman 2007). During 'cold and wet' conditions the SSY at PS1 was greater than PS2, while it was less than PS2 for the other three meteorological conditions. Suspended sediment yield at MS was typically less than any of the proximal sites, indicating sediment storage within the proglacial channel network upstream of MS. The effect of 'storm' events on SSY was striking: compared to the seasonal mean, the minimum increase was 260% for PS3 and the maximum increase was 496% for DS. The increase for RPT, MS, PS2 and PS1 was 430%, 400%, 360%, and 300% respectively. The downstream trend of increasing relative SSY during 'storm' events was likely because of ephemeral stream inputs from diffuse proglacial sediment sources during the events. Warburton (1990) also found that a large proportion of the SSY can be generated in a short period of high stream competency, and Orwin and Smart (2004a) also found that sediment was evacuated during storm events on both of their monitored streams. This triggered response from the proglacial zone should be expected to continue, in declining magnitude, until the end of the paraglacial period (Church and Ryder 1972; Church and Slaymaker 1989; Gurnell *et al.* 1996; Ballantyne 2002a; 2002b).

In summary, 'hot and dry' conditions dominated 44% of the 2011 field season and generated the greatest portion of SSL and Q (Table 4.4), and thus, the greatest total SSY (Table 4.5). However, the mean daily SSY for 'hot and dry' conditions was less than the mean daily SSY for both the 'seasonal average' and 'warm and damp' conditions at all sites. 'Hot and dry' had similar streamflow to 'warm and damp' days but generated lower mean

daily SSL at the catchment outlet (Table 4.3). With the exception of RPT, SSL and Q were primarily derived from the glacier and, with the exception of 'storm' events, sediment storage occurred on the outwash fan complex upstream from MS (Table 4.3). 'Storm' events activated diffuse sediment sources within the proglacial zone and rapidly increased SSY at the catchment outlet to *c.* 500% of the seasonal mean. The range of SSY observed under different conditions at the CCG sites (Table 4.5) fits within the range of observations for alpine glacier systems with comparable catchment areas reported by Gurnell *et al*. (1996); and was greater than that found in a small high arctic glacier basin in Svalbard by Hodson *et al*. (1998), and greater than that found in Greenland reported and summarized by Stott *et al.* (2014). Data presented by Orwin and Smart (2004a) from the SRG have been divided into similar categories which permits a closer comparison.

The SSL results presented by Orwin and Smart have been recomputed in a format that is comparable with this present study (Appendix 7.6). Unit area SSY has not been computed for the SRG results as the catchment area for the individual sites was not reported. At the SRG, similar to this study, the least amount of sediment was generated by the glacier and entrained from the proglacial zone during 'cold and wet' conditions, and sediment was stored in low gradient reaches (Orwin and Smart 2004). 'Storm' events increased SSL by more than 400% of the seasonal mean in their north stream, but just *c.* 100% in the central stream. Although the results show that sediment was stored on the north stream during 'hot and dry' conditions, there was a *c.* 600% increase in SSL on the central stream. Orwin and Smart (2004a) attribute the increase to elevated meltwater flow that mobilized sediment stored within the channel and triggered episodic bank collapses. Their combined evidence showed that short-term storage and release of sediment in the proglacial channels at the SRG

controlled the suspended sediment response pattern. Richards and Moore (2003) also found that fine sediment was temporarily stored between proximal and distal sites at low flow, and then re-entrained at higher flow.

Overall, the differences between the results from the CCG and SRG can be partially explained by the meteorological conditions at the time of monitoring (i.e. the SRG data set was more driven by 'ablation' (55%) than the CCG data set (30%), and data collection started earlier in the ablation season). However, considering the differences between the two streams that were monitored at the SRG and the results from the CCG, the influence of catchment characteristics is highlighted. Particularly the slope and elevation range of the proglacial zone, the type and size of glacier, the stability of proglacial sediment deposits and their connectivity to the fluvial system; which are factors that have been identified previously (Harbor and Warburton 1993; Gurnell *et al.* 1996).

4.2 Proglacial Suspended Sediment Budget

A sediment budget is a useful management tool for assessing where, when and how much sediment is being entrained, transported, stored and evacuated from a watershed to the downstream aquatic environment (Slaymaker 2003; Owens 2005; Walling and Collins 2008). However, sediment budgets can be extremely difficult to establish; even for the *c.* 16 km^2 proglacial catchment in this study. Due to limited field capacity and time constraints, detailed examination of sediment sources was not possible. Field data and observations were used to infer sediment flux processes between the sites. With the information collected, a basic proglacial suspended sediment budget was developed to ascribe SSL to various sources based on the parameters defined by Warburton (1990) for the coarse and fine components of a

proglacial sediment budget (Equation 1, *section 1.6.1*). It was assumed that the error was normally distributed within the data and that the relative accuracy was valid; however, limitations and caveats apply regarding precision (*section* 3.1).

The suspended sediment contribution from the three proximal sites was a combination of direct input from the glacial meltwater stream (**GL**), and input from moraine deposits at the terminus (**M**). Based on field observations, PS1 was predominantly **M**, while PS2 was mostly (80%) **GL** and PS3 may be split equally. Based on stream slope and field observations, change in valley sandur (**ΔVS**) occurred on the outwash fan complex upstream of MS. With the exception of 'storm' events, there was sediment stored upstream of MS, which can be defined as the difference between the SSL input from the proximal sites and the SSL measured at MS. Direct hillslope inputs (**SL**) were observed along the right bank of the meltwater channel, upstream from the outwash fan and immediately downstream from the confluence of PS2 and PS3. The **SL** contribution was typically small, but episodic increases can be expected when triggered by high streamflow, precipitation, overland flow or spring snowmelt and freeze-thaw cycles. Tributary channel inputs (**TR**) to the CCG meltwater stream predominantly came from RPT, and were substantial throughout the field season. The total yield (**Y**) from the proglacial catchment was measured at DS. Following this premise, the seasonal suspended sediment load budget for the 2011 Castle Creek Glacier proglacial zone was defined as:

Y (100%) = GL (39%) + M (20%) + ΔVS (-7%) + SL (0.5%) + TR (49%) **(7)**

Values were used directly or subdivided, as stated in the preceding paragraph, from the seasonal percentage of mean daily SSL (Table 4.3) and, following the same premise, a sediment budget could be drawn from Table 4.3 for any of the meteorological categories. Equation 7 has a slight (1.5%) surplus of sediment input, thus, suggesting additional storage of sediment in the proglacial zone; however, given the error and uncertainty of the data collected, this level of precision is false accuracy and it may be reasonable to accept a net balance.

In the overall suspended sediment budget for the Castle Creek proglacial zone, **TR** from RPT was the dominant source of sediment. Aside from RPT, virtually all of the sediment enters the proglacial stream through **GL** and **M** in the active meltwater channels at the snout of the glacier, accounting for 59% of the SSL input. For the seasonal budget, **ΔVS** was computed as -7%, showing sediment storage on the fan. The balance of contribution shifts moderately under different meteorological and streamflow conditions (Tables 4.3, 4.4, and 4.5); however, 'storm' events were remarkably different and sediment contribution from the proximal sites (**GL** and **M**) became less important as **SL** and **ΔVS** increased. When **TR** from RPT is removed from the budget, the three proximal sites contributed a minimum of 76% during 'storm' events, a maximum of 133% during 'hot and dry' and a seasonal average of 115% of the SSL at DS. Thus, **M** and **GL** contributed 100% of the SSL measured at DS during the 2011 field season and excess SSL went into storage as **ΔVS**, with the exception of 'storm' events when 24% of the SSL is derived from **SL** and **ΔVS**. The CCG pilot study in 2008 found that there was an enrichment of 35% between MS and DS. This enrichment was most likely **TR** from RPT (which was not quantified in 2008), not diffuse sediment sources in the proglacial zone or the proglacial channel. In 2011, the enrichment in the same reach

was *c.* 49% as a seasonal average, which was all attributed to **TR** from RPT. As stated previously, the exception is 'storm' events when ephemeral channels are actively contributing SSL in the MS-DS reach.

Intensive field measurements were conducted by Warburton (1990) to define the proglacial fluvial sediment budget for JD 134 – JD 211 of the 1987 ablation season at the Bas Glacier d'Arolla, Switzerland. The sediment yield was measured at proximal and distal ends of a 300 m proglacial reach. At the distal site, the catchment area was *c.* 8 km^2 and 70% glaciated. Using various sampling approaches, **Y**, **SL**, **TR**, **M** and **ΔVS** were measured or estimated. Proglacial sediment sources contributed 23% of the sediment received at the catchment outlet, and 95% of that contribution was generated from bank and channel erosion of valley sandur during a short period of meltwater flooding from JD 197 – JD 199. While **SL** and **TR** accounted for a small percentage of the total SSY, the **GL** and **M** contribution accounted for *c.* 77%. The **ΔVS** was of overwhelming importance in modifying the sediment load from **GL** and four basic fluvial process subsets were identified: 1) channel marginal; 2) channel; 3) hillslope; and 4) slopewash. Since the **GL** component was estimated by quantifying the other variables and subtracting their total from the overall sediment yield, **Y**, the budget was not truly "closed", and the cumulative error in the measurement of the other terms of the equation made the estimate precise to only ± 26% (Warburton 1990).

Work by Hammer and Smith (1983) on the Hilda Glacier in Alberta found that the proglacial area between a monitoring site at the snout of the glacier and a site 1 km downstream supplied *c.* 50% of the total SSL. Orwin and Smart (2004a) found that **SL** and **ΔVS** in the proglacial zone were the source of 80% of the suspended sediment flux for the central stream, and 30% for the north stream during the 2000 ablation season at the SRG

(Appendix 7.5). They cite sediment availability within the proglacial channels, SSC and Q of glacial inputs, and contribution from extra-channel sediment sources as key differences between the streams they monitored.

The SRG is a small (*c.* 7 km^2) cirque glacier with a relatively steep and small proglacial zone (*c.* 14% and 2 km^2) compared to that of the CCG (*c.* 3% and 6 km^2) which is an alpine valley glacier (*c.* 16 km^2). Also, the deglacierized study area at the SRG had a greater elevation range (*c.* 450 m) compared to the CCG (*c.* 70 m). The differences in the characteristics of the glacier and study site may partially explain the contrasting results. However, inter-annual variability of hydro-meteorological conditions and antecedent conditions such as seasonal snowpack can strongly influence proglacial Q and SSC which would affect the results of the analyses and thus comparisons between different sites and years of data (Gurnell *et al.* 1996; Richards and Moore 2003; Swift *et al.* 2005; Cockburn and Lamoureux 2008; Haritashya *et al.* 2010).

5 Conclusions

5.1 Summary

Divergence between the Q and SSC time-series data sets is common for all sites (Figures 3.1 and 3.5), and it is clear that there is no simple relationship between Q and SSC; thus it is clear that the two variables need to be monitored independently. If Q and SSC were not monitored independently, there would be significant shortcomings in the analysis and the level of detail in the results and discussion section would not be possible. Additionally, the computation of SSL from SSC and Q is much more accurate when the variables are independent.

Objective 1 was to examine the influence of hydro-meteorological conditions on the spatial and temporal pattern of suspended sediment flux in the proglacial zone. The time series were divided into hydrologic days and principal component analysis and cluster analysis were used to categorize days of like conditions and similar suspended sediment response 'shape' and 'magnitude'. Each field season and glacier will be different, and this 2011 data set is a snap shot in time of the conditions in the proglacial zone of the Castle Creek Glacier. From this field season, the following conclusions can be made for the sites along the main Castle Creek meltwater channel:

- 'warm and damp' conditions showed a mixed SSC response pattern that was influenced by antecedent conditions;
- 'hot and dry' conditions tended to generate a 'low' magnitude, 'diurnal' SSC response;

- ‘cold and wet’ conditions tended to generate ‘medium’ or ‘low’ magnitude, ‘irregular’ SSC response;
- ‘storm’ events generated a ‘high’ magnitude, ‘irregular’ response and increased the daily mean SSL by more than 500% of the seasonal mean.

The two small proximal streams, PS1 and PS3, had more ‘diurnal’ data in the ‘cold and wet’ and ‘warm and damp’ conditions, but tended to have more ‘irregular’ data during ‘hot and dry’ days than the sites along the main meltwater channel. While the response ‘magnitude’ at RPT during ‘cold and wet’ and ‘warm and damp’ conditions tended to be lower than PS1 and PS3, the response ‘shape’ was similar. During ‘hot and dry’ conditions, there were more ‘irregular’ data at RPT. The ‘magnitude’ analysis was performed independently for each station and was influenced by the range of the data within the input matrix. It was difficult to make comparisons across sites from this analysis, but the SSC data for each site were successfully categorized into ‘high’, ‘medium’, or ‘low’ magnitude response with respect to the rest of the SSC data collected at the site.

Objective 2 was to determine the sources of Q and SSL under different hydro-meteorological conditions. Aside from the tributary input, RPT, the data collected during the 2011 field season show that glacial stream inputs and the area proximal to the snout of the glacier, exposed within the last few years, were the dominant source of suspended sediment for the majority of the field season. More than 20% of the total SSL evacuated during the field season occurred during two ‘storm’ event days that represented 3% of the field season. During ‘storm’ events, diffuse and point sediment sources throughout the proglacial zone and meltwater channels were activated by intense precipitation or high streamflow. Based on these results, we can expect SSL to be sustained with episodic pulses of high SSL from the

proglacial zone until the completion of deglaciation. Once the catchment has become deglaciated, we can expect episodic pulses of elevated SSL associated with storm events and snowmelt that activate exposed sediment sources in the previously glaciated area. These episodic pulses of high SSL are likely to continue in declining magnitude until the paraglacial period has ended and erosion rates are no different than that of an un-glaciated mountainous catchment (Ballantyne 2002a; Richards and Moore 2003).

This project has built upon the work of past researchers (e.g. Church and Ryder 1972; Hammer and Smith 1983; Warburton 1990; Gurnell *et al.* 1992; Harbor and Warburton 1993; Hodson *et al.* 1998; Hannah *et al.* 2000; Swift *et al.* 2002; Hodgkins *et al.* 2003; Richards and Moore 2003; Orwin and Smart 2004a, 2004b; Swift *et al.* 2005; Jobard and Dzikowski 2006; Stott *et al.* 2007; Stott *et al.* 2009; Moore *et al.* 2009) adding to the growing body of knowledge surrounding deglacial and proglacial processes and paraglacial sedimentation from contemporary glacial environments (Ballantyne 2002b). Most glaciers have experienced rapid recession and/or volume loss since the end of the LIA, and that trend will likely continue at an accelerating rate, even under the most conservative climate projections (Collins *et al.* 2013; Kirtman *et al.* 2013). Glaciers are a major erosive force that increase sediment load to the downstream fluvial system, especially during periods of rapid advance or retreat (Menounos *et al*. 2009). The rate of glacial erosion will likely decrease as the overburden of ice wanes (Church and Ryder 1972; Ballantyne 2002a); however, exposed sediment and channels in proglacial zones have been found to be a significant or dominant source of fine sediment during the ablation season in glaciated catchments (Gurnell *et al.* 1999; Orwin and Smart 2004a; 2004b). Fine sediment affects water quality and is the chemically active component of sediment transported by the fluvial system (Hodson *et al.*

2004; Owens *et al.* 2005). Water quantity and quality are central to life on earth and the information collected during this project may provide useful input parameters for paraglacial sedimentation in water quality modeling for glacially influenced tributaries of socially and ecologically important watersheds, such as the Fraser River basin.

5.2 Limitations

Equipment limitations have compromised the quality of the data that were collected for this study. The two primary issues were the limited number of WL loggers, and the limited range of the Tu data loggers. The four WL loggers available for the study were strategically distributed across six monitoring locations and the WL record for two sites, RPT and PS3, was deduced as the difference between the records collected at the other sites. This method strictly assumes that there is no other source of water entering the channel between the sites and neglects hyporehic interactions. The range of the Tu probes was limited by the data loggers that they were connected to; respectively, their range was 0 – 4V and 0 – 2.5V. Thus, the maximum recorded value was 2.5V, which equates to a site specific SSC (Table 2.2). The range was exceeded at four of the sites (Table 3.2) and missing data was estimated based on composite samples.

Another limitation was encountered with the stream gauging procedure; the main meltwater channel was unsafe to wade when streamflow was greater than 5 m^3/s. This limitation was partially overcome through rating curve extensions and slope-area estimation of peak flow during a high water event. Salt dilution gauging may have been a suitable way to measure flow up to 20 m^3/s (Hudson and Fraser 2005). Obtaining higher Q measurements would have increased the confidence in, or eliminated the need for rating curve extensions.

However, the amount of data that was affected by this limitation was relatively small. The distal site was the worst case, where 13% of the data were greater than the maximum gauged flow, but considered ‘valid’ based on the rating curve extension, and 0.6% of the data were considered an ‘estimate’ since they were greater than two times the maximum gauged flow (WSC 2012).

Aside from the equipment limitations, the study design would have been improved by moving the monitoring site on RPT to the main meltwater channel just upstream of the confluence with RPT. Doing this would have reduced the amount of uncertainty in the reach MS-DS. The difference between DS and the hypothetical site just upstream of the confluence with RPT would have been used to deduce the contribution from RPT. This method would have included any other contributions between the RPT confluence with Castle Creek and DS with RPT, but would have avoided much of the Tu range exceedances. Site maintenance and data collection for RPT was made difficult by high sediment load, low stream volume, and stream bed aggradation. The computations and data analysis for RPT have been the most challenging and required the most exceptions to analytical and computational procedures of all of the sites.

The hydrologic data for RPT were deduced as the difference between MS and DS, which lumps all inputs within the MS-DS reach onto one parameter, RPT. This method is flawed when ephemeral streams are flowing into the MS-DS reach. During storm events, the computations showed that these ephemeral streams contributed *c.* 25% of the SSL at DS. However, there was no streamflow attributed to these streams in the computations. Field observations were used to estimate the flow volume at 5% of the flow at DS. Overestimating the flow from RPT would have caused the SSL to be overestimated in the computations, and

thus the contribution from ephemeral streams to be underestimated. The SSC data collected at RPT and Q derived from the difference between MS and DS has helped refine suspended sediment sources within the MS-DS reach, but there is room for improvement.

The collected data for DS and MS show that there was a SSL enrichment of *c.* 49% and a *c.* 13% increase in Q in the reach, which varied with flow conditions and as the season progressed. Most of this SSL came from RPT. However, during 'storm' events and, likely, early season snowmelt, ephemeral channels that drain diffuse unstable sediment sources in the proglacial zone were also a significant source of sediment to the MS-DS reach.

Error and uncertainty in the data and the analysis were mostly addressed with caveats, using values reported by manufacturers or the work of past researchers as guidance. The 95% confidence intervals were computed and reported for the SSC data; however, the uncertainty terms for SSL values were not reported. These terms will be computed and included for future publications.

The field season did not start early enough to capture spring snowmelt due to equipment logistics and availability of the field team. At the beginning of data collection for the 2011 field season (JD 195), much of the annual snow had already melted from the proglacial zone. It would have been valuable to capture the entire ablation season in the data set.

The diurnal hydrograph was divided at 06:00; however, 08:00 may have better represented the average time of minimum flow. The effect of this difference on the results may be minimal, but it might have made parts of the 'shape' and 'magnitude' analysis more clear.

5.3 Recommendations for Future Research

The proglacial zone of the CCG has a relatively low gradient in comparison to that of the SRG, and it is possible that these two projects could serve as relative endpoints in proglacial sediment modelling for the upper Fraser River basin. As stated previously, and by other researchers, the conditions vary widely from year to year, and additional years of data may be necessary to test the repeatability of the results. For this type of data, a consistent statistical analysis technique will improve the comparability of results. The PCA and CA technique adapted by Orwin and Smart (2004a) from Hannah *et al.* (2000) was an effective method for classifying and categorizing the data; however, parts of the SSC shape and magnitude analysis were subjective, gave unclear results or were not comparable across sites. The most useful and widely applicable part of the analysis may be dividing and summarizing the SSL data based on hydro-meteorological conditions. When the data were summarized in this way it was easier to compare like-conditions from different locations, or to draw information for climate and sediment flux models, such as BQART (Syvitski and Milliman 2007), to help project sediment yield from similar glacially influenced catchments.

The focus of this study was on the sources and flux of suspended sediment within the CCG proglacial zone. However, simplifying the study design to collect SSC and Q data from one site at the outlet of several different proglacial zones over one or a few field seasons could provide a valuable and interesting data set for comparison purposes and regional modelling applications. Having SSL data from the same field season at the outlet of several different proglacial zones within a specific region would reduce the effect of inter-annual variability of hydro-meteorological conditions when making comparisons and allow the effects of catchment characteristics on suspended sediment production to be isolated. The

PCA and CA analysis that was followed for objective two of this study would be an applicable and useful comparison tool. Such a project may permit the development of more spatially precise and temporally responsive proglacial suspended sediment production parameters for modeling applications.

6 Bibliography

Arnott B. 2011. Personal Communication on site at Castle Creek Glacier, British Columbia, August 2011.

Austin MA, Buffet DA, Nicholson DJ, Scudder GGE, Stevens V (eds.). 2008. Taking Nature's Pulse: The Status of Biodiversity in British Columbia. Biodiversity BC, Victoria, B*C.* 268 pp. Available at: www.biodiversitybc.org.

Ballantyne CK. 2002a. A general model of paraglacial landscape response. *The Holocene* **12**: 371 – 376.

Ballantyne CK. 2002b. Paraglacial geomorphology. *Quaternary Science Reviews* **21**: 1935 – 2017.

Beedle MJ, Menounos B, Luckman BH, Wheate R. 2009. Annual push moraines as climate proxy. *Geophysical Research Letters* **36**, L20501.

Bogen J. 1989. Glacial sediment production and development of hydro-electric power in glacierised areas. *Annals of Glaciology* **13**: 6 – 11.

Bolch T, Menounos B, Wheate R. 2010. Landsat-based inventory of glaciers in western Canada, 1985 – 2005. *Remote Sensing of the Environment* **114**: 127 – 137.

Brown GH, Tranter M, Sharp MJ. 1996. Experimental investigations of the weathering of suspended sediment by alpine glacial meltwater. *Hydrological Processes* **10**: 579 – 597.

Church M, Ryder JM. 1972. Paraglacial sedimentation: A consideration of fluvial processes conditioned by glaciation. *Geological Society of America Bulletin* **83**: 3059 – 3072.

Church M, Slaymaker O. 1989. Disequilibrium of Holocene sediment yield in glaciated British Columbia. *Nature* **337**: 452-454.

Cockburn JMH, Lamoureux SF. 2008. Hydroclimatic controls over seasonal sediment yield in two adjacent high arctic watersheds. *Hydrological Processes* **22**: 2013 – 2027.

Collins M, Knutti R, Arblaster J, Dufresne J-L, Fichefet T, Friedlingstein P, Gao X, Gutowski WJ, Johns T, Krinner G, Shongwe M, Tebaldi C, Weaver AJ, Wehner M. 2013. Long-term climate change: projections, commitments and irreversibility. In: *Climate Change 2013: The Physical Science Basis. Contribution of Working Group I to the Fifth Assessment Report of the Intergovernmental Panel on Climate Change.* Stocker TF, Qin D, Plattner G-K, Tignor M, Allen SK, Boschung J, Nauels A, Xia Y, Bex V, Midgley PM (eds.). Cambridge University Press, Cambridge, United Kingdom and New York, NY, USA.

Déry SJ. 2011. Personal Communication at University of Northern British Columbia.

Déry SJ, Stahl K, Moore RD, Whitfield PH, Menounos B, Burford JE. 2009. Detection of runoff timing changes in pluvial, nival and glacial rivers of western Canada. *Water Resources Research* **45**: W04426, DOI: 10.1029/2008WR006975.

Dirszowsky RW. 2004. Bed sediment sources and mixing in the glacierised upper Fraser River watershed, east-central British Columbia. *Earth Surface Processes and Landforms* **29**: 533 – 552.

Eaton BC, Moore RD, Giles TR. 2010. Forest fire, bank strength and channel instability: the 'unusual' response of Fishtrap Creek, British Columbia. *Earth Surface Processes and Landforms* **35**: 1167 – 1183.

Filliben JJ. 1975. The probability plot correlation coefficient test for normality. *Technometrics* **17**: 111 – 117.

Filliben JJ, Devaney J. 2013. Critical values of the normal PPCC distribution. NIST/SEMATECH *e-Handbook of Statistical Methods.* http://www.itl.nist.gov/div898/handbook/eda/section3/eda3676.htm. Accessed 01-03-2014.

Ginting D, Mamo M. 2006. Measuring runoff-suspended solids using an improved turbidometer method. *Journal of Environmental Quality* **35**: 815 – 823.

Gippel CJ. 1989. The use of turbidimeters in suspended sediment research. *Hydrobiologia* **176/177**: 465 – 480.

Gurnell AM, Fenn CR. 1984. Box-Jenkins transfer function models applied to suspended sediment concentration-discharge relationships in a proglacial stream. *Arctic and Alpine Research* **16**: 93 – 106.

Gurnell AM, Clark MJ, Hill CT, Greenhalgh J. 1992. Reliability and representativeness of a suspended sediment concentration monitoring program for a remote alpine proglacial river. *International Association of Hydrological Sciences Publication* **210**: 191 – 200.

Gurnell AM, Hannah D, Lawler D. 1996. Suspended sediment yield from glacier basins. *Erosion and Sediment Yield: Global and Regional Perspectives* (Proceedings of the Exeter Symposium, July 1996). JAHS **236**, 1996.

Gurnell AM, Edwards PJ, Petts GE, Ward JV. 1999. A conceptual model for an alpine proglacial river channel evolution under changing climatic conditions. *Catena* **38**: 223 – 242.

Hammer KM, Smith ND. 1983. Sediment production and transport in a proglacial stream: Hilda Glacier, Alberta, Canada. *Boreas* **12**, 91 – 106.

Hannah DM, Smith BPG, Gurnell AM, McGregor GR. 2000. An approach to hydrograph classification. *Hydrological Processes* **14**: 317 – 338.

Hallet B, Hunter L, Bogen J. 1996. Rates of erosion and sediment evacuation by glaciers: a review of field data and their implications. *Global and Planetary Change* **12**: 213 – 235.

Harbor J, Warburton J. 1993. Relative rates of glacial and nonglacial erosion in alpine environments. *Arctic and Alpine Research* **25**: 1 – 7.

Haritashya UK, Kumar A, Singh P. 2010. Particle size characteristics of suspended sediment transported in meltwater from the Gangotri Glacier, central Himalaya – An indicator of subglacial sediment evacuation. *Geomorphology* **122**, 140 – 152.

Hodgkins R, Cooper R, Wadham J, Tranter M. 2003. Suspended sediment fluxes in a high-arctic glacierised catchment: implications for fluvial sediment storage. *Sedimentary Geology* **162**: 105 – 117.

Hodson A, Gurnell A, Tranter M, Bogen J, Hagen JO, Clark M. 1998. Suspended sediment yield and transfer processes in a small High-Arctic glacier basin, Svalbard. *Hydrological Processes* **12**: 73 – 86.

Hodson AJ, Ferguson RI. 1999. Fluvial suspended sediment transport from cold and warm-based glaciers in Svalbard. *Earth Surface Processes and Landforms* **24**: 957 – 974.

Hodson A, Mumford P, Lister D. 2004. Suspended sediment and phosphorus in proglacial rivers: bioavailability and potential impacts upon the P status of ice-marginal receiving waters. *Hydrological Processes* **18:** 2409 – 2422.

Hodson A, Anesio AM, Tranter M, Fountain A, Osborn M, Priscu J, Laybourn-Parry J, Sattler B. 2008. Glacial ecosystems. *Ecological Monographs* **78(1)**: 41 – 67.

Hudson R, Fraser J. 2005. Introduction to salt dilution gauging for streamflow measurements part IV: the mass balance (or dry injection) method. *Streamline Watershed Management Bulletin* **9/1**: 6 – 12.

Jacobs JL, Dinman JD. 2013. Systematic analysis of bicistronic reporter assay data. http://dinmanlab.umd.edu/statistics/tutorial.html#0. Accessed 02-04-2013.

Jobard S, Dzikowski M. 2006. Evolution of glacier flow and drainage during the ablation season. *Journal of Hydrology* **330**: 663 – 671.

Kirtman B, Power SB, Adedoyin JA, Boer GJ, Bojariu R, Camilloni I, Doblas-Reyes FJ, Fiore AM, Kimoto M, Meehl GA, Prather M, Sarr A, Schär C, Sutton R, van Oldenborgh GJ, Vecchi G, Wang HJ. 2013. Near-term climate change: projections and predictability. In: *Climate Change 2013: The Physical Science Basis. Contribution of Working Group I to the Fifth Assessment Report of the Intergovernmental Panel on Climate Change.* Stocker TF, Qin D, Plattner G-K, Tignor M, Allen SK, Boschung J, Nauels A, Xia Y, Bex V, Midgley PM (eds.). Cambridge University Press, Cambridge, United Kingdom and New York, NY, USA.

Lawson DE. 1995. Sedimentary and hydrologic processes within modern terrestrial valley glaciers. In *Modern Glacial Environments Processes, Dynamics and Sediments.* Menzies J (ed.). Glacial Environments: Volume 1, Butterworth-Heinemann; **Ch. 11**: 337 – 362.

McVan 2003. Analite 180 and 190 series manual. Copyright 1995-2003 - McVan Instruments PTY. LTD.

Menounos B, Clague JJ, Gilbert R, Slaymaker O. 2005. Environmental reconstruction from varve network in the southern Coast Mountains, British Columbia, Canada. *The Holocene* **15**: 1163 – 1171.

Menounos B, Osborn G, Clague JJ, Luckman BH. 2009. Latest Pleistocene and Holocene glacier fluctuations in western Canada. *Quaternary Science Reviews* **28**: 2049 – 2074.

Milner AM, Brown LE, Hannah DM. 2009. Hydroecological response of river systems to shrinking glaciers. *Hydrological Processes* **23**: 62 – 77.

Moore RD, Fleming SW, Menounos B, Wheate R, Fountain A, Stahl K, Holm K, Jakob M. 2009. Glacier change in western North America: influences on hydrology, geomorphic hazards and water quality. *Hydrological Processes* **23**: 42 – 61.

Morehead MD, Syvitski JP, Hutton EWH, Peckham SB. 2003. Modeling the temporal variability in the flux of sediment from ungauged river basins. *Global Planetary Change* **39**: 95-110.

Naden PS. 1988. *Modeling Geomorphic Systems, Chapter 8: Models of suspended sediment in natural streams,* edited by M. G. Anderson, John Wiley & Sons Ltd.

Navratil O, Esteves M, Legout C, Gratiot N, Nemery J, Willmore S, Grangeon T. 2011. Global uncertainty analysis of suspended sediment monitoring using turbidimeter in a small mountainous river catchment. *Journal of Hydrology* **398**: 246 – 259.

O'Connor BP. 2000. SPSS and SAS programs for determining the number of components using parallel analysis and Velicer's MAP test. *Behavior Research Methods, Instrumentation, and Computers* **32(3)**: 396-402.

Onset 2013. Hoboware User's Guide. www.onsetcomp.com.

Orwin JF, Smart C*C.* 2004a. Short-term spatial and temporal patterns of suspended sediment transfer in proglacial channels, Small River Glacier, Canada. *Hydrological Processes* **18**: 1521 – 1542.

Orwin JF, Smart C*C.* 2004b. The evidence for paraglacial sedimentation and its temporal scale in the deglacierizing basin of Small River Glacier, Canada. *Geomorphology* **58**: 175 – 202.

Orwin JF, Smart C*C.* 2005. An inexpensive turbidimeter for monitoring suspended sediment. *Geomorphology* **68**: 3 – 15.

Owens PN. 2005. Conceptual models and budgets for sediment management at the river basin scale. *Journal of Soils and Sediments* **5**: 201 – 212.

Owens PN, Batalla R, Collins AJ, Gomez B, Hicks DM, Horowitz AJ, Kondolf GM, Marden M, Page MJ, Peacock DH, Petticrew EL, Salomons W, Trustrum NA. 2005. Fine-grained sediment in river systems: environmental significance and management issues. *River Research and Applications* **21**: 693 – 717.

Pickup G. 1988. *Modeling Geomorphic Systems, Chapter 7: Hydrology and sediment models.* Anderson MG (ed.). John Wiley & Sons Ltd.

Resource Inventory Standards Committee (RISC). 2009. Manual of British Columbia Hydrometric Standards. *Prepared by the Ministry of Environment Science and Information Branch.* **V 1.0.** http://www.ilmb.gov.bc.ca/risc. Accessed 07-06-11.

Richards G, Moore RD. 2003. Suspended sediment dynamics in a steep, glacier-fed mountain stream, Place Creek, Canada. *Hydrological Processes* **17**: 1733 – 1753.

Ritter D, Kochel C, Miller J. 2002. *Process Geomorphology.* Fourth Edition. McGraw-Hill Higher Education.

Schiefer E, Slaymaker O, Klinkenberg B. 2001. Physiographically controlled allometry of specific sediment yield in the canadian Cordillera: a lake sediment-based approach. *Geografiska Annaler* **83(A)**: 55 – 65.

Schiefer E, Menounos B, Wheate R. 2007. Recent volume loss of British Columbian glaciers, Canada. *Geophysical Research Letters* **34**: L16503. doi: 10.1029/2007GL030780, 2007.

Scheifer E, Hassan MA, Menounos B, Pelpola CP, Slaymaker O. 2010. Interdecadal patterns of total sediment yield from a montane catchment, southern Coast Mountains, British Columbia, Canada. *Geomorphology* **118**: 207 – 212.

Shea J. 2011. Personal Communication at University of Northern British Columbia, Prince George.

Slaymaker O. 2003. The sediment budget as conceptual framework and management tool. *Hydrobiologia* **494**: 71 – 82.

Stott TA, Grove J. 2001. Short-term discharge and suspended sediment fluctuations in the proglacial Skeldal River, NE Greenland. *Hydrological Processes* **15**: 407 – 423.

Stott TA, Mount NJ. 2007. Alpine proglacial suspended sediment dynamics in warm and cool ablation seasons: Implications for global warming. *Journal of Hydrology* **332**: 259-270.

Stott TA, Owens PN, Forrester BJ, Lee J. 2009. Suspended Sediment Fluxes in the Castle Creek Glacier Proglacial Zone, Cariboo Mountains, British Columbia. *Innovations in Practice* **3**: 49-70.

Stott T, Nuttall A-M, Biggs E. 2014. Observed run-off and suspended sediment dynamics from a minor glacierised basin in south-west Greenland. *Geografisk Tidsskrift-Danish Journal of Geography* , doi: 10.1080/00167223.2013.862911.

Swift DA, Nienow PW, Spedding N, Hoey TB. 2002. Geomorphic implications of subglacial drainage configuration: rates of basal sediment evacuation controlled by seasonal drainage system evolution. *Sedimentary Geology* **149**: 5 – 19.

Swift DA, Nienow PW, Hoey TB, Mair DWF. 2005. Seasonal evolution of runoff from Haut Glacier d'Arolla, Switzerland and implications for glacial geomorphic process. *Journal of Hydrology* **309**: 133 – 148.

Swada M, Johnson PG. 2000. Hydrometeorology, suspended sediment and conductivity in a large glacierised basin, Slims River, Yukon Territory, Canada (1993 – 94). *Arctic* **53**: 101-117

Syvitski JPM, Milliman JD. 2007. Geology, geography, and Humans battle for dominance over the delivery of fluvial sediment to the coastal ocean. *The Journal of Geology* **115**: 1 – 19.

Tabachnick BG, Fidell LS. 1989. Using multivariate statistics, second edition. Harper Collins Publishers, Inc.

Tennant C, Menounos B, Wheate R, Clague JJ. 2012. Area change of glaciers in the Canadian Rocky Mountains, 1919 to 2006. *The Cryosphere* **6(6)**: 1541-1552.

Tunnicliffe JF, Church M. 2011. Scale variation of post-glacial sediment yield in Chilliwack Valley, British Columbia. *Earth Surfaces Processes and Landforms* **36**: 229 – 243.

Walling DE. 1978. Reliability considerations in the evaluation and analysis of river loads. *Zeitschrift fur Geomorphologie*, Supplementband **29**: 29 – 42.

Walling DE. 2005. Tracing suspended sediment sources in catchments and river systems. *Science of the Total Environment* **344**: 159 – 184.

Walling DE, Collins AL. 2008. The catchment sediment budget as a management tool. *Environmental Science and Policy* II: 136 – 143.

Warburton J. 1990. An alpine proglacial fluvial sediment budget. *Geografiska Annaler* **72(A)**: 261 – 272.

Water Survey of Canada (WSC). 2012. Hydrometric manual: data computations. Weather and Environmental Monitoring Directorate, issued under the authority of the Assistant Deputy Minister, Meteorological Services of Canada. qSOP-NA037 (Beta Version) 2012-12-17. Water Survey of Canada. http://www.wsc.ec.gc.ca

7 Appendix

7.1 Hydrometric

Barometric Data:

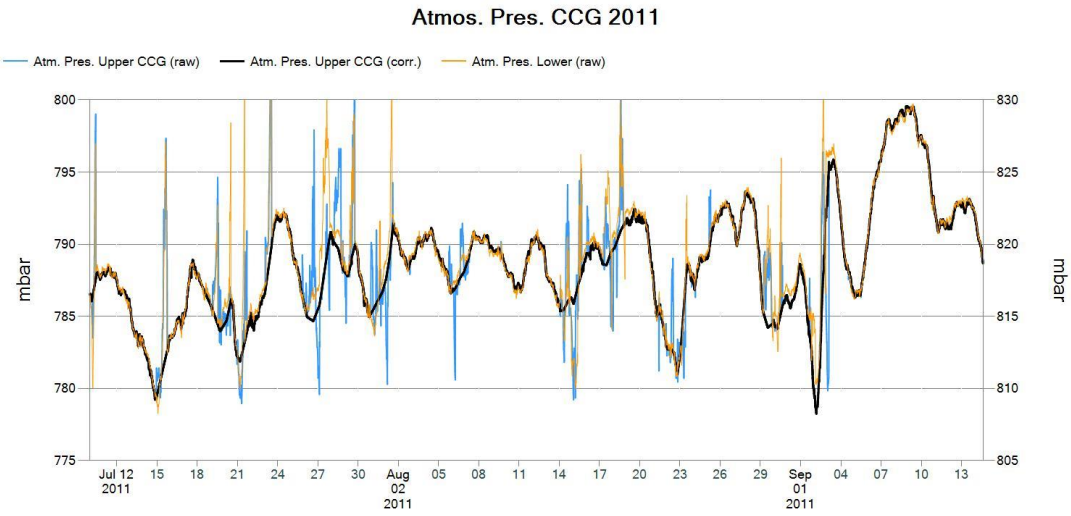

Figure 7.1 Barometric pressure from Castle Creek Glacier upper and lower meteorological stations. Rate of change threshold used to remove erroneous raw data, time-series averaged to give corrected time-series for use in computations.

Rating Curves:

The relationship between Q and WL can change over time, and thus, it is necessary to apply ‘shifts’ to the base rating curve to compensate for changes in water level reference point, section control, or channel control. A change in the WL reference point will affect the entire relationship by the same value and can be compensated for with a single offset shift. Section control often defines the lower end of the rating curve and is affected by scour and aggradation processes that have a greater influence on the lower end of the relationship.

Changes to section control can be compensated for with “knee-bend” shifts; however, the point at which the shift blends back onto the base rating curve may be difficult to define with limited data. Channel control defines the upper end of the rating curve and refers to the general configuration of the stream such as flood plain elevations, breakpoints, channel slope and width which tend to be more stable over time.

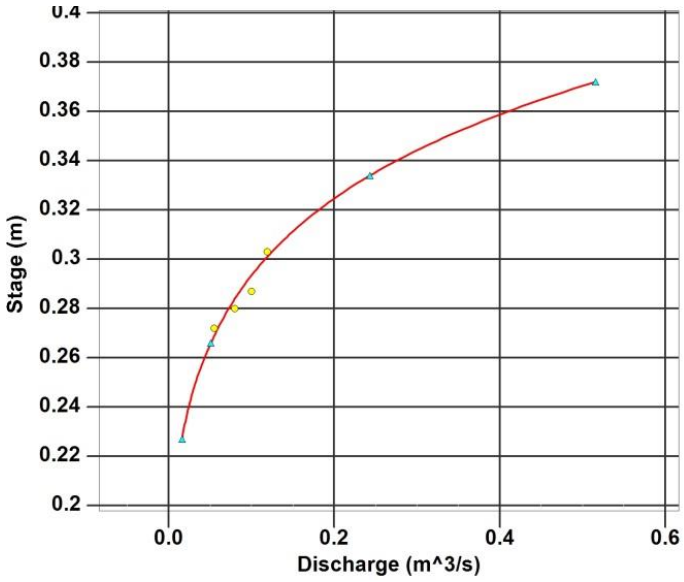

Figure 7.2 PS1 rating curve. No shifts applied.

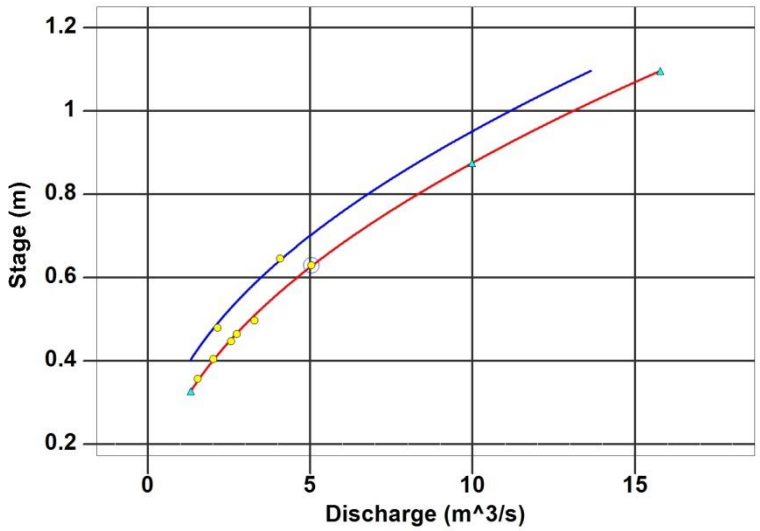

Figure 7.3 PS2 rating curve. The shift applies to data after Aug. 22, 2011; the site was moved just before the high flow event. Data considered an estimate above 10 m^3/s.

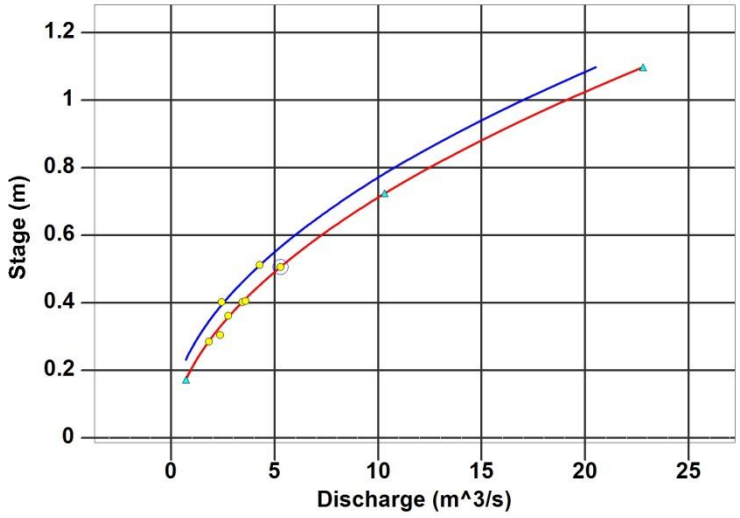

Figure 7.4 MS Rating curve. The shift accounts for stilling well movement during the Aug. 22 event, and is applied to data thereafter. Data considered an estimate above 10 m^3/s.

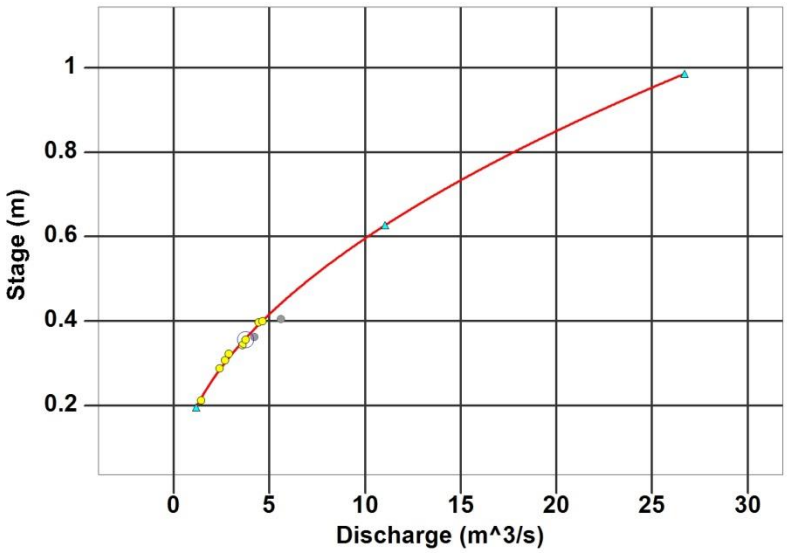

Figure 7.5 DS rating curve. No shifts applied. The two grey rating points are outside acceptable range of 5%, and were not used for rating curve development. Data considered an estimate above 10 m^3/s.

7.2 Suspended Sediment

Floating apparatus used to collect Tu and SSC samples:

Tu – SSC computations

Table 7.1 Fourth-spread method Tu - SSC

Site	PS1*	PS2	PS3*	MS	RPT	DS
q(100)	707.41	2506.653	585.65	3205.77	997.77	970.72
q(75)	399.40	356.01	263.59	279.09	467.36	418.37
Median, x~	289.27	292.22	172.27	232.70	371.96	371.39
q(25)	270.67	254.29	138.96	198.35	249.41	311.89
q(0)	177.31	128.22	100.03	96.50	111.08	76.46
fourth spread	128.73	101.72	124.63	80.74	217.95	106.48
upper outlier boundary	482.36	444.81	359.21	353.81	698.88	531.11
lower outlier boundary	96.18	139.64	-14.68	111.58	45.04	211.67
Number of samples (n)	24	205	110	202	179	183
Outliers?	6	49	28	26	4	14
Actual Sample Size (N)	**18**	**156**	**82**	**176**	**175**	**169**
mean, xbar	279.73	274.82	161.15	230.09	361.57	361.32
VAR(xbar)	2815.30	1392.81	1155.56	2249.15	17315.3	4864.57
STDEV(xbar)	53.06	37.32	33.99	47.43	131.59	69.75
Standard Error, se(xbar)	12.51	2.99	3.75	3.57	9.95	5.37
PPCC	0.9939	0.9960	0.9883	0.9943	0.9904	0.9940
Critical Value (0.05)	0.9452	0.9913	0.9842	0.9921	0.9921	0.9919
Normal?	YES	YES	YES	YES	**NO**	YES
Min. Sample Size (N~)	56	29	69	66	204	58

If Probability Plot Correlation Coefficient > Critical Value then we fail to reject that the data is drawn from a population with a normal distribution.

*additional outlier (s) removed qualitatively prior to "F-S Method", PS1 =1, PS3=8

Normal Probability Plots:

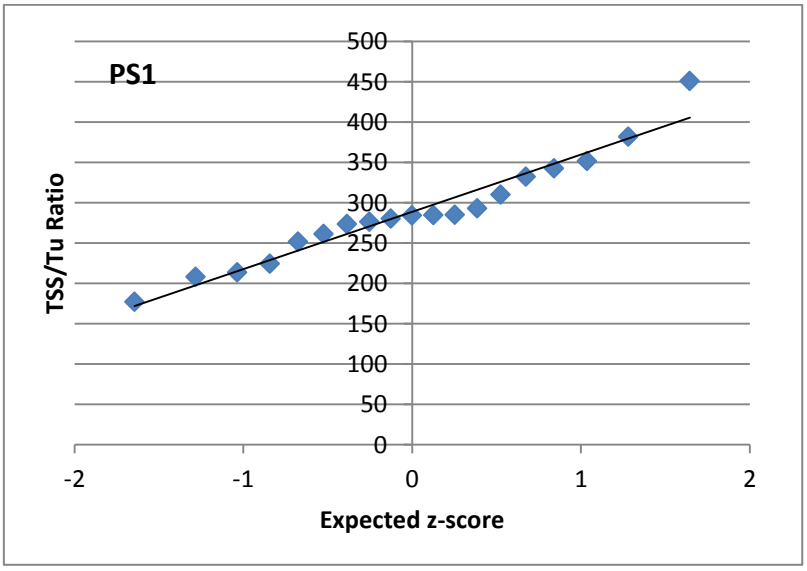

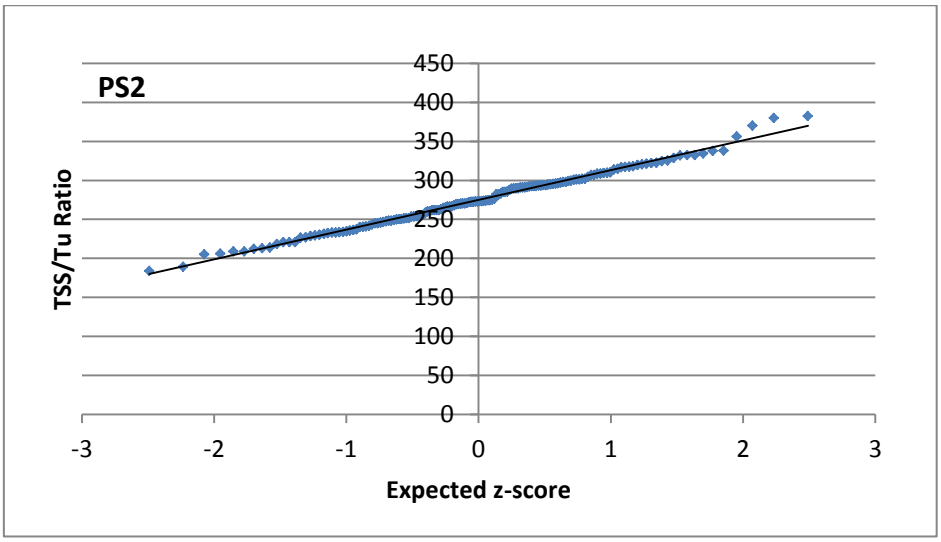

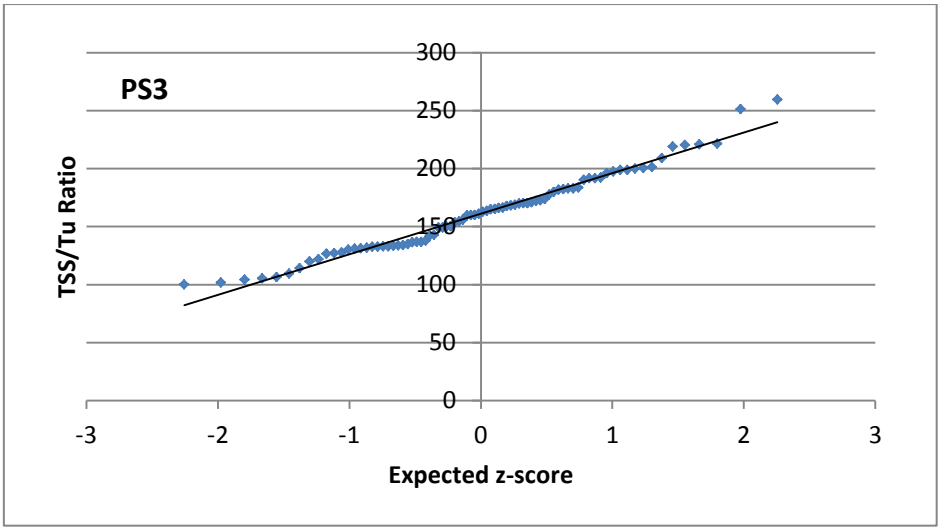
PS3
TSS/Tu Ratio
300
250
200
150
100
50
0
-3
-2
-1
0
1
2
3
Expected z-score

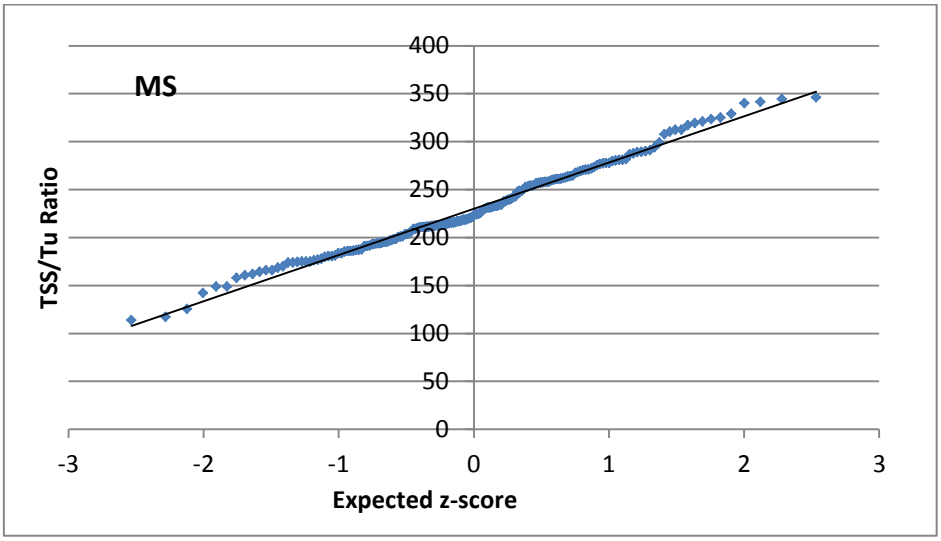
MS
TSS/Tu Ratio
400
350
300
250
200
150
100
50
0
-3
-2
-1
0
1
2
3
Expected z-score

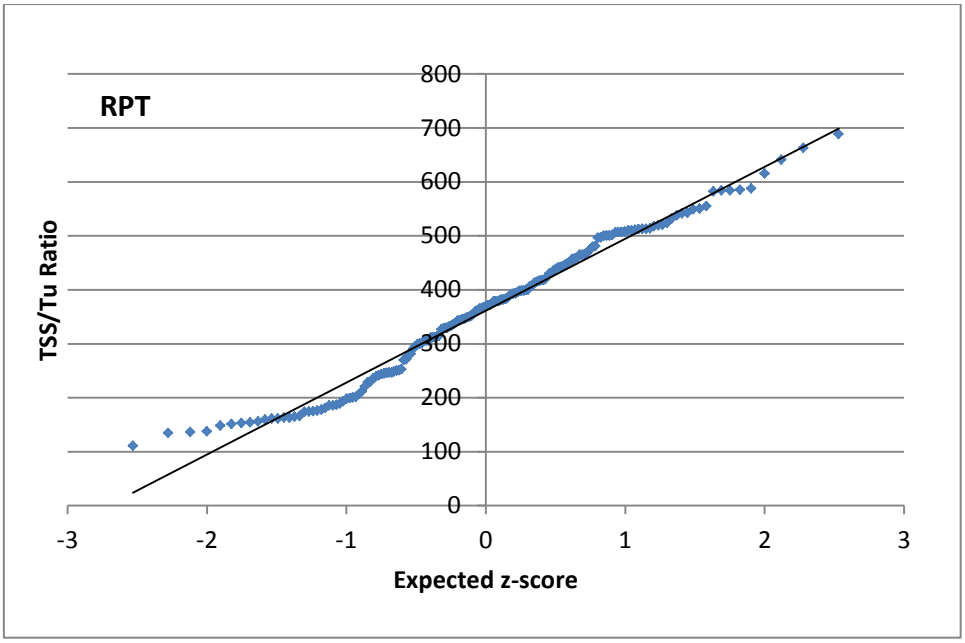
RPT
TSS/Tu Ratio
800
700
600
500
400
300
200
100
0
-3
-2
-1
0
1
2
3
Expected z-score

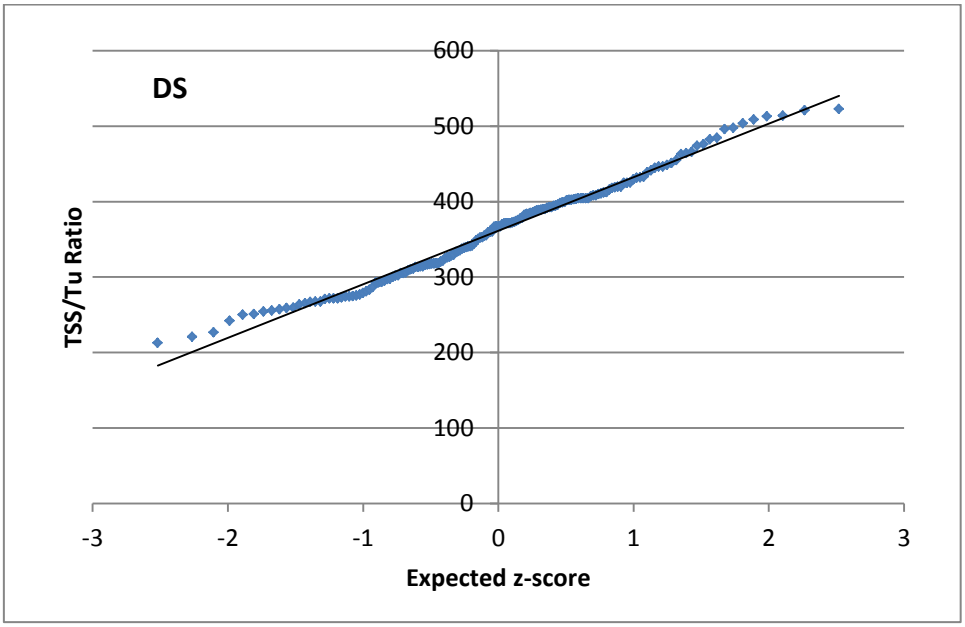
DS
TSS/Tu Ratio
600
500
400
300
200
100
0
-3
-2
-1
0
1
2
3
Expected z-score

	PS1	PS2	PS3	MS	RPT	DS
SSC Samples	24	205	110	202	179	183
Corroded samples	n/a	47	22	23	n/a	n/a
Outliers	6	2	6	3	4	14
Actual Sample (N)	18	156	81	176	175	169
Normality	Yes	Yes	Yes	Yes	No	Yes
Equation, y=	305x-54	252x+9	183x-28	213x+8	469x-107	413x-23
R^2 value	0.43	0.79	0.85	0.67	0.76	0.77
95% C.I. (Δy)	57.6	2.8	9.1	3.6	20.5	5.4

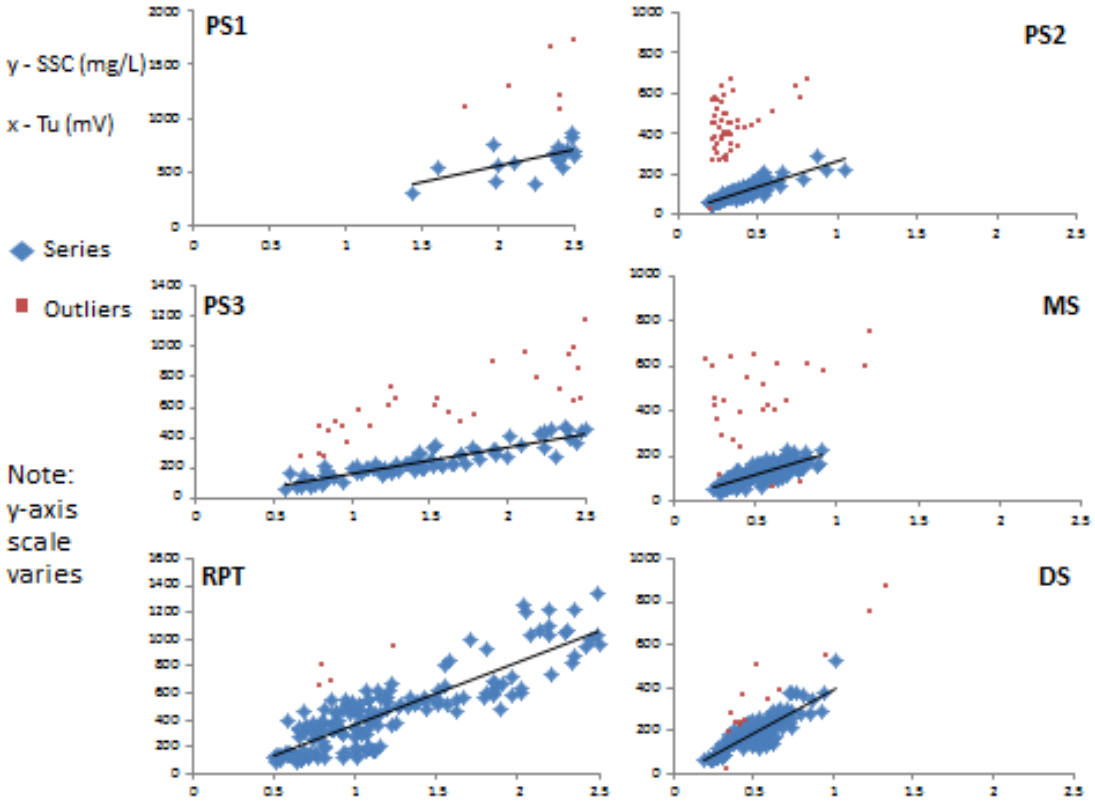

Figure 7.6 Turbidity and suspended sediment concentration regressions; all outliers presented

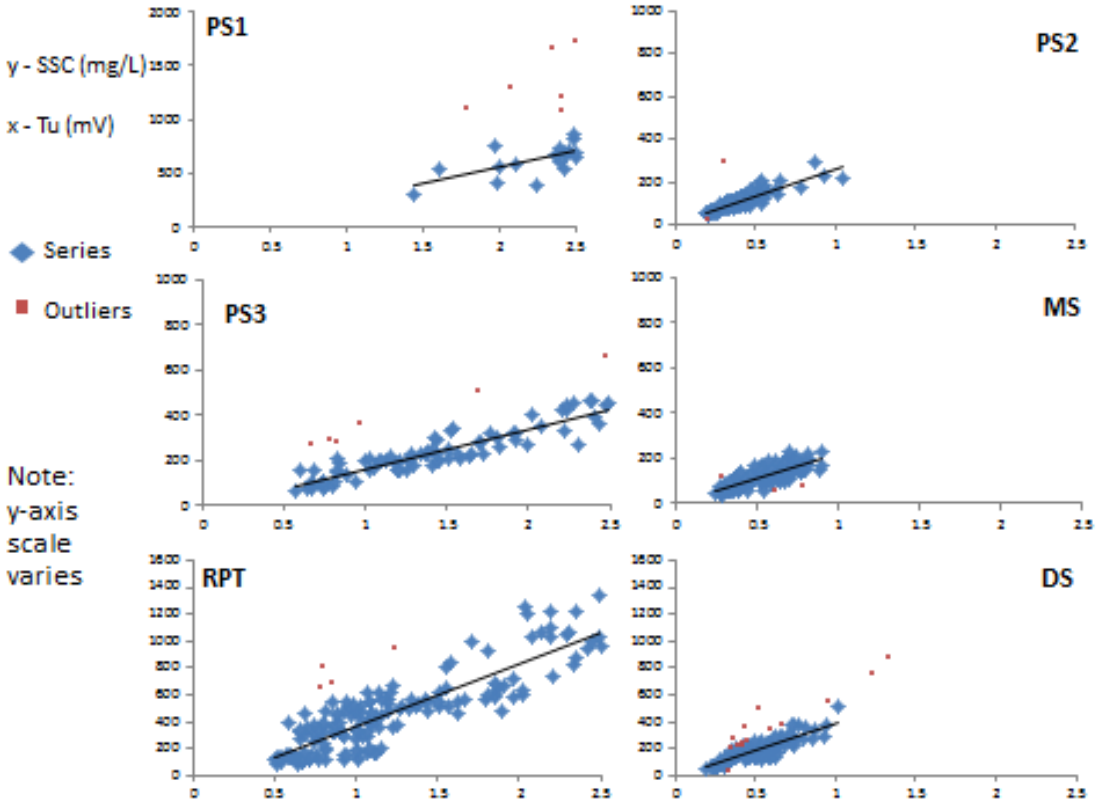

Figure 7.7 Turbidity and suspended sediment concentration regressions. Corroded samples removed.

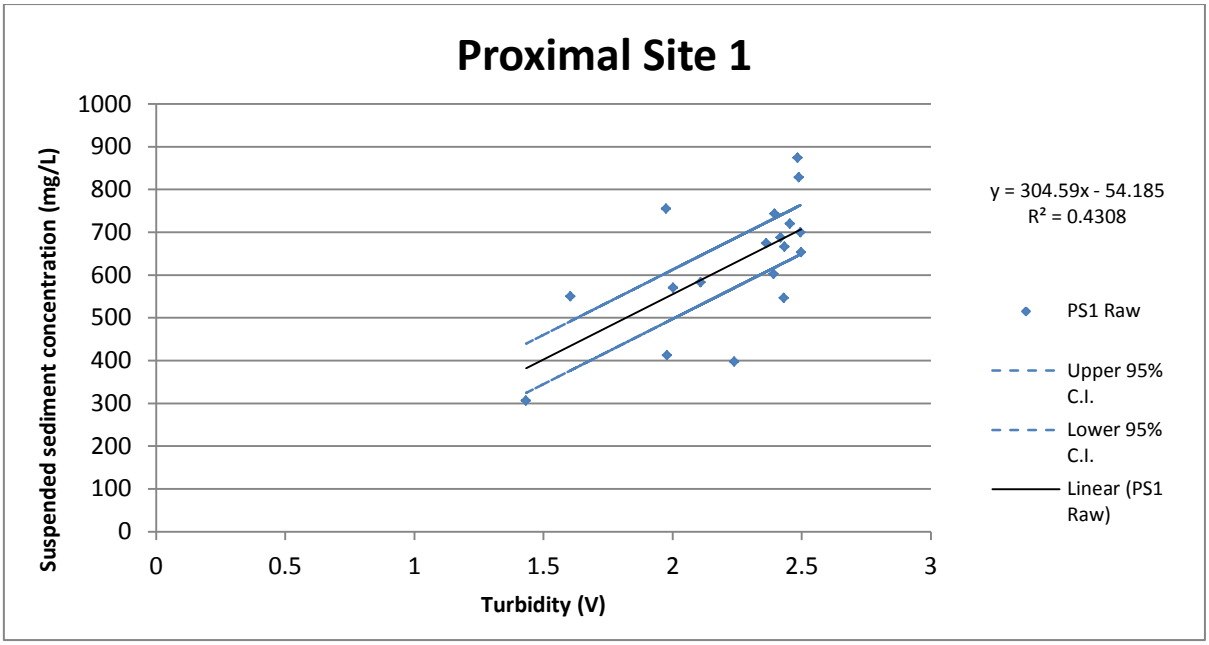
Proximal Site 1
Suspended sediment concentration (mg/L)
1000
900
800
700
600
500
400
300
200
100
0
0
0.5
1
1.5
2
2.5
3
Turbidity (V)
y = 304.59x - 54.185
R² = 0.4308
PS1 Raw
Upper 95% C.I.
Lower 95% C.I.
Linear (PS1 Raw)

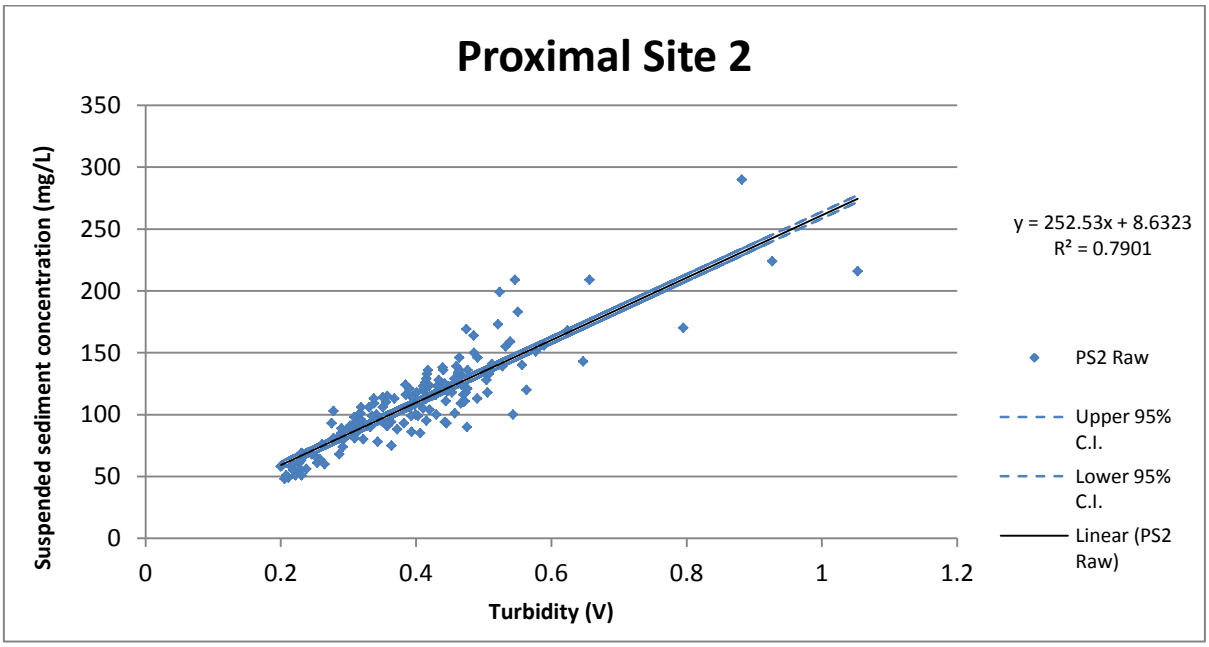
Proximal Site 2
Suspended sediment concentration (mg/L)
350
300
250
200
150
100
50
0
0
0.2
0.4
0.6
0.8
1
1.2
Turbidity (V)
y = 252.53x + 8.6323
R² = 0.7901
PS2 Raw
Upper 95% C.I.
Lower 95% C.I.
Linear (PS2 Raw)

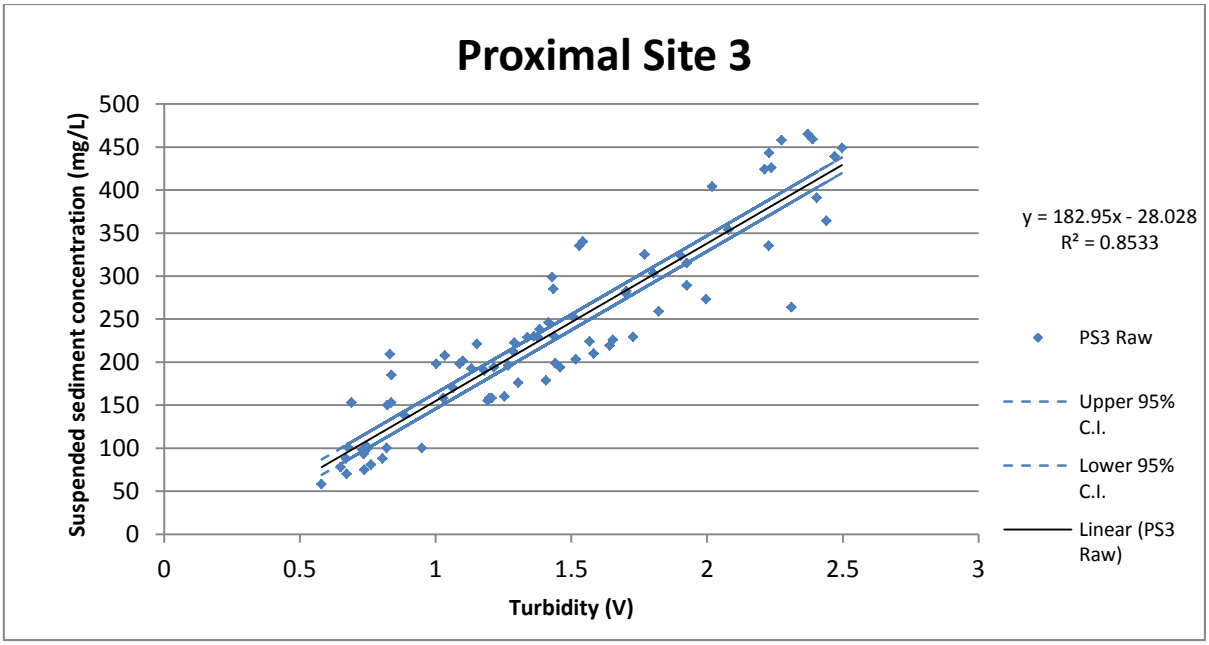
Proximal Site 3
Suspended sediment concentration (mg/L)
500
450
400
350
300
250
200
150
100
50
0
0
0.5
1
1.5
2
2.5
3
Turbidity (V)
y = 182.95x - 28.028
R² = 0.8533
PS3 Raw
Upper 95% C.I.
Lower 95% C.I.
Linear (PS3 Raw)

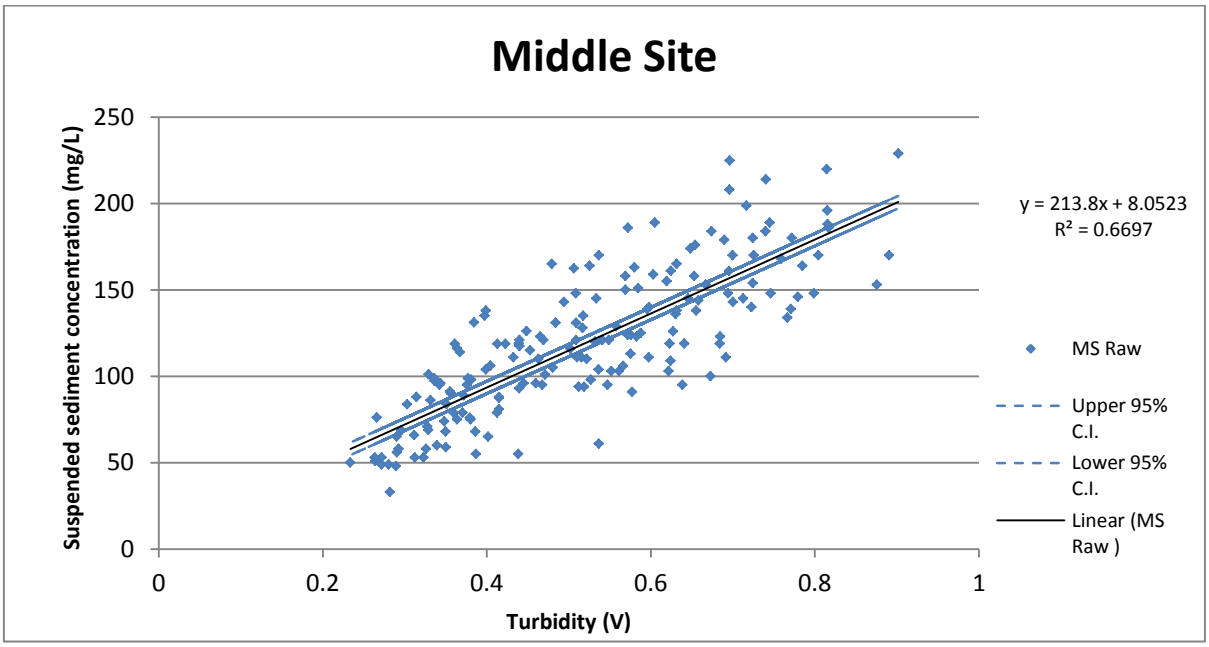
Middle Site
Suspended sediment concentration (mg/L)
250
200
150
100
50
0
0
0.2
0.4
0.6
0.8
1
Turbidity (V)
y = 213.8x + 8.0523
R² = 0.6697
MS Raw
Upper 95% C.I.
Lower 95% C.I.
Linear (MS Raw)

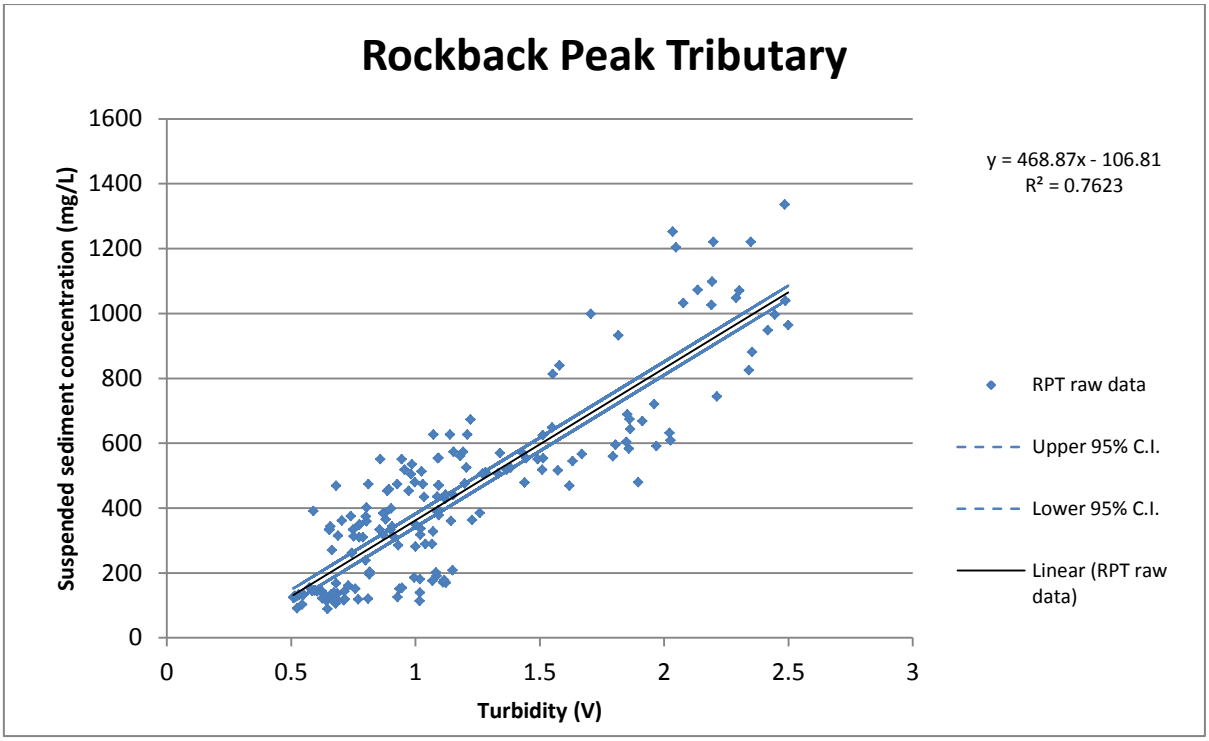

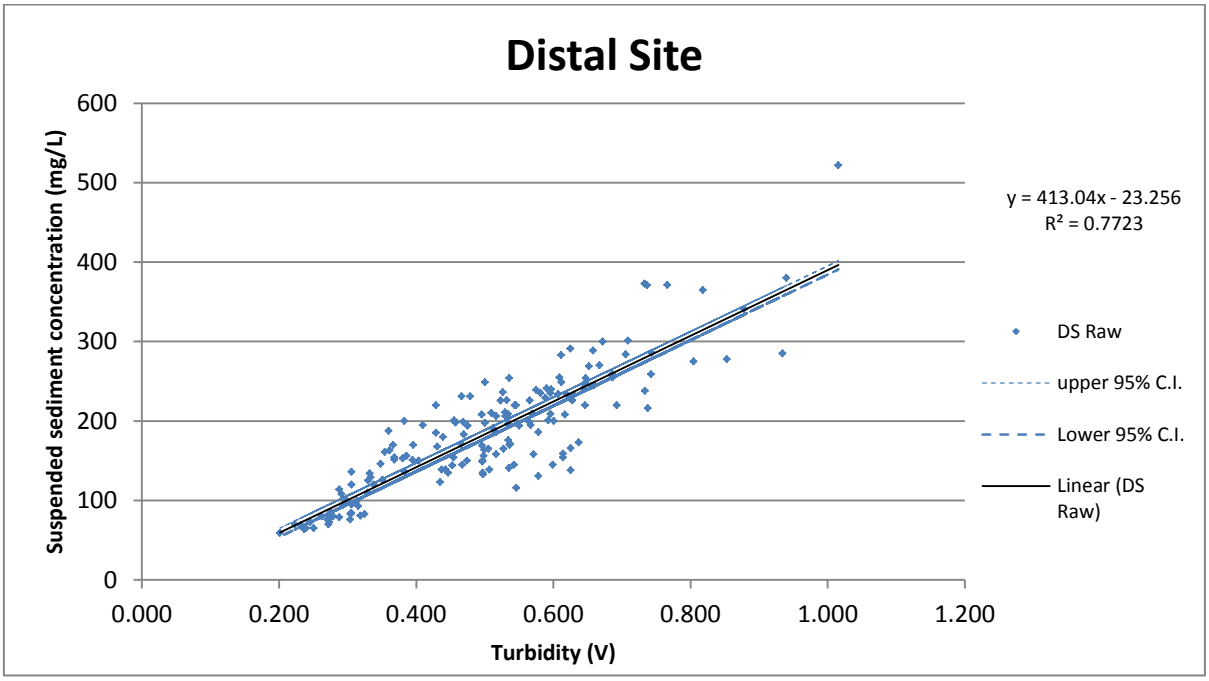

Figure 7.8 - Turbidity and suspended sediment concentration regressions. Outliers removed, 95% confidence interval included. Figures presented for all six sites over three preceding pages.

7.3 Meteorological

Table 7.2 Meteorological Parameters

	Met. Stn.	Upper	Upper	Upper	Lower	Lower	Lower	Upper	Lower	Lower	Upper
	Parameter	**AT min**	**AT max**	**AT mean**	**AT min**	**AT max**	**AT mean**	**PT mean**	**Rel. Hum.**	**T.Sol. Rad.**	**W.Spd. mean**
Cold and Wet (17days)	Min	-1.9	1.6	-0.2	-0.3	4.9	2.5	0.8	76.3	6265	2.0
	Max	3.9	14.2	6.7	4.4	9.2	6.7	19.1	90.1	22772	6.0
	Average	1.0	5.6	3.0	2.0	7.3	4.8	8.0	84.4	14553	4.1
	Std.Dev.	1.6	2.7	1.5	1.4	1.3	1.2	5.9	4.3	5133	1.1
Warm and Damp (15 days)	Min	0.2	5.4	2.6	2.4	8.8	5.6	0.0	61.5	9326	1.7
	Max	6.4	12.6	9.5	6.1	13.5	9.7	6.9	88.6	25597	5.5
	Average	3.0	8.2	5.5	4.3	10.7	7.9	2.5	72.5	18195	3.6
	Std.Dev.	1.9	1.9	1.8	1.3	1.5	1.2	2.5	7.9	3658	1.0
Hot and Dry (26 days)	Min	4.2	10.8	7.7	4.9	12.2	8.9	0.0	40.0	13792	2.4
	Max	13.3	18.2	15.4	9.9	18.6	13.2	8.6	73.0	28782	7.5
	Average	7.5	13.1	10.3	7.4	14.7	10.9	1.2	58.6	22041	3.6
	Std.Dev.	1.9	1.9	1.8	1.2	1.2	1.0	2.0	7.2	3718	1.0
Storm (2 days)	JD 211	5.7	11.5	7.9	4.5	14.6	9.4	31.2	73.9	20485	4.3
	JD 234	4.7	9.3	7.5	5.7	10.9	8.4	31.0E	84.0	8001	5.9
	Average	5.2	10.4	7.7	5.1	12.7	8.9	31.1	79.0	14243	5.1
	Std.Dev.	0.5	1.1	0.2	0.6	1.9	0.5	0.1	5.1	6242	0.8

7.4 Suspended Sediment Load Summary – 'Shape', 'Magnitude' and Hydro-Meteorological Categories

Table 7.3 Total suspended sediment load summary (kg/*x* days) for categories determined through PCA and CA. Table 3.5 reports the number of days in each category.

Station	Cluster Classification	Cold and Wet	Warm and Damp	Hot and Dry	Storm	Category Sum	Sum_T
PS1	Diurnal (Irregular)	73906 (5829)	42658 (9472)	51594 (33503)	(34400)	168158 (83204)	251362
	High	64305 (5829)	34414 (9472)	20219 (33503)	(34400)	118938 (83204)	202142
	Medium	8961	8244	31375	--	48580	48580
	Low	640	--	--	--	640	640
PS2	Diurnal (Irregular)	20774 (351764)	188116 (215052)	579493 (92464)	285759	1074142 (659280)	1733422
	High	(74606)	(109527)	74572	285759	360331 (184133)	544464
	Medium	20774 (158067)	151802 (23263)	336154 (65821)	--	508730 (247151)	755881
	Low	(119091)	36314 (82262)	168767 (26643)	--	205081 (227996)	433077
PS3	Diurnal (Irregular)	99130 (33315)	77113 (21069)	60350 (87018)	59199	295792 (141402)	437194
	High	76527 (15130)	45512 (10915)	23649 (50209)	59199	204887 (76254)	281141
	Medium	8460	31601 (9060)	29092 (29946)	--	69153 (39006)	108159
	Low	14143 (18185)	(1094)	7609 (6863)	--	21752 (26142)	47894
MS	Diurnal (Irregular)	66218 (445241)	240890 (291981)	754191 (124541)	383598	1444897 (861763)	2306660
	High	--	--	--	301577	301577	301577
	Medium	(161716)	(138134)	163088	82021	245109 (299850)	544959
	Low	66218 (283525)	240890 (153847)	591103 (124541)	--	898211 (561913)	1460124
RPT	Diurnal (Irregular)	426592 (41420)	296581 (238462)	138975 (672463)	343410 (42929)	1205558 (995273)	2200831
	High	257233 (18039)	222085 (235113)	123601 (543805)	343410	946329 (796957)	1743286
	Medium	58110 (18153)	--	15374 (93531)	(42929)	73484 (154613)	228097
	Low	111249 (5228)	74495 (3349)	(35127)	--	185744 (43704)	229448
DS	Diurnal (Irregular)	150697 (854988)	427579 (596198)	1346120 (210365)	888649	2813045 (1661651)	4474596
	High	(213187)	--	--	888649	888649 (213187)	1101836
	Medium	56034 (286429)	248039 (406369)	563048 (148311)	--	867121 (841109)	1708230
	Low	94663 (355372)	179540 (189829)	783072 (62054)	--	1057275 (607255)	1664530

7.5 Julian Day Calendar

Table 7.4 Julian Day (JD) Calendar for 2011 simplified to focus on typical ablation season. The 2011 field season at Castle Creek Glacier has been shaded.

Julian Day Calendar									
May	JD	June	JD	July	JD	Aug.	JD	Sept.	JD
1	121	1	152	1	182	1	213	1	244
2	122	2	153	2	183	2	214	2	245
3	123	3	154	3	184	3	215	3	246
4	124	4	155	4	185	4	216	4	247
5	125	5	156	5	186	5	217	5	248
6	126	6	157	6	187	6	218	6	249
7	127	7	158	7	188	7	219	7	250
8	128	8	159	8	189	8	220	8	251
9	129	9	160	9	190	9	221	9	252
10	130	10	161	10	191	10	222	10	253
11	131	11	162	11	192	11	223	11	254
12	132	12	163	12	193	12	224	12	255
13	133	13	164	13	194	13	225	13	256
14	134	14	165	14	195	14	226	14	257
15	135	15	166	15	196	15	227	15	258
16	136	16	167	16	197	16	228	16	259
17	137	17	168	17	198	17	229	17	260
18	138	18	169	18	199	18	230	18	261
19	139	19	170	19	200	19	231	19	262
20	140	20	171	20	201	20	232	20	263
21	141	21	172	21	202	21	233	21	264
22	142	22	173	22	203	22	234	22	265
23	143	23	174	23	204	23	235	23	266
24	144	24	175	24	205	24	236	24	267
25	145	25	176	25	206	25	237	25	268
26	146	26	177	26	207	26	238	26	269
27	147	27	178	27	208	27	239	27	270
28	148	28	179	28	209	28	240	28	271
29	149	29	180	29	210	29	241	29	272
30	150	30	181	30	211	30	242	30	273
31	151			31	212	31	243		

7.6 Suspended Sediment Load Summary for the Small River Glacier

Orwin and Smart reported total suspended sediment load (kg) for common days of monitoring, and computed percentage increase based on the uppermost site that was monitored. Their summary differed from the summary presented for the CCG in that daily mean SSLs and weighted averages were used for summaries to avoid bias in the results due to missing days of data and use as much of the data as possible. Table 7.5 presents the results of Orwin and Smart (2004a) in a format that is comparable with results presented in section 4.1.

Table 7.5 Re-computed results from Orwin and Smart 2004a, pg. 1539; suspended sediment totals have been computed as mean daily suspended sediment load (SSL) (kg/day) and percent of total SSL observed at the downstream site. NPG – North Proglacial; NPM – North Proglacial Middle; NPL – North Proglacial Lower; CPU – Central Proglacial Upper; CPL – Central Proglacial Lower.

Meteorological period	Cold and Wet 25% (7 days)		Snowmelt 25% (7 days)		Hot and Dry 43% (12 days)		Storm 7% (2 days)		Seasonal 100% (28 days)	
Site	% of Total SSL	mean SSL	% of Total SSL	mean SSL	% of Total SSL	mean SSL	% of Total SSL	mean SSL	% of Total SSL	mean SSL
NPG	**91**	764	**43**	1100	**87**	1250	**55**	7000	**64**	1502
NPM	**134**	1129	**103**	2600	**119**	1704	**98**	12400	**108**	2548
NPL	**100**	843	**100**	2529	**100**	1430	**100**	12700	**100**	2363
CPU	**42**	232	**38**	486	**15**	367	**47**	1735	**26**	461
CPL	**100**	551	**100**	1286	**100**	2500	**100**	3680	**100**	1794